PhD-FSTC-31-2010
The Faculty of Sciences, Technology and Communication

DISSERTATION

Defense held on 24/11/2010 in Luxembourg

to obtain the degree of

DOCTEUR DE L'UNIVERSITÉ DU LUXEMBOURG

EN BIOLOGIE

by

Thomas Georges Victor DENTZER
Born on 9th March 1977 in Luxembourg (Luxembourg)

FUNCTIONS OF THE HEPATITIS C VIRUS NON-STRUCTURAL PROTEIN 2

Dissertation defense committee

Dr Carsten Carlberg, dissertation supervisor
Professor, Université du Luxembourg

Dr Charles Rice, member
Professor, The Rockefeller University, New York

Dr Johan Neyts, member
Professor, University of Leuven

Dr Jean-Pierre Bronowicki, member
Professor, CHU de Nancy

Dr Jean-Claude Schmit, deputy chairman
CEO, CRP- Sante Luxembourg

Dr Jean-Luc Bueb, Chairman
Professor, Université du Luxembourg

Abstract

An estimated 170 million people are infected with hepatitis C virus (HCV). 15-30% of HCV-induced chronic hepatitis progresses to cirrhosis within years to decades after infection, and 3-4% of them will develop hepatocellular carcinoma. There is no vaccine available, and current HCV therapy of pegylated interferon-α in combination with ribavirin leads to a sustained response only in about 50% of infected patients.
The HCV non-structural protein NS2 (MW 23 kDa) is a dimeric multifunctional hydrophobic protein with an essential but poorly understood role in infectious virus production. The N terminal region of NS2 interacts with membranes whereas the C-terminal region, together with the N-terminal third of NS3, forms the NS2-3 protease. NS2 is not required for RNA synthesis, although cleavage at the NS2/3 junction is necessary for replication. Further, NS2 has been shown to interact with a number of viral and host proteins; it has been reported to activate transcription factors, inhibit apoptosis, and is a substrate for host kinase phosphorylation and proteosomic degradation.

NS2 determinants and their respective function in the HCV life cycle were investigated. Based on the crystal structure of the post-cleavage form of the NS2 protease domain, we mutated conserved features and analyzed the effects of these changes on polyprotein processing, replication, and infectious virus production. We found that mutations around the protease active site inhibit viral RNA replication by preventing NS2/3 cleavage. Supplementary assays indicated a dimerization defect for these mutant constructs, which prevented cleavage and RNA replication. In contrast, alterations in the dimer interface and at the C-terminal region did not affect replication, NS2 stability, or NS2 protease activity, but decreased infectious virus production. Analysis of the NS2/3 cleavage site revealed an additional function for several residues besides cleavage, notably in infectious virus production. A more comprehensive deletion and mutagenesis analysis of the C-terminal end of NS2 revealed the importance of its C-terminal residue in infectious particle production. Structural data suggests that the C-terminal leucine is locked in the active site, and mutation or deletion

of this residue could therefore alter the NS2 folding and disrupt potential protein-protein interactions important for infectious particle production. Further, we established an NS2-3 interaction model based on the solved $NS2^{pro}$ and NS3 crystal structures and assessed the importance of proximal residues for viral propagation. We were able to show genetic interactions between the viral proteins NS2 and E1 as well as NS2 and NS3. Additionally a pull down assay of strep-tagged NS2 followed by a mass spectrometry analysis divulged the physical interactions between NS2-E2, and NS2-NS3. Numerous host cell proteins could be identified to interact with NS2, involved in various pathways such as membrane trafficking, actin/myosin interactions or actin polymerization.

In this study we dissected the residues of NS2 involved in its multiple essential roles and interactions in the HCV life cycle and established NS2 as a new viable target for HCV-specific inhibitors for future anti-viral therapeutics.

1 Acknowledgments

I would like to thank Dr. Charles Rice, for giving me the opportunity to work in his laboratory. I am very grateful for Charlie's support, especially during the difficult times and can't be appreciative enough for his valuable insights and scientific discussions during my stay in the Rice lab.

I am extremely grateful to Jean-Claude Schmit who gave me the opportunity to work in his laboratory and who supported me all through my thesis. I am thankful for his advice, help and endless support. Without Jean-Claude this thesis would not have been possible.

I express my sincere gratitude to Carsten Carlberg who generously gave of his time and provided me with guidance.

I am very thankful to Jean-Luc Bueb for his support and heading the thesis committee. Many thanks to my thesis committee members Johan Neyts, and Jean-Pierre Bronowicki for their advice.

A special thank you to Nolwenn Jouvenet for assistance and help with the microscope and the FRET data analysis.

I want to thank the numerous past and present Rice lab members that created an exceptional work atmosphere and shared their ideas, knowledge and friendship.

I acknowledge the Retrovirology laboratory Luxembourg from the CRP-santé for their support, especially Carole Devaux for her help over all these years.

I am grateful to the Fonds National de la Recherche Luxembourg, which in part supported this work.

2 Table of contents

Table of Contents

3 List of figures

4 List of tables

5 List of abbreviations

2A	Foot and mouth disease virus 2A peptide
APS	Ammonium persulfate
BDV	Border disease virus
BSA	Bovine serum albumin
BVDV	Bovine viral diarrhea virus
CARD	Caspase-recruitment domain
CD	Cluster of differentiation
CD81	Cluster of differentiation 81
cDNA	Complementary DNA
CHAPS	3-(3-Cholamidopropyl)dimethylammonio-1-propansulfat
CLDNI	Claudin-1
CsA	Cyclosporine A
CSFV	Classical swine fever virus
DAB	3,3'-Diaminobenzidine
DC-SIGN	Dendritic cell-specific intercellular adhesion molecule-3-grabbing non- integrin
DC-SIGNR	Dendritic cell-specific intercellular adhesion molecule-3-grabbing non- integrin receptor
DENV	Dengue virus
DHF	Dengue hemorrhagic fever
DMEM	Dulbecco's modified eagle's medium
DMSO	Dimethylsulfoxid
dNTP	Desoxynucleosid-5'-triphosphat
DSS	Dengue shock syndrome
DSS	Disuccinimidyl suberate
DTT	Dithiothreitol
EDTA	Ethylene-diamine-tetraacetic acid
eIF3	Eukaryotic initiation factor 3
EMCV	Encephalomyocarditis virus
ER	Endoplasmic reticulum
ESCRT	Endosomal sorting complex required for transport
FCS	Fetal Calf Serum
FRET	Fluorescence resonance energy transfer

GLUC	Gaussia Luciferase
GNN	HCV Polymerase-defective control construct
H77	Genotype 1a strains of HCV
HCC	Hepatocellular carcinoma
HCV	Hepatitis C virus
HCVcc	Hepatitis C virus cell culture
HCVpp	Hepatitis C virus pseudo particle
HDL	High-density lipoprotein
HIFI	High fidelity
HIV	Human immunodeficiency virus
HRP	Horse Radish Peroxidase
HUH-7.5	Human Hepatoma cell line
HVR	Hypervariable region
IFN	Interferon
IHC	Immunohistochemistry
IRES	Internal ribosomal entry site
IRF	Interferon regulatory factor
J6	Genotype 2a
JEV	Japanese encephalitis virus
JFH1	HCV genotype 2a
kb	Kilobase
kDa	Kilodalton
LDs	Lipid droplets
LDL	Low-density lipoprotein
LDLR	Low-density lipoprotein receptor
m.o.i	Multiplicity of infection
mRNA	Messenger RNA
MVE	Murray valley encephalitis virus
NCR	Non coding region
NS	Non-structural
NS2pro	NS2 protease
nt	Nucleotide
NTP	Nucleoside triphosphate
NTPase	Nucleoside triphosphatase

OCLN	Occludin
ORF	Open reading frame
PAGE	Polyacrylamide gel electrophoresis
PBS	Phosphate buffered saline
PBS-T	Phosphate buffered saline + 0.1% Tween
PEG	Polyethylene glycol
PMSF	Phenylmethylsulfonyl fluoride
PTB	Polypyrimidine tract binding
qRT-PCR	Quantitative reverse transcription polymerase chain reaction
RC	Replicase complex
RdRp	RNA-dependent RNA polymerase
RNA	Ribonucleic acid
rRNAs	Ribosomal RNA
RT-PCR	Reverse transcription-polymerase chain reaction
SARS	Severe acute respiratory syndrome
SDS	Sodium dodecyl sulfate
SDS-PAGE	SDS- polyacrylamide gel electrophoresis
SFM	Serum Free Medium
SR-BI	Scavenger receptor class B type I
ssDNA	Single stranded DNA
SVR	Sustained virologic response
TAE	Tris-acetate-EDTA
TBE	Tick-borne encephalitis
TCID50	Tissue culture infectious dose 50
TEMED	N,N,N',N'-tetramethylethylenediamine
TLR	Toll like receptor
TM	Transmembrane domain
U2OS	Human osteosarcoma cell line
Ubi	Ubiquitin
VLDL	Very low-density lipoprotein receptor
WN	West nile virus
WT	Wild type
YFV	Yellow fever virus

6 List of original publications

Ivo C. Lorenz, Joseph Marcotrigiano, Thomas G. Dentzer, and Charles M. Rice.
Structure of the catalytic domain of the hepatitis C virus NS2-3 protease, Nature, 2006 Aug 17;442(7104):831-5

Thomas G. Dentzer, Ivo C. Lorenz, Matthew J. Evans, Charles M. Rice.
Determinants of the hepatitis C virus nonstructural protein 2 protease domain required for production of infectious virus, Journal of Virology, 2009 vol. 83 (24) pp. 12702-12713

Thomas G. Dentzer, Meigang Gu, and Charles M. Rice.
Importance of NS2 and NS3 interplay in infectious hepatitis C virus production, Journal of Virology, to be submitted

7 Chapter 1: Introduction

Mankind has overcome many burdens and solved many problems over the last 50 to 100 years concerning health care. Medical diagnostics, treatment and therapies have had a tremendous impact on life, while only mentioning the discovery of antibiotics to fight bacterial infections or the development of a poliovirus vaccine. Even today, infectious diseases continue to challenge the human population with vaccine preventable diseases like yellow fever, which kills over 30 000 people each year (273) to newly emerging threats like SARS (Severe acute respiratory syndrome), influenza or well described pathogens notably the human immunodeficiency virus (HIV) and hepatitis C virus (HCV). Numerous pathogens with a human or agriculture impact belong to the family of the *Flaviviridae*, a group of small, enveloped viruses that is divided into *Flavivirus, Pestivirus,* and *Hepacivirus* (151).

7.1 The Flaviviridae Family

Currently the family consists of three genera: the flaviviruses (from the latin flavi, yellow), the pestiviruses (from the Latin *pestis*, plaque), and the hepaciviruses (from the Greek *hepar*, *hepatos*, liver). Further, a group of unassigned viruses, the GB (GBV-A, GBV-B, GBV-C) agents, are awaiting their formal classification within the family.

Flaviviruses are named after the first human virus discovered, the yellow fever virus (YFV), and consists of nearly 80 viruses, many of which are arthropod-borne human pathogens causing a variety of diseases including fevers, encephalitis, and hemorrhagic fevers. Major diseases are Dengue Hemorrhagic Fever (DHF), Dengue Shock Syndrome (DSS), Japanese encephalitis, and yellow fever. Other *flaviviruses* of regional or endemic concern include Kyasanur Forest disease, Murray Valley encephalitis (MVE), St. Louis encephalitis, tick-borne encephalitis (TBE), and West Nile (WN) viruses (91, 151, 178, 273). The development of a live-attenuated *flavivirus* vaccine, YFV strain 17D by Max Theiler was awarded the Nobel price in 1951. Very few *flavivirus* vaccines are currently available, notably TBEV and JEV for humans and WNV for use in animals.

The *Pestiviruses* genus comprise a group of animal pathogen pestiviruses, bovine viral diarrhea virus (BVDV), border disease virus (BDV), and classical swine fever virus (CSFV), which show similarities with HCV (198). Bovine viral diarrhea virus (BVDV) shares a similar structural

organization with HCV, and both viruses generally cause chronic long-term infections in their respective hosts. Together with the closely related border disease virus of sheep (BDV) and European Swine fever virus (CSFV), also referred to as Hog Cholera virus, BVDV is now classified in the genus pestivirus of the *Flaviviridae* family. BVDV exists in two biotypes, non-cytopathic and cytopathic, the latter differing in structural proteins from the non-cytopathic biotypes. In virus-free animals infection is transient and mostly subclinical or mild but may also lead to an array of diverse symptoms such as pneumoenteritis (often in combination with other microorganisms) (152).

Hepaciviruses contain only one member, the HCV with an estimated 170 million people infected worldwide. HCV can be resolved spontaneously or it progresses from an acute, to a chronic infection, which potentially leads to liver cirrhosis and hepatocellular carcinoma (HCC) over a period of years (82). HCV is the leading cause for liver transplantations in developed countries (282). Current therapies account for a sustained virological response (SVR) of about 50% of genotype 1 infected patients and there is no vaccine available.

7.2 Genome organization of the *Flaviviridae*

The *Flavivirus* genome consists of a single positive-stranded RNA of 9-12 kilobases (kb) with a type I 5' cap ($M^7GpppAmpN_2$) at the 5' end and lacks a polyadenylated tail (152). In contrast, HCV and the *Pestiviruses* possess an internal ribosomal entry site (IRES) but no 5' end cap (150, 238, 276). Upon binding of the virions to their corresponding receptor at the cell surface, endocytosis of the particle and a low-pH induced fusion events releases the genomic RNA into the cytoplasm where it is immediately translated, similar to cellular mRNAs. As for all positive-stranded RNA viruses, *Flavivirus* genomic RNA is infectious. Genomes encode a single long open reading frame flanked by 5'- and 3'-non-coding regions (NCR) of ~100 and 400 to 700 nucleotides (nt), respectively. The genomic RNA is the messenger RNA for translation of a single long open reading frame (ORF) as a large polyprotein. After translation, the polyprotein is processed co- and post-translationally by cellular and viral encoded proteases into ten or eleven discrete products. These proteins are named NH_2-C-prM-E-NS1-NS2A-NS2B-NS3-NS4A-NS4B-NS5-COOH for *Flaviviruses*, NH^2-N^{pro}-C-E^{rns}-E1-E2-p7-NS2-NS3-NS4A-NS4B-NS5A-NS5B-COOH for *Pestiviruses*, and NH_2-C-E1-E2-p7-NS2-NS3-NS4A-NS4B-NS5A-NS5B-COOH for *Hepaciviruses*. Proteins can be divided into structural proteins at the amino terminal

region of the polyprotein and non-structural (NS) proteins. Structural proteins include capsid (C) and the envelope proteins that form the virion that are predominantly processed by cellular enzymes such as signal peptidase. The NS proteins encode viral proteases, helicases, replicase components and the RNA- dependent RNA polymerase and are primarily liberated by viral protease NS3 (20, 41, 297) along with its cofactor NS4A (70, 298) or NS2B (*Flaviviruses*, (41)). The NS proteins NS3 to NS5B (NS1 to NS5 in *Flaviviruses*) group together to form the replicase complex in the cytoplasm in close proximity of modified intracellular membranes (203). NS5B and NS5 (*Flaviviruses*) represent the viral RNA-dependent RNA polymerase, which is part of the replicase complex and catalyzes the accumulation of genomic RNA (25, 262, 320). NS3 possesses many essential functions for viral RNA replication, including a protease and helicase as well as nucleoside triphosphatase (NTPase) activity (260, 261, 294). The roles of other NS proteins have yet to be defined although some of them seem to be crucial for RNA replication or infectious virus production (151).

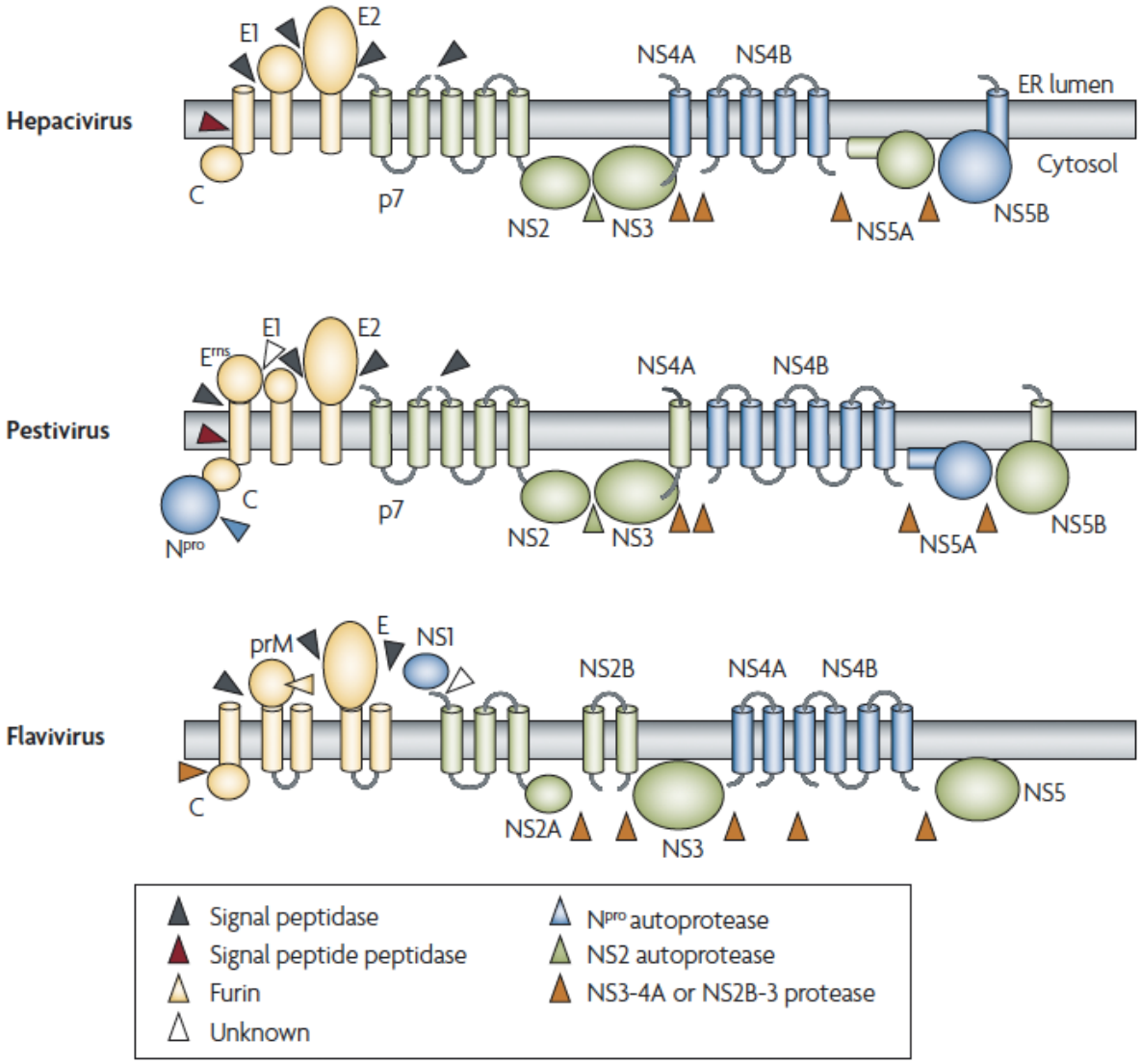

Fig. 1-1. Processing and putative topologies of the *Flaviviridae* polyproteins. Proposed topologies of viral proteins with respect to the endoplasmic reticulum (ER) membrane. Enzymes that are involved in their liberation from the polyprotein are indicated. Structural proteins are shown in yellow and NS proteins are shown in green (required for infectious virus production) or blue (have not been implicated in infectious virus production). C, core protein (or capsid protein in flaviviruses); N^{pro}, amino-terminal protease (210).

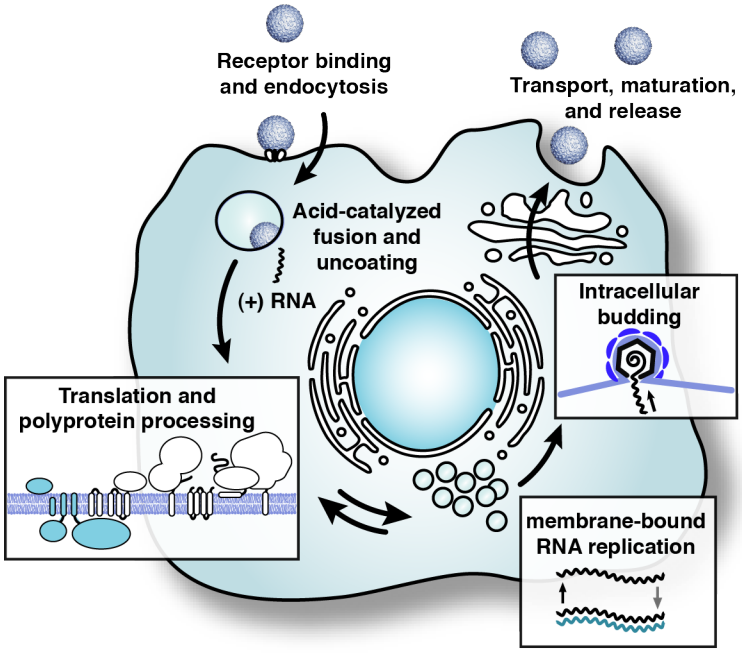

Fig. 1-2. Life cycle of the *Flaviviridae*. *Flaviviridae* particles enter the cell by endocytosis, introducing a single-stranded RNA molecule into the cytoplasm. Translation of this genomic RNA is followed by processing of the polyprotein to yield the viral gene products. The replicase proteins catalyse RNA accumulation in close association with modified intracellular membranes. Packaging of the RNA into virus particles is thought to occur at cytoplasmic membranes, and is followed by egress of the progeny virions through the secretory pathway (151).

7.3 Lifecycle of the *Flaviviridae*

Flaviviridae virion morphogenesis occurs in association with intracellular membranes where the C protein and genomic RNA aggregate and are budding into the ER derived membranes (39). Cryo-electron microscopy (EM) suggests that virions do not contain an ordered nucleoprotein interior and subviral particles without the C protein or RNA are present in flavivirus infections (135, 209, 314, 315, 317). Particles are then transported via the secretory pathway and released at the cell surface without cell lysis of the host cell (177).

The maturation process of *Flaviviruses* is based on an acid-induced reorganization and conformational change of the glycoproteins whereas the *Pestiviruses* and *Hepaciviruses* seem

to be readily infectious upon formation, although they still undergo a maturation process before egress (81, 137, 180, 208, 255, 308).

7.4 Structure of the *Flaviviridae*

Flavivirus particles appear to be spherical, 40 to 60 nm in diameter with an electron dense core surrounded by a lipid bilayer (Fig.1-3) (152). Because of the lipid envelope, organic solvents and detergents can inactivate flaviviruses.

The surface of virus particles contains two viral proteins, E (envelope) and M (membrane) where E is the major antigenic determinant and mediates binding and fusion during viral entry. The structure of a flavivirus has been determined by using a combination of cryo-EM and fitting of the known structure of glycoprotein E into the electron density map. The virus core, within a lipid bilayer, lies underneath an external, icosahedral scaffold of 90 glycoprotein E dimmers the so-called “herring-bone” pattern with icosahedral symmetry. The three E monomers per icosahedral asymmetric unit do not have quasiequivalent symmetric environments. E dimers are thought to undergo rotational rearrangements around 3- and 5-fold axes of symmetry to form fusogenic trimeric complexes (137). Immature DENV-2 and YFV particles are larger (60 nm) with 60 spikes, each composed of three E monomers surrounding a prM trimer (315). The mature form represents 90 anti-parallel E dimmers due to the cleavage of prM and the dissociation and rotation of the E trimers. In addition to these two types of virions, smaller non-infectious particles are released from infected cells.

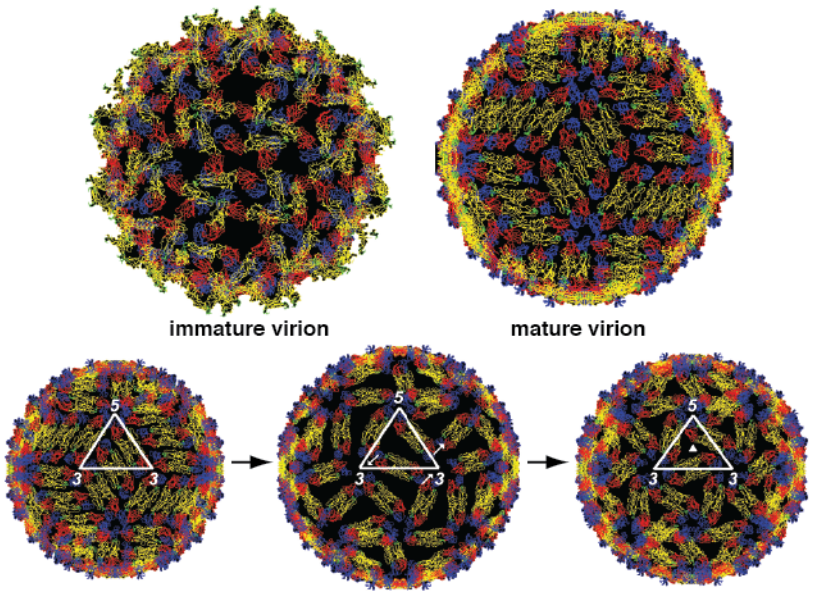

Fig. 1-3. Virion particles. B. Cryo-EM reconstruction of immature DENV-2 particles. C. Cryo-EM reconstruction of mature DENV-2 particles. D. Model of the low pH-induced fusogenic state (151).

7.5 The hepatitis C virus (HCV)

HCV is the sole member of the genus Hepacivirus within a large family of related positive-strand RNA viruses, the *Flaviviridae*. Humans are the only natural host, and HCV affects roughly 3% of the human population (8). Blood or blood products primarily transmit HCV. Other routes of transmission are untested samples and parental risk factors, most notably “needle sharing” among users of intravenous drugs. Sexual transmissions and intrauterine infections are also possible but rare.

Diagnostic tests based on the use of recombinant antigens generated from this genome demonstrated a clear association between antibodies against HCV antigens and a liver disease that was originally designated non-A, non-B hepatitis. After the successful cloning of its genome in 1989 (44), molecular studies of HCV became possible.
Phylogenetic analysis of full-length or partial sequences of HCV has identified 6 genotypes based on genomic variability in a small region of NS5B (genotype 1-6) and numerous subtypes designated by lower case letters (i.e. a, b, c) (151, 239).

The six genotypes differ in their nucleotide sequence by 31 to 34% (21). Within an HCV genome, subtypes can be defined that differ in their nucleotide sequence by 20 to 23%. The most frequent genotype in Western Europe and the United States is genotype 1a, whereas in Japan genotype 1b is the most common. Genotypes 2 and 3 are less frequent, and the other genotypes are very rare and are mostly found in distinct geographical regions like Egypt (genotype 4), South Africa (genotype 5) and Southeast Asia (genotype 6). This genomic variability is due to the high error rate (about 10^{-4}) of the viral RNA-dependent RNA polymerase (RdRp). It is not clear if the distinct HCV genotypes are associated with a more severe course of the disease. However, the distinction is of importance for predicting the outcome of anti-viral therapy of those infected with chronic hepatitis C.

7.6 Genome structure

Similar to other members of the *Flaviviridae*, HCV RNA synthesis is likely to be semi-conservative and asymmetric: the positive-strand genome serves as a template to make a negative-strand intermediate; the negative strand then serves as a template to produce multiple nascent genomes.

The HCV genome is a highly structured positive-stranded and uncapped, 9.6-kb RNA containing a 5' and 3' NCR. The 5' non-coding region (NCR) contains a 341 nt well-conserved sequence element that folds into a structure of four domains and a pseudoknot, a *cis* acting RNA element that is essential for RNA replication (151). The first 122 nt serve as a minimal replication element (80, 87, 129, 173, 237). The 5' NCR also directs the cap-independent translation of the large open reading frame (3,011 codons). Conserved secondary structures have been predicted for various parts of the genome, as core and NS5B (277). Interestingly, HCV seems to contain a high amount of internal base pairing which is a feature common among viruses causing persistent infections (251).

The 3' NCR consists of a short (~40 nt) variable domain, a polyuridine/polypyrimide (polyU/UC tract, followed by a highly conserved 3'X region of 98 nt which is critical for RNA replication (132, 263, 301). One particular stem loop at the 3'-reminal coding region of NS5B, was found to be indispensable for replication, since mutational disruption of the loop structure severely reduced or completely blocked RNA replication (307). Additional, a 3´X domain and the

5BSL3.2 element interaction, the 'kissing' loop, within the ORF is also required for RNA replication (79).

A number of cellular factors have been described to bind to the HCV 3' NCR including RNA binding proteins polypyrimidine-tract binding protein (PTB), heterogeneous ribonuclear protein C, glyceraldehyde-3-phosphate dehydrogenase, HuR, and La autoantigen (21, 151, 154).

7.7 Hepatitis C

Acute infections are frequently asymptomatic or associated with mild symptoms that disguise the medical problem and raise the risk of a chronic infection. About 80% of the infected individuals are unable to eliminate the virus (103). 10 to 20% of persistently infected individuals develop liver cirrhosis within 20 years and eventually HCC. There is no vaccine available, and current HCV therapy of pegylated interferon-α in combination with ribavirin leads to a sustained response only in about 50% of genotype 1 infected patients. However, 80 to 90% of patients persistently infected with genotype 2 or genotype 3 viruses elicit a sustained response and are able to eliminate the virus.

All current treatment protocols for hepatitis C are based on the use of various preparations of interferon alpha (IFN-α), which is administered by intramuscular or subcutaneous injection. Interferon alpha is a naturally occurring glycoprotein that is secreted by cells in response to viral infections. It exerts its effects by binding to a membrane receptor, which leads to phosphorylation, dimerization, and nuclear import of latent transcription factors known as signal transducers and activators of transcription (STATs), a series of intracellular signaling events that ultimately leads to enhanced expression of certain genes (95). This leads to the enhancement and induction of certain cellular activities including augmentation of target cell killing by lymphocytes and inhibition of virus replication in infected cells.

More recently, peg interferon α (polyethylene glycol (PEG)-conjugated interferon-α (IFN-α)), sometimes called pegylated interferon, has been available for the treatment of chronic hepatitis C. The addition of ribavirin to IFN-α or PEG-IFN-α is superior to IFN-α alone in the treatment of chronic hepatitis C. Ribavirin, a guanosine analog is a synthetic nucleoside that has activity against a broad spectrum of viruses (95). It enhances the interferon effect to a more powerful

immune reaction, due to its immune modulating properties. The effect of ribavirin plus interferon on viral clearance may lead to reduced mortality and morbidity in patients with chronic hepatitis C infection. However, combination therapy is associated with increased risk for adverse events. Ribavirin monotherapy for patients with chronic hepatitis C has no significant beneficial effect. HCV exhibits many potential targets and while some are not in development for new antiviral drugs, others are already in clinical trial phases and could enter the market in the near future. Viral targets include a wide range from entry factors, helicases, HCV IRES, to immunosuppressive agents like cyclosporine A (CsA). Small molecules directed against host factors represent another class of currently evaluated potent HCV antivirals with a high threshold for resistance, as their mechanism is independent from HCV replication. An additional approach consists of manipulating the immune response to enhance adaptive immunity against HCV-specific epitopes, with the alteration of the cytokine milieu. Other modulators affect interleukin balance, anti-inflammatory agents and immune enhancers or inhibition of IFN-**α**-mediated activation of the Janus activated kinase and signal transducer and activators of transcription (JAK-STAT) pathway. Polymerase and protease inhibitors are however the most commonly developed antivirals nowadays. Inhibitors of HCV NS5B RNA dependent RNA polymerase (RdRp) are divided into two classes, the nucleoside (NI) and non-nucleoside inhibitors (NNI).

Nucleoside inhibitors metabolites act as nonobligate chain terminators in the active triphosphate (TP) form while competing with the natural substrate nucleotides for the HCV NS5B RdRp, thereby reducing the efficiency of further RNA elongation through steric resistance.
Non-nucleoside inhibitors target different and less conserved allosteric sites of the HCV NS5B polymerase. The mechanism of the inhibitory effect differs from the NI by binding the active site of HCV. Multiple NS5B HCV inhibitory compounds have been described and are under clinical investigation. Several NS5B polymerase inhibitors are undergoing early stages of clinical investigation and present promising results. Protease inhibitors represent a large group of potent antivirals, targeting specifically viral components. The HCV NS3/NS4A serine protease is responsible for polyprotein processing that is essential for the production of infections virions and therefore provides an attractive target for inhibition of viral replication. The protease inhibitors telapravir and boceprevir, currently in phase 3 clinical trials will be among the first HCV specific antivirals that could enter the market in 2011.

Many compounds and HCV specific inhibitors are currently in various stages of development and clinical trials, which will hopefully improve current anti-viral therapies (53). A major concern is the emergence of resistant mutations, conferring cross-resistance to multiple therapies and significantly diminishing treatment. This obstacle emphasizes the importance of elucidating multiple mechanisms to inhibit HCV and conferring several methods for concomitant inhibition of viral replication.

Although the liver and hepatocytes seem to be the primary organ for HCV replication, persistent infections are often (40% of patients) associated with other symptoms of at least extrahepatic disease, renal complications, neuropathy, lymphoma, Sjorgen syndrome with or without cryoglobulinemia, porphyria cutanea, and diabetes (21). An HCV infection is present at 80% of patients with cryoglobulinemia type II and type II. HCV is a leading cause for liver transplantations in Europe and the United States, but reinfection of the newly transplanted liver occurs almost universally (69).

7.8 Tools to study HCV

Hepatitis C has long been hampered by the lack of a small animal model or an appropriate cell culture system. This presumably results from defects at one or multiple steps of the replication cycle. For positive-strand RNA viruses such as HCV, transfection with infectious RNA can circumvent the entry steps, allowing translation and initiation of RNA replication in permissive cells. Full-length cDNA clones of HCV have been constructed for genotypes Ia, 1b, and 2a and the infectivity of transcribed RNAs validated by intrahepatic inoculation of chimpanzees (304). However, replication in tissue culture is limited.

7.8.1 HCV Replicon System

It was shown for bovine virus diarrhea virus (BVDV) that a subgenomic RNA, originally identified as a defective interfering particle and lacking all the structural proteins can replicate autonomously in cells (24). This observation could be confirmed with HCV and led to the construction of RNAs capable of replicating in a human hepatoma cell line (164). The culture system recapitulates the intracellular part of the HCV life cycle, allowing detailed molecular studies. HCV replication appears to be restricted to the human hepatoma cell line HuH-7, and therefore a subpopulation of these cells was screened. Self-replicating subgenomic RNA was eliminated from HuH-7 clones by prolonged treatment with alpha interferon (IFN-α). A higher frequency of cured cells could support both subgenomic and full-length HCV replication. The increased permissiveness of one of the cured cell lines named Huh-7.5 allowed to readily detect HCV RNA and antigens early after RNA transfection, eliminating the need for selection of replication-positive cells.

The efficiency of HCV replication in cell culture is determined both by adaptation of the viral sequence and by the host cell itself (26-28, 164).

7.8.2 HCV pseudoparticles (HCVpp)

Due to poor infection in cell culture, HCV entry has been notoriously difficult to study so far. In 2003, a system was developed to generate infectious pseudo-particles (HCVpp), which are assembled by displaying unmodified and functional HCV glycoproteins onto retroviral and lentiviral core particles (22, 104). The presence of a luciferase marker gene packaged within these HCV pseudo-particles allows reliable and fast determination of infectivity, mediated by the HCV glycoproteins.

High infectivity of the pseudo-particles requires both E1 and E2 HCV glycoproteins. Sera from HCV-infected patients and some anti-E2 monoclonal antibodies are able to neutralize the particles (162, 309). Thus, this system provided a valuable tool to identify neutralizing antibodies. In addition, these pseudo-particles allowed investigation of the role of putative HCV receptors.

HCVpp has provided the most insight into HCV entry. In the future, the HCVpp, together with the recently developed infectious tissue culture system (see below), will be useful tools to investigate the different steps of HCV entry into host cells. (26, 164, 286, 319)

7.8.3 HCV infectious cell culture system (HCVcc)

Genome-length replicon RNAs used in studies carried adaptive mutations, which increased the efficiency of viral RNA replication. One subgenomic replicon of the HCV genotype 2a strain JFH1, which was isolated from a Japanese patient with acute fulminant hepatitis (124), replicated efficiently in cell culture without adaptive changes. Several groups developed infectious systems based on the full-length JFH genome (286, 319) or chimeras containing the core-NS2 region from the genotype 2a J6 strain (154). These replicons were able to replicate ant to produce infectious viral particles in human hepatoma cells. Although the titers of particles released into the medium were relatively low in HuH-7 cells (286), enhanced levels were obtained in more permissive HuH-7.5 sublines, and virus could be passaged in tissue culture (154, 319). Efficiently replicating JFH1 genotype 2a replicons produced particles with a density of about 1.15-1.17g/ml and a spherical morphology with an average diameter of about 55nm (286). Particle density varied between 1.10 to 1.15 g/cm3 in sucrose density gradient centrifugation (286, 319) or 1.09 to 1.14 g/cm3 in iodixanol equilibrium sedimentation (154). Supplementary, inoculation of a chimpanzee with cell-culture generated particles induced viremia and clearly demonstrated *in vivo* infectivity of cell culture grown virus (286).

The development of an infectious tissue culture system represented a major breakthrough in the field. For the first time, more than 15 years after the isolation of the virus, an experimental tool to study a complete viral life cycle in cell culture has been available.

7.9 Animal system

The chimpanzee remains the only animal model that reproduces a human like infections, including viral persistence and development of specific innate and adaptive immune responses whereas disease progression is typically milder in chimpanzees and rarely progresses to end stage liver disease or HCC (287). Various small animal models for example transgenic mouse models are being developed although none is currently available which mimics the whole HCV life cycle (148, 151, 191, 192).

7.10 Life cycle of HCV

In contrast to other *flaviviruses*, little is known about the life cycle of HCV. During the first decade after its discovery, it was not possible to study HCV replication in tissue culture. A breakthrough came with the first functional 'subgenomic' replicons in cell culture (26, 164). This system still had a limited range of use, since analysis of replication can only be done in tissue culture and no infectious particles are produced. After the recent development of an infectious cell culture system based on a particular isolate of the virus, the analysis of the molecular biology and the virus-host interactions of HCV became possible (154, 286, 312).

Based on findings from the replicon system and in analogy to other *flaviviruses* like BVDV, an HCV life cycle was suggested as shown in Fig. 1-4. After receptor binding and endocytosis of the virions, the positive-stranded RNA is translated, the large polyprotein is processed, and RNA is replicated. Finally, virions are assembled and leave the cell through the secretory pathway (Fig. 1-4).

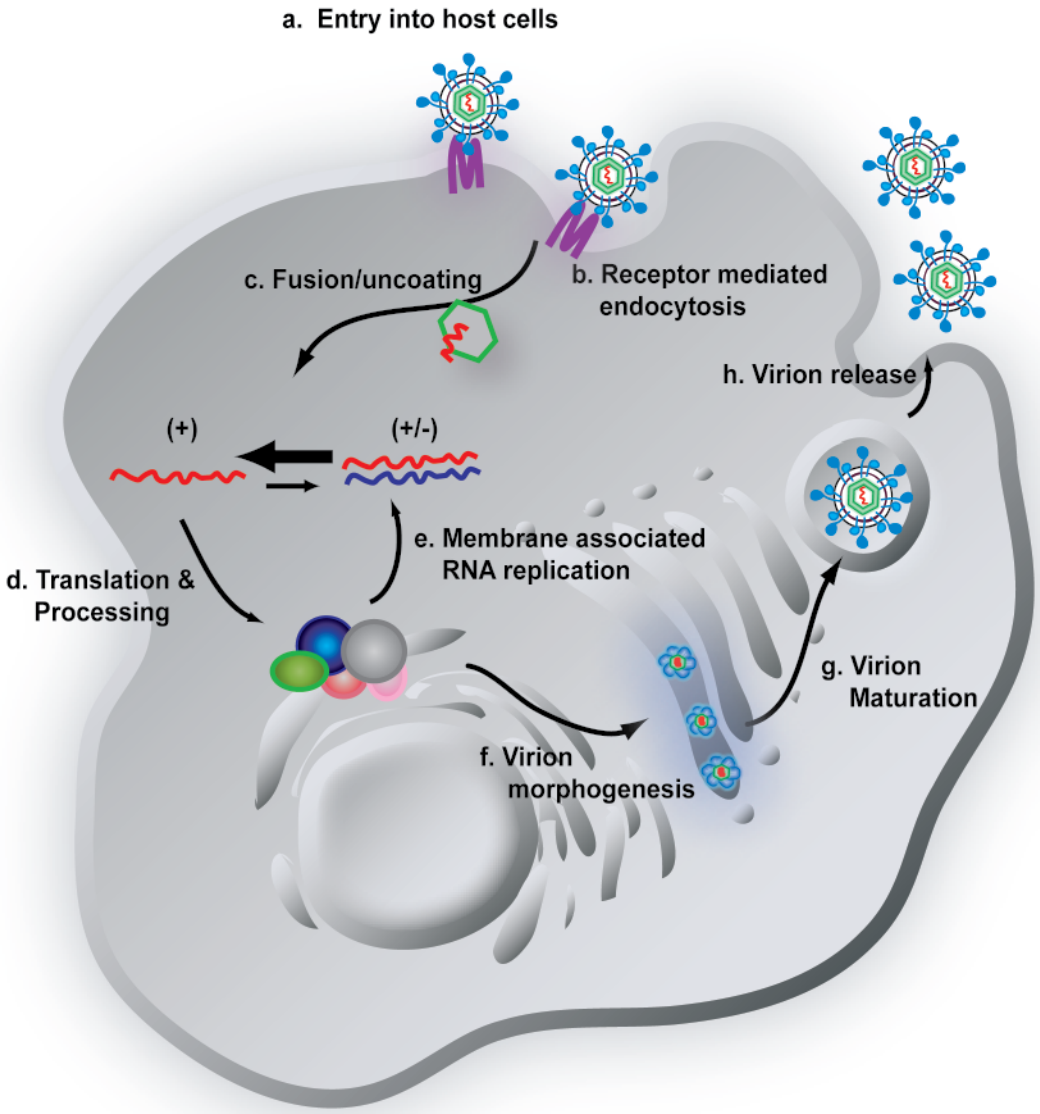

Fig. 1-4. The HCV life cycle. HCV virions enter the cell via receptor-mediated endocytosis, followed by fusion with the host cell membrane and uncoating. The positive-strand RNA genome is then translated and the viral polyprotein is processed into single proteins. RNA is replicated and premature virions are assembled. Viral particles are transported via the secretory pathway before being released from the cell (154).

7.11 Receptor binding and fusion

Over the last years with the development of the HCVcc system, there have been many advances in HCV entry research. There have been a number of HCV receptors identified that seem to participate in HCV entry.

An important receptor is CD81, a member of the tetraspanin family that is critical for cell infections with HCVpp (51, 143, 188, 312) and HCVcc (38, 150, 286). The extracellular loop of CD81 binds to the HCV glycoprotein E2 to mediate entry, but CD81 alone is not sufficient (59, 98, 225, 231). It is thought to act in later entry steps as CD81 antibodies can inhibit entry even after virus adsorption (51). CD81 is expressed on most cell types, including B and T cells, making it unlikely to be the only determinant of HCV hepatotropism.

Another candidate, scavenger receptor class B type I (SR-BI) is probably involved in initial attachment of viral particles by binding to HCV glycoprotein E2 (243). SR-BI also plays a role in the uptake of cholesterol and cholesterol esters from high-density lipoproteins (HDL) and the catabolism of oxidized low-density lipoproteins (LDL). HDL is known to enhance HCVpp uptake via the E2-HVR1 region and apolipoprotein C1 (23, 193, 283), whereas oxidized LDL inhibits HCVcc and HCVpp entry at a post-attachment step (284).

Further, the LDL receptor itself is also part of the HCV receptor-binding complex and mediates binding and internalization of HCV. This is also true for other related *flaviviridae* like BVDV and GBV-C (3, 199, 300). LDLR has been an attractive candidate HCV receptor since the discovery of the association between infectious HCV and low-density lipoprotein (LDL) or very low density lipoprotein (VLDL) (199). Coating of virions with serum lipoproteins during their secretion from hepatocytes or after release into circulation could shield the virus from neutralizing antibodies and provide a mechanism for binding and entry that is independent of the HCV glycoproteins.

CLDN1, a member of the claudin family and a component of the tight junction strain, is essential for HCV entry and is highly expressed in the liver and other epithelial tissues. CLDN1 consists of four transmembrane (TM) helices, intracellular amino and carboxy termini and two extracellular loops (EL) where the N-terminal third of the CLDN1 EL1 is sufficient to confer susceptibility for HCVpp entry (280). Anti-CLDN1 antibodies can block an HCV infection and

kinetics indicate that CLDN1 is active in later entry steps after virus binding where it is acting as a co-receptor (68).

The most recently discovered HCV entry molecule is OCLN, a tight junction protein with four TM domains that is thought to regulate paracellular permeability and cell adhesion (232). OCLN seems to be the missing factor since expression of CD81, SR-BI, CLDN1 and OCLN allow non-susceptible cell lines like murine cells to be infected with pseudoparticles in the HCVpp system.

The C-type lectins DC-SIGN, L-SIGN, and DC-SIGNR are able to bind to the HCV E2 protein and are thought to direct HCV to new host cells rather than being implicated in infection (50, 169, 170).

HCV is thought to follow a coordinated entry pathway using several receptors and co-receptors to migrate from the cell surface to the tight junction for internalization presumably via clathrin-mediated endocytosis. Fusion of the viral and cellular membranes is presumably triggered by the low pH of the endocytic compartment, which leads to the release of a single-stranded, positive-sense RNA genome into the cytoplasm (151, 274).

7.12 Genome structure

Similar to other members of the *Flaviviridae*, HCV RNA synthesis is likely to be semi-conservative and asymmetric: the positive-strand genome serves as a template to make a negative-strand intermediate; the negative strand then serves as a template to produce multiple nascent genomes.

The 5' to the 3' end of the HCV genome is a highly structured and uncapped, 9.6-kb RNA. The 5' non-coding region (NCR) contains a 341 well-conserved sequence element that folds into a structure of four domains and a pseudoknot, a *cis* acting RNA element, essential for RNA replication (151). The first 122-nt serve as a minimal replication element (80, 87, 129, 173, 237). The 5' NCR also directs the cap-independent translation of the large open reading frame (3,011 codons). Conserved secondary structures have bee predicted for various parts of the genome, ie C and NS5B (277). Interestingly, the HCV seems to contain a high amount of internal base pairing which is a feature common among viruses causing persistent infections (251).

The 3' NCR consists of a short (~40 nt) variable domain, a polyuridine/polypyrimide (polyU/UC tract, followed by a highly conserved 3'X region of 98 nt which is critical for RNA replication (132, 263, 301). Interestingly, the 5BSL3.2 element interaction, the 'kissing' interaction, within the ORF is also required for RNA replication (79). One particular stem loop at the 3'-terminal coding region of NS5B, was found to be indispensable for replication, since mutational disruption of the loop structure severely reduced or completely blocked RNA replication (307).

A number of cellular factors have been described to bind to the HCV 3' NCR including RNA binding proteins PTB, heterogeneous ribonuclear protein C, glyceraldehyde-3-phosphate dehydrogenase, HuR, and La autoantigen (21, 151, 154).

7.13 Translation and polyprotein processing

Translation of the HCV genome depends on an internal ribosome entry site (IRES) within the 5' NCR. The HCV IRES binds 40S ribosomal subunits directly, bypassing the need for pre-initiation factors (21, 217, 224, 254). The IRES-40S complex binds to the initiation factor eIF3 to form a 48S intermediate complex to place the initiating AUG codon at nt 342 within the ribosomal P-site (111, 217). These IRES/eIF3 interactions mimic a functional 5' cap binding complex eIF4F (252).

The translation product of the viral genome is a large polyprotein containing the structural proteins core (C) and the glycoproteins E1 and E2 in the N-terminal region, and the nonstructural proteins (NS) p7, NS2, NS3, NS4A, NS4B, NS5A, and NS5B in the C-terminal region (Fig. 1-5). The structural proteins are required for genome packaging and cell fusion, whereas the NS proteins are mainly responsible for host cell interactions, virus replication and assembly. The individual functional proteins are processed co- and post-translational from the polyprotein by various cleavage events of host cell signalases and two viral proteinases (21).

Cleavage at the junctions between C/E1, E1/E2, E2/p7, and p7/NS2 is mediated by the ER resident cellular enzyme signal peptidase. An additional processing step, mediated by the cellular enzyme signal peptide peptidase, removes the El signal sequence from the C-terminus of core, leading to mature core protein (190). In genotype 1a, processing at the E2/p7 and p7/NS2 junctions is incomplete or inefficient and leads to the presence of uncleaved E2/p7/NS2

protein (40, 197).

Processing in the NS region of the polyprotein is mediated by two virus-encoded proteases. The NS2 cystein protease cleaves at the NS2/3 junction, and the NS3 serine protease(84, 182), which utilizes NS4A as a cofactor for efficient processing at the 3/4A, 4A/4B, 4B/5A, and 5A/5B sites.

In addition to these structural and NS proteins, the large ORF encodes for small proteins of unknown function in the +1 frame of the core gene (33). ARFP/F (frame shift), ARFP/DF (double frame shift), or ARFP/S (short form) are most likely produced by a ribosomal frame shift, although alternate translational initiation sites may also be involved (18, 33, 281).

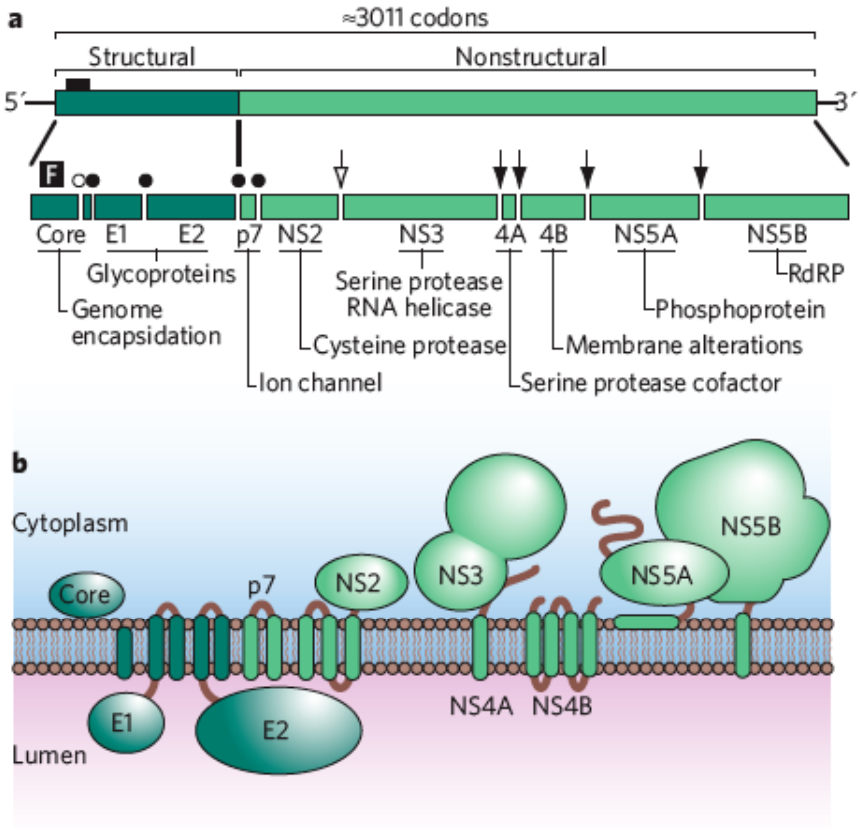

Fig. 1-5. HCV genes and products. a. Structure of the viral genome, including the long open reading frame encoding structural and NS genes, 5' and 3' NTRs. The polyprotein processing scheme is shown below. Closed circles refer to signal peptidase cleavage sites; the open circle refers to the signal peptide peptidase cleavage site. **b.** The topology of HCV proteins is shown with respect to a cellular membrane (154).

7.14 RNA replication

In vivo data shows that RNA replication occurs in the liver, as well as in PBMC's. Subgenomic replicon-bearing cells produce a 1000 to 1 molar ratio of viral proteins to viral RNA (234). Translation and RNA replication are highly regulated processes since they proceed in opposite directions on a given RNA template. There have been a couple of HCV regulators described such as the La protein or PTB that modulate IRES activity by binding to the 5' NCR and core region while binding to the 3' end represses replication (6, 13, 109, 271, 275). It is thought that low levels of HCV core protein can enhance HCV IRES-mediated translation, while high concentrations inhibit translation (29, 313).

The site of RNA replication is a membrane-associated complex, the replicase complex. RNA associates with perinuclear matrix of ~85 nm vesicles called the "membranous web" that is most likely derived from the rough ER and induced by HCV NS4B expression (63, 64, 83, 202, 205, 230). A large excess number of viral non-structural proteins can be found in active replicase complexes, which include a channel for NTP exchange with nascent RNA and pyrophosphate (234). Formation of a replicase complex associated with intracellular membranes and cellular proteins is typical for plus-strand RNA viruses like Polio or flaviviruses. The error rate of the NS5B, the RNA dependent RNA polymerase generates a vast amount of virus variants that help the virus to evade the immune system, as well as drug treatments.

HCV replication also induces the expression of other genes involved in lipid metabolism like ATP citrate lyase and acetyl-CoA synthetase and is stimulated by saturated fatty acids, while polyunsaturated fatty acids inhibit replication (122, 259).

HCV RNA replication initiates with the synthesis of a genome-length negative-strand RNA that serves as a template for nascent positive-strand synthesis with a ratio ten positive-strands per negative strand (5, 142, 165, 196, 234).

7.15 Virion Assembly and Secretion

The assembly of viral structural proteins and RNA into new virus particles is still largely unanswered. Initiation of virion assembly is thought to take place on the cytosolic site of the ER at lipid droplets (LDs) and requires at least viral genomes from the site of replication in the membranous web, and translated HCV core protein (316). The preferred binding for core-RNA interactions seems to be the 5' half of the HCV genome that selects for plus strand RNA. Mature core contains two distinct domains (D1 and D2) where N-terminal hydrophobic residues of the D2 domain are responsible for core-LD association and also virus release (81, 83, 136, 180, 274), while the hydrophobic C-terminus of core was reported to interact with the TM domain of E1 (159, 174).

It is thought that NS5A is involved in the process of transporting the replicase complex (RC) to the site of assembly, to facilitate the viral RNA and core interactions. Further, NS proteins, essential for assembly, are also recruited to the surface of LDs (89, 140, 274). Core could induce LD clustering at the periphery of the nucleus and therefore concentrate core-coated LDs in proximity of replicase complexes (220, 257). Otherwise, RCs could simple be transported on the microtubule network, mediated by NS3 and NS5A interactions with tubulin and actin (48).

The process of recruiting and transportation of all assembly factors still remains unclear and there is no evidence for specific signal sequences or packaging motifs. Packaging may occur rather through protein-protein than protein-RNA interactions. Nucleocapsids acquire their viral envelope by budding into the ER membrane, where the HCV envelope proteins are retained.

The maturation process is believed to take place along transportation of the virions in the very low-density lipoprotein (VLDL) assembly pathway (213), a lipid release pathway in hepatocytes. VLDL components can also be found in RCs and NS5A-apoE interactions have also been detected (97, 190) and an NS5A-apoE within RCs could facilitate the transport of lipoprotein to lipid droplets coated with core for virion assembly. Circulating virus particles form complexes with VLDLs that are called LVPs. Intracellular and extracellular infectious particles differ by their buoyant densities where circulating particles display lower densities (10, 138, 145, 150, 158, 176, 286). LVPs contain the core protein, viral RNA, VLDL structural elements apoB and apoE and are rich on triglycerides (138, 160) but it still remains unclear what role VLDL factors play in the release of infectious HCV virus. HCV is not restricted to the VLDL pathway as the endosomal sorting complex required for transport (ESCRT) has also been identified to be involved in particle egress (115, 175). Transport of the newly assembled virions is thought to

occur along compartments of these secretory pathways, followed by release of the particles from the cell (Fig. 1-6).

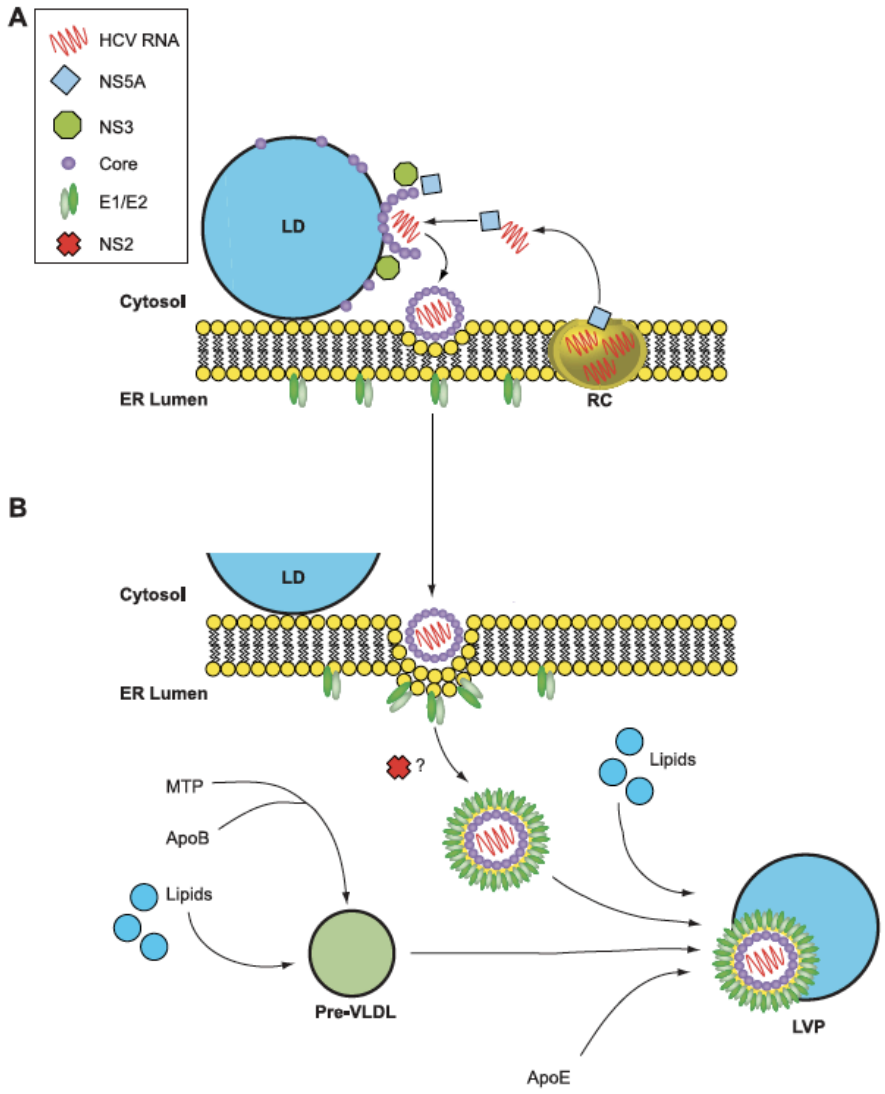

Fig. 1-6. Model for HCV virion assembly. Assembly is thought to initiate on the cytosolic side of the ER membrane (A), and complete maturation occurs in the ER lumen (B) prior to release from the cell. **A**. In early steps of assembly, core protein is targeted to LDs, where it coats the organelle surface. Viral RCs are recruited to LD surfaces in a core- and NS5A-dependent manner. Replicated RNA is transferred from RCs for association with core to permit encapsidation of the genome. NS3 is then required for the formation of fast-sedimenting core-containing particles, which are presumed to represent non-infectious virions that will undergo further stages of maturation. **B**. Late assembly steps involve the acquisition of a lipid envelope and the incorporation of the E1 and E2 glycoproteins into virions. NS2 confers infectivity to virions, possibly by mediating an interaction between glycoprotein complexes (E1 and E2) and immature particles. During maturation, nascent virus particles combine with pre-VLDLs (produced by initial lipidation

of apoB by MTP), lipids in the form of lumenal LDs, and other lipoprotein components such as apoE to generate LVPs. The role of p7 in this model remains unclear (116).

7.16 Structure and genomic organization

7.16.1 Structure of virions

Analysis of particles isolated from patient sera demonstrated that the size of infectious virus was between 30 and 80 nm, whereas virions from HCVcc showed 50 nm in diameter (32, 94). There is considerable heterogeneity between different clinical samples, and many factors can affect the behavior of particles containing HCV RNA (101, 269, 291).

The infectivity of the enveloped virus can be destroyed by chloroform treatment (31, 73). The buoyant density is very low with 1.10 g/ml compared to other enveloped RNA viruses (*flavivirus* >1.2 g/ml) measured in sucrose gradients (30). Interestingly, less infectious samples seem to present an increased buoyant density, at least in acute phase chimpanzee serum (101). Production of non-enveloped nucleocapsids and the binding to immunoglobulin may account for the heterogeneity (12, 101, 121, 181, 270) as well as delipidation of particles with a diameter of only 33 nm.

7.16.2 Features of HCV proteins

7.16.3 Structural proteins

The core, E1 and E2 proteins are major constituents of the virus particle required for genome packaging (core), attachment of the virus to its target cell (E2) and the fusion into the cytoplasm (E1 or E2). Core assembles into multimers and interacts with viral RNA to form the nucleocapsid, while E1 and E2 are retained in the ER and form non-covalent heterodimers through determinants in their TM domains. (154)

7.16.3.1 Core protein

The core or capsid protein is a highly conserved basic protein. Different sizes have been observed, from a 19 to 23 kDa. Core protein undergoes multiple processing events upon translation. The C protein consists of three-domains: a hydrophilic approximately 120 aa N-terminal domain followed by a approximately 50 aa hydrophobic domain and a approximately 20 aa membrane anchor (fields 81,110). The core C-terminus is cleaved by host signal peptidase; to produce a 23 kDa membrane anchored form that serves as a signal peptide to translocate E1 into the ER (99). Subsequent signal peptide peptidase cleavage occurs within the C-terminal membrane anchor around residue 173 to 182 to form a 21 kDa mature form (107, 156, 190, 201, 215, 216, 241).

The C protein associates with membranes, particularly the cytoplasmic surface of the ER (101, 200, 201) and has been shown to interact with the 5´ NCR, inhibit IRES function (71, 249, 264) and to mediate dimerization of the 3´-terminal 98 nt (52). It is essential for virus assembly and accumulates at the surface of LDs that are also the unique morphological feature of non-hepatic cells transfected with core (16). Non-specific RNA binding, multimerization and interaction with E1 has been observed for the C protein (108, 159, 174, 241), however, no direct interaction with E2 has been shown so far.

In addition the core protein co-localizes with apolipoprotein AII at the surface of the LDs. Analysis of liver biopsies from chronically HCV-infected chimpanzees revealed that HCV core is cytoplasmic and localized on the ER and on LDs (16). Core is essential for virus assembly, but has been described to be involved in other cellular pathways like altered signaling, cellular transformation, and transcriptional control (189, 267).

7.16.3.2 Envelope Proteins E1 and E2

The HCV envelope proteins E1 (31-35 kDa) and E2 (70 kDa) mediate virus attachment and fusion during entry and are glycoproteins containing type I C-terminal TM anchors, which are heavily modified by N-linked glycosylation and contain multiple disulfide-linked cysteines. E1 folds slowly, whereas folding of E2 occurs rapidly (54, 61). E1 interacts non-covalently with the membrane-proximal domain of E2 to form E1E2 heterodimeric complexes (61, 221, 306). The

ectodomains of both E1 and E2 containing several disulfide bonds are translocated into the lumen of the ER, and are modified by N-linked glycosylation (21). El and E2 have been shown to be retained within the lumen of the ER (46, 49) and signals for ER retention have been mapped to the TM domains of both glycoproteins (49, 74). Both proteins are cleaved of the polyprotein by cellular peptide peptidase.

Calnexin, calreticulin, and immunoglobulin binding protein (BiP) have been shown to interact with E1 and E2 for maturation (45, 60).

E1 residues 264 to 290 bear similarity to suspected or known fusion peptides from *Flavivirus* and *paramyxovirus* glycoproteins and may thus perform an analogous function during HCV entry (152).

E2 contains two hypervariable regions, (HVR1 and HVR2), where HVR1 at the N-terminus is the major antigenic determinant of neutralizing antibody response. Early induction of HVR1 specific antibodies correlates with clearance and can protect chimpanzees from infection (7, 72, 322).

The ectodomain of E2 binds to the human tetraspanin-family cell surface membrane protein CD81 (231), an interaction that appears to involve a conformationally sensitive region of E2 and an extracellular subdomain of CD81. This interaction is supposed to play a key role in HCV binding and entry, since infectivity can be neutralized by E2 reactive antibodies (152).

7.16.4 NS proteins

7.16.4.1 p7 protein

The hydrophobic p7 protein (7 kDa) adopts a double membrane-spanning topology and is a member of a small protein family of viroporins that enhance membrane permeability forming ion channels (89, 222). The viroporins are believed to be required for the late steps in virus assembly. *In vitro* assays show that p7 can multimerize and form cation-conductive membrane channels that can be inhibited by amantadine, iminosugar derivatives, and hexamethylene amiloride (89, 222, 233).

P7 is not necessary for RNA replication but essential for infectious virus production (165, 240) and can be localized at the ER and mitochondrial membranes (88, 90).

7.16.4.2 NS2 protein

NS2 (23 kDa) is a hydrophobic protein containing several TM segments in the N-terminal half. One to four TM segments have been proposed and recent data suggest that NS2 contains three TM domains, with a fourth region close to the membrane in the cytosol in close proximity to NS3. The C-terminal half of NS2 and the N-terminal third of NS2 form the NS2/NS3 protease (84, 101). The N-terminus is cleaved by signal peptide peptidase and is oriented towards the ER lumen whereas the C-terminus processed by the NS2/NS3 protease.

NS2-3 processing is inhibited by metal chelators and stimulated by zinc (84, 101). This led to speculation that the enzyme might be a metalloprotease. Limiting zinc could indirectly inhibit NS2-3 cleavage by affecting NS3 folding (278), and mutations in zinc-coordinating residues in NS3 were shown to inhibit NS2-3 protease activity (85, 101).

Identification of conserved residues at the C-terminus in NS2 required for proteolysis (His 143, Glu 163 and Cys 184) (85, 101), and comparison with other classes of viral proteases gave evidence that NS2-3 might be a cysteine protease that cleaves at the NS2/3 junction (85, 99, 167, 218, 268). NS2 is not required for replication of subgenomic replicons, which span NS3 to NS5B (164). However, cleavage at the NS2-3 junction is necessary in chimpanzees (133), full-length replicon system (292), and tissue culture (55, 114). Uncleaved NS2-3 retains serine protease activity and it rapidly degraded by the proteasome (85, 99, 293).

In vitro studies showed, that purified protein can efficiently reproduce processing at the NS2/3 site in the absence of additional cofactors (218, 268). The minimal region for in vitro cleavage at the NS2-3 junction required amino acid residues 94 to 217 of NS2 and residues 1 to 181 of NS3. Size-exclusion chromatography and a dependence of the processing rate on the concentration of truncated NS2/3 suggested a functional multimerization of the precursor protein. Although cleavage can occur in vitro in the absence of microsomal membranes, synthesis of the polyprotein precursor in the presence of membranes greatly increases processing at this site (242).

NS2 has been shown to interact with E2 and other NS proteins (58, 126, 155, 236, 246). Cellular protein interactions with NS2 include the cellular pro-apoptotic molecule CIDE-B that is inhibited upon NS2 binding and the down-regulation of cellular transcription (62, 66). NS2 can be phosphorylated at the conserved residue Ser 977 (Ser 168) by casein kinase 2, leading to the rapid degradation of NS2 by the proteasome (78).

Cyclosporine A (CsA) inhibits HCV RNA replication in an NS2 dependent way, mediated through cellular cyclophilin A. NS2 may act as a secondary target to CsA dependent inhibition or modulates the anti-viral activity against NS3 to NS5B (47).

NS2 is essential for infectious virus production. Interestingly chimeric HCVcc genomes when fused together after the first and the second TM domain of NS2 produce the highest amount of infectious virus (228).

7.16.4.2.1 Structure of NS2 Protease Domain

More recently, we solved the crystal structure of the protease domain of NS2 ($NS2^{pro}$, residues 94 to 217). The protein was recombinantly expressed in bacteria and purified to homogeneity in the presence of detergents. $NS2^{pro}$ consists of two subdomains connected by an extend linker to form a dimeric structure (Fig. 1-7). In the N-terminal subdomain, two anti-parallel α-helices (H1 + H2) are connected by a short loop. These helices are followed by a random-coil conformation that contacts both H1 and H2. The protein continues into a long, extended coil before entering an anti-parallel β-sheet in the C-terminal subdomain. The last β strand continues to the C-terminal residue, leucine 217.

7.16.4.2.2 Catalytic Mechanism of NS2^{pro}

The crystal structure of NS2^{pro} demonstrated that the protein is a dimeric cysteine protease containing two composite active sites (Fig. 1-7) (167). For each active site, the catalytic histidine and glutamate residues are contributed by one monomer and the nucleophilic cysteine by the other. After cleavage, the C-terminus remains bound to the active site, thereby preventing further proteolysis by the same active site (Fig. 1-8). Thus, each molecule can mediate a single cleavage. The geometry at the active site of NS2^{pro} is similar to other viral and cellular cysteine and serine proteases like poliovirus 3Cpro, Sindbis virus capsid, subtilisin, and papain suggesting that the composite active site formed by NS2^{pro} dimerization is competent for catalysis (167).

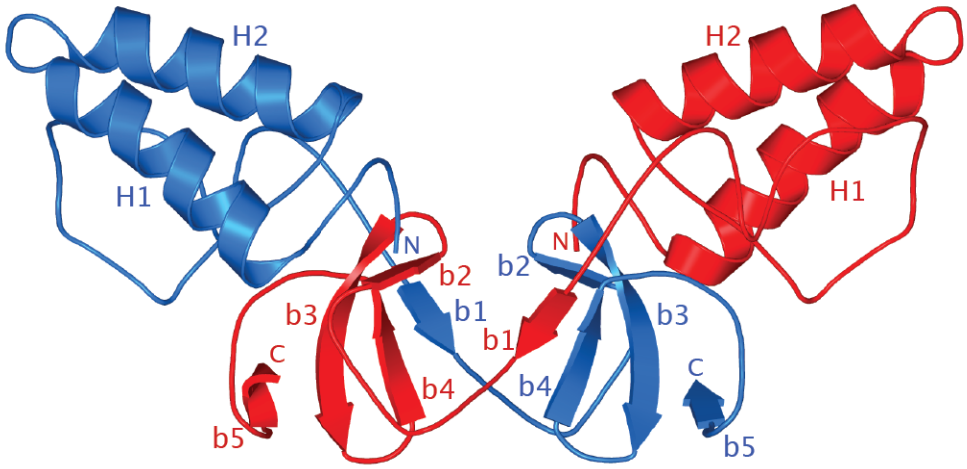

Fig. 1-7. Crystal structure of HCV NS2. NS2 is a dimer in the form of a 'butterfly'. Each monomer contains two subdomains connected by an extended linker arm. One monomer is drawn in blue, while the second monomer is shown in red. H1 and H2 denote helices 1 and 2, respectively. N, N-terminus; C, C-terminus (167).

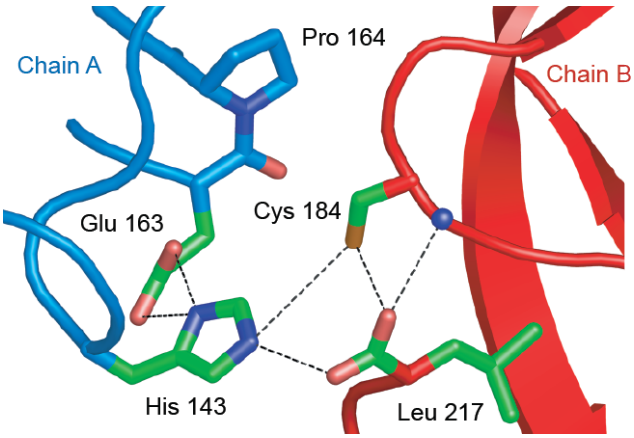

Fig. 1-8. HCV NS2 active site. Chain A is shown in blue, while the second chain is shown in red. His 143 and Glu 163 are contributed by one monomer, whereas Cys 184 originates from the other monomer. The C-terminal residue of NS2, Leu 217 is coordinated to the active site, blocking access of other substrates to the active site. Dashed lines indicate contacts between catalytic residues and the C-terminus. The carboxylic acid of Leu 217 contacts the side chains of the catalytic triad (His 143 and Cys 184) and the backbone nitrogen of Cys 184. Pro 164, which lies adjacent to the active site, has a *cis*-peptide conformation.

7.16.4.2.3 A cis-Proline residue near the Active Site of NS2^{pro}

The conserved Pro 164 (HCV and GB), which is adjacent to Glu 163 of the catalytic triad, has a *cis*-peptide conformation with the pyrrolidine ring lying on the same side as the carbonyl group of Glu 163. The proximity of Pro 164 to Glu 163 may bend the peptide backbone to establish the correct geometry of the glutamate side chain for catalysis. Moreover, the cis-proline confirmation is thought to contribute to dimer stabilization since the linker that connects the two subdomains follows Pro 164.

7.16.4.2.4 Membrane association of NS2

The NS2 amino terminus is generated by signal peptidase in the lumen of the ER and several additional TM or membrane-associated segments precede the NS2 protease domain (21). Furthermore, NS2^{pro} possesses a hydrophobic N-terminal domain with several hydrophobic residues on the outside of helix H2. In addition, detergent molecules were co-crystallized with

NS2 interacted with helices H1 and H2. This suggests that the N-terminal end of helix H2 of each monomer might be inserted into a cellular membrane (fig. 1-9). In this model, helix H2 interacts with fatty acid tails of the membrane lipids, while basic residues in the N-terminal subdomain neutralize the polar head groups. Peripheral membrane association of helix H2 would place the amino termini of the two protein monomers in close proximity to the membrane (Fig. 1-9).

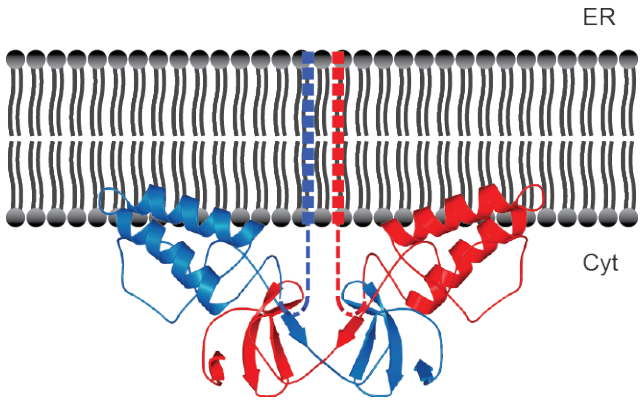

Fig. 1-9. Model for NS2 membrane association. Helix H2 of each monomer is peripherally inserted into the membrane. Dashed lines represent a putative TM segment upstream of the N-terminal end of $NS2^{pro}$ for each chain. The blue colour indicates monomer A, while monomer B is marked in red.

7.16.4.3 NS3 protein

The NS3 protein (~70 kDa) encodes a serine protease domain in the N-terminal one third of the protein, and an NTPase/helicase domain in the C-terminal two thirds (152) that are both essential for viral replication (21, 151).

NS3 in conjunction with NS2 cleaves at the NS2/3 junction to produce a free NS3 N-terminus. Then NS3 associates with the cofactor NS4A and coordinates ZN^{2+} to residues distal from the protease activity: Cys-1123, Cys-1125, Cys-1171, and His-1175 to process the polyprotein at downstream cleavage sites NS3/4A, NS4A/4B, NS4B/5A, and NS5A/5B (19, 70, 149).

The NS3 serine protease contains three active site residues His 1083, Asp 1107, and Ser 1165 and a substrate binding surface (17, 127, 168, 303).

In addition to its roles in HCV polyprotein processing and RNA replication, several other functions have been proposed for NS3. The NS3-4A serine protease activity antagonizes innate anti-viral defenses by blocking activation of the transcription factors IRF-3 and NF-κB (76, 77, 147).
Toll-like receptor 3 (TLR3), the recently identified cytosolic RNA helicases RIG-I (retinoic acid inducible gene I) and Mda5 (melanoma differentiation-associated gene 5) sense viral 'signatures' like double-stranded (ds) RNA. Then, through CARD domains, transcription factors interferon regulatory factor 3 (IRF3) and NF-κB are activated. The CARD-containing adaptor, called Cardif, was discovered that interacts with RIG-I (retinoic acid inducible gene-I) and recruits IKK, and IKK kinases by means of its C-terminal region, leading to the activation of NF-kB and IRF3. Cardif is targeted and inactivated by NS3-4A, the serine protease from HCV known to block interferon-β production. Disruption of this signaling pathway by HCV might provide a foundation for viral persistence (113, 194).

NS3 has been shown to unwind RNA and DNA homo- and heteroduplexes by binding to an unpaired region of a template strand and translocating in a 3´ to 5´ direction (21). The RNA helicase at the C-terminus of NS3 most likely serves to unwind RNA secondary structures, presumably during RNA replication and viral activity (132, 141).

A number of cellular and viral interacting proteins have been described for NS3 (146, 161, 179, 247).

7.16.4.4 NS4A protein

The NS4A protein (~8 kDa) is a cofactor of the NS3/4A serine protease activity, critical for all serine protease dependent cleavages except NS5A/5B. NS4A facilitates the recognition of RNA by the NS3 protease/helicase (219). It associates with membranes, probably through the hydrophobic N-terminal region, and interacts with other replicase components, such as NS3, NS4A, NS4B, and NS5B (299). The C-terminal region is involved in NS5A hyperphosphorylation (120, 130).

7.16.4.5 NS4B protein

The NS4B protein (~30 kDa) contains four TM domains (65, 106, 171). NS4B organizes primarily the replication process in a specialized membrane compartment, the membranous web (63, 83, 106), and reduces ER to Golgi traffic, induces ER stress mediated protein unfolding, inhibits protein synthesis, and causes cythopathic effect (75, 106, 123, 134, 318). A set of highly adaptive mutations was found in NS4B, suggesting an important role of NS4B for HCV replication (164).

7.16.4.6 NS5A protein

NS5A is a hydrophilic protein that exists in at least two forms with apparent molecular masses of 56 and 58 kDa due to differential phosphorylation (101). It is membrane-anchored via an N-terminal, amphipathic helix and localizes to active replication complexes (34, 83, 202). NS5A is an active component of the HCV replicase, as well as a pivotal regulator of replication and a modulator of cellular processes ranging from innate immunity to dysregulated cell growth (reviewed in (154). Pharmacologic inhibition of NS5A hyperphosphorylation increases RNA replication (212).

NS5A is organized into three domains: The N-terminal domain (domain I) coordinates a single zinc atom per protein molecule and the predicted binding motif consists of four cysteine residues (266). These are conserved among the *Hepacivirus* and *Pestivirus* genera. Mutations disrupting either the membrane anchor or zinc binding of NS5A are lethal for RNA replication (266). NS5A contains large number of cell culture-adaptive mutations in the replicon system, suggesting that it may play a role in RNA replication (26, 28). The crystal structure of domain I, revealed a novel and different fold, a new zinc-coordination motif and an unusual disulphide bond (150). Little is known about domain two and domain three is poorly conserved and tolerant to deletions and insertions (14, 105, 157, 186). NS5A Domain I is responsible for interactions with LDs and the association of other NS proteins and viral RNA (195). Association of replicase complexes with LDs occurs in a core- and NS5A-dependent manner (184, 265).

An interaction between NS5A and the human vesicle-associated membrane protein-associated protein A (hVAP-A), a cellular target N-ethylmaleimide-sensitive factor attachment protein receptor, required for efficient RNA replication was discovered. (67). NS5A mutations that block the interaction with hVAP-A reduce HCV RNA replication. Additional analyses revealed an inverse correlation between NS5A phosphorylation and hVAP-A interaction.

NS5A has been reported to be involved in resistance to interferon treatment (151), oxidative stress, activation of signalling pathways (STAT-3, PI3K, and NF-kB), and transcriptional regulation (92, 96, 258).

7.16.4.7 NS5B protein

The NS5B protein (~68 kDa) is the viral RNA-dependent RNA polymerase (RdRP) and has a “right hand” structure, with distinct finger, palm, and thumb domains (4, 35, 144) where RNA templates slide into a hydrophilic groove within the finger domain (128, 214). The overall structure of NS5B is remarkably similar to the RdRP of bacteriophage phi6 (37), and co-crystallization of these enzymes with model substrates and nucleoside triphosphates has yielded a credible model for de novo initiation.(279). The enzyme forms the catalytic center of a highly ordered replication complex composed of viral and cellular factors that interact on a membranous scaffold to multiply the HCV genome and is a major target for development of HCV-specific antivirals. NS5B is tethered to membranes by a C-terminal peptide anchor and

interacts with itself to form higher-order RdRP complexes that may have functional relevance to the membrane bound replicase (110, 153, 244).

NS5B has been shown to elongate annealed primers or self-priming templates (25, 163, 166, 302, 310) and uses divalent cations Mg+ or Mn+ to catalyze nucleotide incorporation for RN synthesis (521,656) although in vivo, HCV RNA synthesis is thought to initiate de novo, i.e. without a primer (172, 235, 248, 321). NTP analogs containing 2'C-methyl groups are potent inhibitors of HCV by terminating RdRP, but confer easily resistance (53). RdRP activity is also modulated by interaction with other NS proteins like NS3 that enhances RNA synthesis, or NS4B and NS5A that inhibit RNA synthesis activity (227, 250).

Various host factors have been identified to bind NS5B such as proline *cis-trans* isomerase cyclophilin B that is critical for RNA replication (290), serine kinase PRK2 that enhances replication or cyclophilin B that is inhibited by CsA, which inhibits HCV replication (128, 289).

7.16.4.8 F protein

HCV encodes an additional protein, called F (frame shift) or ARF-protein, with a molecular weight of 17 kDa. However, no function has been associated to F/ARF yet. Translation initiates at the core gene, but ribosomes shift into an alternative reading frame to produce an eleventh polypeptide (33).

7.17 Objectives

NS2, one of two viral proteases had been described to be essential for NS2/3 cleavage, but abundant for RNA replication. The $NS2^{pro}$ crystal structure predicted the necessity of an NS2 dimer to mediate cleavage.

Our first objective was to demonstrate the presence of dimeric or oligomeric NS2. Via crosslinking and FRET assays, we were able to show the dimeric form of NS2. Further, several mutations around the active site (Y141A, P164A/G) revealed a lack of dimerization, which explained their cleavage deficiency.

Further, we wanted to identify possible additional functions of the NS2 protease in NS2/3 cleavage and infectious virus production by a comprehensive analysis of $NS2^{pro}$ residues. We found that the residues around the active site are mainly involved in NS2/3 cleavage events and dimerization while the crossover region, and the C-terminal region are mostly important for infectious particle production. The C-terminal requires a leucine as deletions or substitutions of this residue resulted in inhibited infectious virus production. Additional residues attached to the NS2 C-terminus were not tolerated for infectious particle production. We also demonstrated that the minimal required length of NS3 residues that was thought to be 181 aa is not necessary as a 31 residue construct already illustrated protease activity. A secondary aim was to identify and characterize the role(s) of the NS2/3 cleavage site, focusing on the C-terminal amino acids of NS2 and the four N-terminal NS3 residues. We identified an essential function in infectious virus production for several residues in addition to their function in NS2/3 cleavage.

The last aim was to identify NS2 interacting host proteins, as well as characterizing viral protein interactions to create an NS2 network map. We build an NS2-NS3 interaction model, and identified several residues potentially important in their interactions. We were also able to establish genetic evidence for NS2 interactions with E2 and NS3, which could be confirmed by NS2 strep tagged pull downs and mass spectrometry. In addition, mass spectrometry identified numerous host cell proteins involved in NS2 functions.

8 Chapter 2: Material and Methods

Plasmid constructs. Mono- and bicistronic genomes were generated by standard molecular biology techniques and verified by restriction enzyme digestion and sequencing of PCR-amplified segments. Descriptions of the cloning strategies are provided below.

(i) J6/H77NS2/JFH and mutant derivatives. J6/H77NS2/JFH constructs contain genotype 2a (J6) from core to p7, genotype 1a (H77) NS2 and genotype 2a (JFH) NS3 to NS5B. To create this construct the plasmid J6/JFH (17) was used as template to PCR amplify the J6/JFH E2 3' end through p7 sequence with forward oligo RU-O-5739 (5' - CCGCCTTGTCGACTGGTC) and reverse oligo RU-O-5855 (5' - CTCCGTGTCCAacGC gTAAGCCTGTTGGGGC). The H77 NS2 through half of JFH-1 NS3 region was PCR amplified from H77/JFH (17) with the forward oligo RU-O-5854 (5' - CAGGCTTAcGCg tTGGACACGGAGGTGGCC) and reverse oligo RU-O-5721 (5' - GCTACCGAGGGGTTAAGCACT). Since these PCR products overlap at the p7/NS2 junction, they were used as template in a second round of PCR with the outside oligos RU-O-5855 and RU-O-5721 to generate a PCR product encoding the J6 E2 C-terminal region though p7, the H77 NS2, and JFH-1 NS3 N-terminal region. This product was digested with restriction endonucleases BsaBI and AvrII and ligated into the BsaBI/AvrII digested J6/JFH plasmid, to create the final J6/H77NS2/JFH plasmid. An adaptive change at G1145A (chimeric genome numbering) encoding substitution A269T (chimeric polyprotein numbering) was found to increase infectious virus titers of J6/H77NS2/JFH, and was included in all J6/H77NS2/JFH-based genomes constructed. Mutant derivatives of J6/H77NS2/JFH were created by site directed mutagenesis using the AfeI/BbvCI restriction sites.

(ii) J6/H77NS2/JFH(NS2-IRES-NS3) and mutant derivatives. J6/H77NS2/JFH(NS2-IRES-NS3) encodes a stop codon after NS2, an EMCV IRES, a start codon, and the remainder of the JFH-1 polyprotein starting with NS3. Mutant derivatives of J6/H77NS2/JFH(NS2-IRES-NS3) were created by site directed mutagenesis using the PmeI/MluI restriction sites.

(iii) J6/H77NS2/JFH(NS2-IRES-nsGluc2AUbi) and mutant derivatives. J6/H77NS2/JFH(NS2-IRES-nsGluc2AUbi) is similar to J6/H77NS2/JFH(NS2-IRES-NS3) but encodes a *Gaussia* luciferase gene followed by the foot and mouth disease virus 2A peptide and a ubiquitin monomer (nsGluc2AUbi cassette) between the EMCV IRES and NS3 (13). The N-terminal signal sequence of *Gaussia* luciferase has been deleted so that the reporter is not secreted.

Mutant derivatives of J6/H77NS2/JFH(NS2-IRES-nsGluc2AUbi) were created by site directed mutagenesis using the PmeI/MluI restriction sites. NS2 extensions into NS3 were subcloned using BbvCI/SpeI/KpnI restriction sites.

(iiii) Jc1(5'C19nsGluc2AUbi) was subcloned using a *Gaussia* luciferase construct J6/JFH(5'C19Gluc2AUbi) (274) as backbone while inserting the BsaBI/BbvCI fragment from Jc1. Monocistronic mutant derivatives were created by site directed mutagenesis using the same BsaBI/BbvCI restrictions sites.

(iiiii) Jc1(NS2-IRES-nsGluc2AUbi) was created by site directed mutagenesis inserting a stop codon and a PmeI site into Jc1, which was then digested with BsaBI/PmeI and inserted into the opened vector J6/JFH(NS2-IRES-nsGluc2AUbi) (114). Bicistronic mutant derivatives were created by site directed mutagenesis using NotI/SpeI restrictions sites.

(iiiiii) The FRET pair constructs pCMV-p7-NS2-NS3 and derivatives (Venus/Cerulean and mCherry/sGFP) were created by site directed mutagenesis using the BamHI/HindIII cloning sites.

(iiiiiii) Jc1 NS2 OST-tag was created using site directed mutagenesis and a Jc1 J6/JFH backbone. The PCR fragment were digested with NotI/BsaBI and ligated into the opened Jc1 vector.

Cell culture. Huh-7.5 cells were cultured in Dulbecco's modified Eagle medium (Invitrogen) supplemented with 0.1 mM non-essential amino acids and 10% fetal bovine serum (complete medium). Cells were grown at 37 °C in 5% CO_2.

vTF7-3 Vaccinia Helper Virus Infection. Huh-7.5 cells were seeded in 6-well plates at a density of 2.5 to 5 x 10^5 cells per well. The number of cells approximately doubled overnight. On the following day, the amount of vTF7-3 vaccinia helper virus required for the desired m.o.i. was calculated, and the virus stock was diluted in PBS 1% FCS. Cells were washed once with PBS. The virus dilution in PBS was added, and the cells were incubated at 37 °C / 5% CO_2 with gentle rocking for 1 h. After the incubation, the inoculum was removed, and cells were washed

once with PBS. Complete medium was added, and cells were transfected with plasmid DNA (see below), followed by incubation at 37 °C / 5% CO_2.

DNA transfection. DNA was diluted into serum-free medium (SFM) in a microfuge tube (1.5 µg DNA in 100 ml SFM per well for a 6-well plate). In a separate tube, 7 µl Lipofectamine 2000 were diluted in 100 µl SFM per well for a 6-well plate. The two solutions were mixed and incubated for 20 min at room temperature. Cells previously infected with vTF7-3 vaccinia helper virus were washed once with PBS, and fresh complete medium was added. Finally, the DNA:lipid complex solution was added to the cells.

***In vitro* crosslinking.** A dilution series of crosslinker was prepared, corresponding to a 0.5x to 50x molar ratio of crosslinker:protein. 2 µl of each crosslinker dilution were added to 18 µl purified NS2 protein, followed by incubation at room temperature in the dark for 90 min. After adding 2x SDS loading buffer, the samples were separated by SDS-PAGE. Proteins were visualized by staining of the gel with Coomassie Blue solution.

***In vivo* crosslinking.** 16 to 18 h post-transfection, crosslinking solution was added, followed by incubation of the cells on ice for 30 min. Two different crosslinking methods were used: addition of crosslinker either before or after lysis of the cells. Depending on the properties of the crosslinker and the lysis buffer used (CHAPS Triton X-100 or SDS).

Crosslinking before lysis: Cells were washed once with cold PBS, followed by addition of 500 µl Crosslinker/PBS solution per well. After incubation on ice for 30 min, the crosslinker was removed and 300 µl PBS/glycine (final glycine concentration: 50 mM) was added to quench the excess crosslinker. After a 5-min incubation on ice, 200 µl SDS lysis buffer was added. Cells were scraped and passed 10 times through a $26^{1/2}$ G needle to shear genomic DNA and transferred to a 1.5 ml microfuge tube. The lysates were either immediately tested by SDS-PAGE and immunoblot, or stored at -20 °C.

Crosslinking during lysis: After cells were washed with cold PBS, 150 µl lysis buffer/crosslinking solution containing crosslinker and 2% CHAPS was added and incubated for 5 min on ice. The cells were scraped, transferred to 1.5 ml microfuge tubes and incubated on ice for 30 min. Subsequently, glycine was added to a final concentration of 50 mM to stop the crosslinking reaction. After incubation on ice for 5 min, lysates were centrifuged at 1500 x g (5000 rpm) for

10 min at 4 °C. The lysates were either immediately tested by SDS-PAGE and immunoblot, or stored at -20 °C.

FRET analysis. Huh-7.5 cells were plated on glass-bottomed dishes (MatTek) and DNA constructs were transfected with a total of 2 µg DNA (1 µg NS2-Venus, and 1 µg NS2-Cerulean) using lipofectamine 2000. Cells were imaged 12-16 h after transfection, without fixation. TIR-FM was performed with cells immersed in CIM and using an inverted Olympus IX-70 microscope equipped with an APO 60x, N.A. 1.49 TIR objective (Olympus Scientific) and a 12-bit cooled CCD camera (ORCAER; Hamamatsu Photonics, Hamamatsu), as previously described (Nolvenn ref 19). The microscope was enclosed in a chamber and all imaging was performed at 37 °C. eGFP was excited with the 488-nm line of an argon laser (Omnichrome; Melles Griot) reflected off a dichroic beamsplitter (z488rdc) while mCherry was excited with the 587-nm laser (model 05-LGR-193, Melles Griot) reflected off a 488/587 polychroic mirror. All mirrors and filters were obtained from Chroma Technologies Corp (118).

The camera and shutters were controlled using MetaMorph software (Molecular Devices), which was also used for all data analyses. For measuring the intensity of fluorescent puncta, a region was drawn around an area of interest of 10 x 10 pixels and the maximum intensity within this region recorded. We measured a bleedthrough from CFP into YFP of about 60% for the Venus/Cerulean FRET pair, while the eGFP/mCherry pair showed a bleedthrough into mCherry of about 15%. In total, three different regions were analyzed with 50 spots per cell to acquire representative data.

RNA transcription. In vitro transcripts were generated as previously described (17). Briefly, plasmid DNA was linearized by XbaI and purified by using a Minelute column (QIAGEN, Valencia, CA). RNA was transcribed from 1 µg of purified template by using the T7 Megascript kit (Ambion, Austin, TX) or the T7 RNA polymerase kit (Promega, Madison, WI). Reactions were incubated at 37 °C for 3 h, followed by a 15 min digestion with 3 U of DNase I (Ambion). RNA was purified by using an RNeasy kit (QIAGEN) with an additional on-column DNase treatment. RNA was quantified by absorbance at 260 nm and diluted to 0.5 µg/µl. Prior to storage at -80 °C, RNA integrity was determined by agarose gel electrophoresis and visualization by ethidium bromide staining.

RNA electroporation. Huh-7.5 cells were electroporated with RNA as previously described (17). Briefly, Huh-7.5 cells were treated with trypsin, washed twice with ice-cold RNase-free AccuGene phosphate-buffered saline (PBS; Bio-Whittaker, Rockland ME), and resuspended at 1.75 x 107 cells/ml in PBS. Then, 2 µg of each RNA was combined with 0.4 ml of cell suspension and immediately pulsed using a BTX ElectroSquare Porator ECM 830 (820 V, 99 µs, five pulses). Electroporated cells were incubated at room temperature for 10 min prior to resuspension in 15 ml or 30 ml complete medium for non-reporter and reporter constructs, respectively. Resuspended cells were plated into 24-well, 6-well and P100 tissue culture dishes.

Assays for RNA replication. At 4 or 8, 24, 48, and 72 h post-electroporation, cells in 24-well plates were washed with Dulbecco PBS (DPBS) and lysed by the addition of *Renilla* lysis buffer (Promega, Madison WI) or RLT buffer (QIAGEN) containing 10% ß-mercaptoethanol for assay of replication by luciferase activity or quantitative reverse transcription-PCR (qRT-PCR), respectively. For luciferase assays, lysates were thawed prior to addition of *Renilla* substrate (Promega) according to the manufacturer's instructions. The luciferase activity was measured by using a Berthold Centro LB 960 96-well luminometer. For qRT-PCR analysis, prior to storage at -80 °C, lysates were homogenized by centrifugation through a QiaShredder column (QIAGEN) for 2 min at 14,000 x g. Total RNA was isolated by RNeasy kit (QIAGEN) and quantified by determining the absorbance at 260 nm. A total of 50 ng of total cellular RNA was used per reaction. qRT-PCRs were performed on a LightCycler 480 (Roche, Basel Switzerland) using the LightCycler amplification kit (Roche) with primers directed against the viral 3' NTR. We assembled 20 µl reactions according to the manufacturer's instructions as previously described (13).

Assays for infectious virus production. At 4 or 8, 24, 48, and 72 h post-electroporation, the cell culture media was harvested and replaced with fresh complete medium. Harvested cell culture supernatants were clarified by using a 0.45-µm pore-size filter and stored in aliquots at -80 °C. For detection of infectious virus production by qRT-PCR or luciferase assay, naive cells were infected with clarified cell culture supernatants and incubated for 72 h prior to analysis. Determination of infectious virus production by limiting dilution assay was performed as described previously (13, 17). Briefly, clarified cell culture supernatants were serially diluted and used to infect approximately 3 x 103 cells plated in 96-well dishes. At 3 days post-infection, cells were washed with DPBS, fixed with ice-cold methanol, and stained for the presence of NS5A

expression as described previously. The 50% tissue culture infectious dose ($TCID_{50}$) was calculated using the Reed & Muench method (17).

Passaging for revertants. Jc1 reporter constructs were electroporated into Huh-7.5 cells and 72 h post-electroporation, supernatant was transferred to naïve Huh-7.5 cells. Cells were split upon confluency, passaged for a total of seven passages and samples of each passage were stored at -80 °C. Lysates were thawed prior to addition of Renilla substrate (Promega) according to the manufacturer's instructions. The luciferase activity was measured by using a Berthold Centro LB 960 96-well luminometer.

Reverse transcription (RT) PCR. For analysis of revertants and verification of infectious viruses, total RNA was isolated by RNeasy kit (QIAGEN) and quantified by determining the absorbance at 260 nm. A total of 2 ug of total cellular RNA was used per reaction of the SuperScript III First-Strand Synthesis System for RT-PCR (Invitrogen) according to the manufacturer's instructions with primers RU-5716 (5'-CTGCGGAACCGGTGAGTACAC-3'), RU-5927 (5'-CAAGGTCTCCCACTTTCAG-3'), RU-5999 (5'-GTGTACCTAGTGTGTGCCGCTCTACCACCEPTED 3'), and RU-6000 (5'-ATGCCGCTAATGAAGTTCCAC-3'). 1ul of the RT mix (RNA/primer/dNTP mix) was used to amplify the Jc1 genome using appropriate primers. The amplified fragments were then gel purified sequenced and analyzed for revertants or second site mutations.

Immunohistochemistry. Immunohistochemical detection of NS5A was performed as described previously (150). Briefly, cells were fixed with 100% methanol at 48 h post-electroporation, blocked for 1 h with PBS/0.2% milk/1.0% BSA/0.1% saponin, and incubated for 5 min with 3% hydrogen peroxide. After washing with PBS and PBS/0.1% saponin (PBSS), cells were incubated for 1 h at RT with 1:200 dilution of anti-NS5A mAb (9E10, ref 29). The secondary antibody, ImmunPress goat-anti-mouse peroxidase (Vector, Burlingame, CA), was diluted 1:10 and incubated for 30 min at RT. After washing, staining was developed with DAB substrate (Vector) for 5 min. Nuclei were counterstained with Hemotoxylin-2 (Sigma).

Titer by limiting dilution. Limiting dilution assay was performed as described previously (150). Briefly, clarified cell culture supernatants harvested at various time points post-electroporation were serially diluted an 50 ul of each dilution used to infect approximately 3x103 15 cells. At 72

h post-infection, cells were fixed and infected cells detected by immunohistostaining for NS5A. Fifty percent tissue culture infectious dose ($TCID_{50}$) was calculated (150).

SDS-PAGE and Immunoblot. Cells were lysed at 72 h post-electroporation with RLT buffer (QIAGEN) containing 1% ß-mercaptoethanol and homogenized by centrifugation through a QiaShredder column (QIAGEN) for 2 min at 14,000 x g. Lysates were separated by SDS-polyacrylamide gel electrophoresis (PAGE). After transfer to nitrocellulose membrane, blots were blocked for 1 h with 5% milk/PBS-T (phosphate buffered saline, 0.1% Tween). For NS2 detection, mAb 6H6 (1.0 mg/ml), was diluted 1:1000 in PBS-T. For NS5A detection mAb 9E10 (17) was diluted 1:1000 in PBS-T. For β-actin detection mouse-anti-β-actin mAb (Sigma, St Louis, MO) was diluted 1:20000 in PBS-T. After 1 h incubation at room temperature, and extensive washing with PBS-T, rabbit-anti-mouse immunoglobulin-horseradish peroxidase (HRP) secondary antibody (Pierce, Rockford, IL) was added at 1:10000 dilution in 5% milk/PBS-T for 45 min at RT. After additional washing, blots were developed with SuperSignal West Pico chemiluminescent substrate (Pierce).

Expression and pull-down of OST-tagged HCV proteins. *In vitro* transcribed HCV genomic RNA into Huh-7.5 cells for expression of One-STrEP-tag (OST; IBA, St. Louis MO) tagged NS2 proteins.

Lysates from ten P150 plates of electroporated cells were pooled and used for pull-down with Strep-Tactin resin (IBA) 72 h post-electroporation. The Strep-tactin Superflow resin was pre-washed, then incubated with the lysates for 2 h at 4 °C using the rotator. Following the incubation, samples were washed and after adding 30 µl 2x SDS loading buffer (Invitrogen) boiled at 90 °C for 5 min. The resin was then loaded on a 4-20% Bis-Tris gradient gel (Invitrogen). The gel was then stained with Colloidal Blue and sent to a mass spectrometry facility for analysis.

Analysis and evaluation of mass spectrometry hits. Three different databases were used to compare the acquired data from mass spectrometry: Swiss-prot., an HCV virus, and a human protein database (unconcrete). This data was inserted in a newly created database called ‘receptor’. Receptor allowed to apply different cut off values (Score: > 40 and Matches: > 2) to narrow down the list to only highly confident hits.

9 Chapter 3: Role of the NS2 protease domain in infectious particle production

9.1 Introduction

After publication of the $NS2^{pro}$ structure, we wanted to focus on the role(s) of the NS2 protein, and specifically the protease domain. We analyzed critical NS2 residues based on structural data and biophysical properties. We found that the NS2 protease domain is essential for virus production and that deleting or mutating the C-terminal residue, Leu 217 abolishes infectious virus production. The results were published in 2009 in the *Journal of Virology* with the title:

9.2 "Determinants of the Hepatitis C Virus non-structural protein 2 protease domain required for production of infectious virus" (Publication 1)

JOURNAL OF VIROLOGY, Dec. 2009, p. 12702–12713 Vol. 83, No. 24
0022-538X/09/$12.00 doi:10.1128/JVI.01184-09

Determinants of the Hepatitis C Virus Nonstructural Protein 2 Protease Domain Required for Production of Infectious Virus▽

Thomas G. Dentzer,[1,2] Ivo C. Lorenz,[1]† Matthew J. Evans,[1]‡ and Charles M. Rice[1]*

Center for the Study of Hepatitis C, Laboratory of Virology and Infectious Disease, The Rockefeller University, 1230 York Avenue, New York, New York 10065,[1] and Laboratoire de Rétrovirologie, Centre de Recherche Public-Santé, 84 rue Val Fleuri, Luxembourg L-1526, Luxembourg[2]

Received 9 June 2009/Accepted 28 September 2009

The hepatitis C virus (HCV) nonstructural protein 2 (NS2) is a dimeric multifunctional hydrophobic protein with an essential but poorly understood role in infectious virus production. We investigated the determinants of NS2 function in the HCV life cycle. On the basis of the crystal structure of the postcleavage form of the NS2 protease domain, we mutated conserved features and analyzed the effects of these changes on polyprotein processing, replication, and infectious virus production. We found that mutations around the protease active site inhibit viral RNA replication, likely by preventing NS2-3 cleavage. In contrast, alterations at the dimer interface or in the C-terminal region did not affect replication, NS2 stability, or NS2 protease activity but decreased infectious virus production. A comprehensive deletion and mutagenesis analysis of the C-terminal end of NS2 revealed the importance of its C-terminal leucine residue in infectious particle production. The crystal structure of the NS2 protease domain shows that this C-terminal leucine is locked in the active site, and mutation or deletion of this residue could therefore alter the conformation of NS2 and disrupt potential protein-protein interactions important for infectious particle production. These studies begin to dissect the residues of NS2 involved in its multiple essential roles in the HCV life cycle and suggest NS2 as a viable target for HCV-specific inhibitors.

An estimated 130 million people are infected with hepatitis C virus (HCV), the etiologic agent of non-A, non-B viral hepatitis. Transmission of the virus occurs primarily through blood or blood products. Acute infections are frequently asymptomatic, and 70 to 80% of the infected individuals are unable to eliminate the virus. Of the patients with HCV-induced chronic hepatitis, 15 to 30% progress to cirrhosis within years to decades after infection, and 3 to 4% of patients develop hepatocellular carcinoma (17). HCV infection is a leading cause of cirrhosis, end-stage liver disease, and liver transplantation in Europe and the United States (7), and reinfection after liver transplantation occurs almost universally. There is no vaccine available, and current HCV therapy of pegylated alpha interferon in combination with ribavirin leads to a sustained response in only about 50% of genotype 1-infected patients.

The positive-stranded RNA genome of HCV is about 9.6 kb in length and encodes a single open reading frame flanked by 5′ and 3′ nontranslated regions (5′ and 3′ NTRs). The translation product of the viral genome is a large polyprotein containing the structural proteins (core, envelope proteins E1 and E2) in the N-terminal region and the nonstructural proteins (p7, nonstructural protein 2 [NS2], NS3, NS4A, NS4B, NS5A, and NS5B) in the C-terminal region. The individual proteins are processed from the polyprotein by various proteases. The host cellular signal peptidase cleaves between core/E1, E1/E2, E2/p7, and p7/NS2, and signal peptide peptidase releases core from the E1 signal peptide. Two viral proteases, the NS2-3 protease and the NS3-4A protease, cleave the remainder of the viral polyprotein in the nonstructural region (22, 27). The structural proteins package the genome into infectious particles and mediate virus entry into a naïve host cell; the nonstructural proteins NS3 through NS5B form the RNA replication complex. p7 and NS2 are not thought to be incorporated into the virion but are essential for the assembly of infectious particles (14, 36); however, their mechanisms of action are not understood.

NS2 (molecular mass of 23 kDa) is a hydrophobic protein containing several transmembrane segments in the N-terminal region (5, 9, 32, 39). The C-terminal half of NS2 and the N-terminal third of NS3 form the NS2-3 protease (10, 11, 26, 37). NS2 is not required for the replication of subgenomic replicons, which span NS3 to NS5B (20). However, cleavage at the NS2/3 junction is necessary for replication in chimpanzees (16), the full-length replicon (38), and in the infectious tissue culture system (HCVcc) (14). Although cleavage can occur in vitro in the absence of microsomal membranes, synthesis of the polyprotein precursor in the presence of membranes greatly increases processing at the NS2/3 site (32). In vitro studies indicate that purified NS2-3 protease is active in the absence of cellular cofactors (11, 37). In addition to its role as a protease, NS2 has been shown to be required for assembly of infectious intracellular virus (14). The N-terminal helix of NS2 was first implicated in infectivity by the observation that an intergenotypic breakpoint following this transmembrane segment resulted in higher titers of infectious virus (28). Structural and

* Corresponding author. Mailing address: Laboratory of Virology and Infectious Disease, Center for the Study of Hepatitis C, The Rockefeller University, 1230 York Ave., New York, NY 10065. Phone: (212) 327-7046. Fax: (212) 327-7048. E-mail: ricec@rockefeller.edu.

† Present address: International AIDS Vaccine Initiative, AIDS Vaccine Design & Development Laboratory, Brooklyn, NY 11220.

‡ Present address: Department of Microbiology, Mount Sinai School of Medicine, New York, NY 10029.

▽ Published ahead of print on 7 October 2009.

functional characterization of the NS2 transmembrane region has shown that this domain is essential for infectious virus production (13). In particular, a central glycine residue in the first NS2 helix plays a critical role in HCV infectious virus assembly (13). The NS2 protease domain, but not its catalytic activity, is also essential for infectious virus assembly, whereas the unprocessed NS2-3 precursor is not required (13, 14).

The crystal structure of the postcleavage NS2 protease domain ($NS2^{pro}$, residues 94 to 217), revealed a dimeric cysteine protease containing two composite active sites (Fig. 2C; [21]). Two antiparallel α-helices make up the N-terminal subdomain, followed by an extended crossover region, which positions the β-sheet-rich C-terminal subdomain near the N-terminal region of the partner monomer. Two of the conserved residues of the catalytic triad (His 143, Glu 163) are located in the loop region after the second N-terminal helix of one monomer, while the third catalytic residue, Cys 184, is located in the C-terminal subdomain of the other monomer. Creation of this unusual pair of composite active sites through NS2 dimerization has been shown to be essential for autoproteolytic cleavage (21). The structure of $NS2^{pro}$ further demonstrated that the C-terminal residue of NS2 remains bound in the active site after cleavage, suggesting a possible mechanism for restriction of this enzyme to a single proteolytic event (21). Here we have used the crystal structure of $NS2^{pro}$, along with sequence alignments, to target conserved residues in each of the $NS2^{pro}$ structural regions. Our mutational analysis revealed that the residues in the dimer crossover region and the C-terminal subdomain are important for infectious virus production. In contrast, the majority of amino acids in the active site pocket were not required for infectivity. Interestingly, we observed that the extreme C-terminal leucine of NS2 is absolutely essential for generation of infectious virus, as mutations, deletions, and extensions into NS3 are very poorly tolerated. This analysis begins to dissect the determinants of the multiple functions of this important protease in the HCV life cycle.

MATERIALS AND METHODS

Plasmid constructs. Mono- and bicistronic (see Fig. 1A) genomes were generated by standard molecular biology techniques and verified by restriction enzyme digestion and sequencing of PCR-amplified segments. Descriptions of the cloning strategies are provided below, and plasmid and primer sequences are available upon request.

(i) J6/H77NS2/JFH and mutant derivatives. J6/H77NS2/JFH constructs contain genotype 2a (J6) from core to p7, genotype 1a (strain H77) NS2 and genotype 2a (JFH) NS3 to NS5B. To create this construct, the J6/JFH plasmid (18) was used as a template to PCR amplify the J6/JFH E2 3′ end through the p7 sequence with forward oligonucleotide RU-O-5739 (5′-CCGCCTTGTCGA CTGGTC) and reverse oligonucleotide RU-O-5855 (5′-CTCCGTGTC-CAACGCGTAAGCCTGTTGGGGC). The H77 NS2 through half of JFH-1 NS3 region was PCR amplified from H77/JFH (18) with the forward oligonucleotide RU-O-5854 (5′-CAGGCTTACGCGTTGGACACGGAGGTGGCC) and reverse oligonucleotide RU-O-5721 (5′-GCTACCGAGGGGTTAAGCA CT). Since these PCR products overlap at the p7/NS2 junction, they were used as template in a second round of PCR with the outside oligonucleotides RU-O-5855 and RU-O-5721 to generate a PCR product encoding the J6 E2 C-terminal region though p7, the H77 NS2, and JFH-1 NS3 N-terminal region. This product was digested with restriction endonucleases BsaBI and AvrII and ligated into the BsaBI/AvrII-digested J6/JFH plasmid to create the final J6/H77NS2/JFH plasmid. An adaptive change at G1145A (chimeric genome numbering) encoding substitution A269T (chimeric polyprotein numbering) was found to increase infectious virus titers of J6/H77NS2/JFH, and was included in all J6/H77NS2/JFH-based genomes constructed. Mutant derivatives of J6/H77NS2/JFH were created by site-directed mutagenesis using the AfeI/BbvCI restriction sites.

(ii) J6/H77NS2/JFH(NS2-IRES-NS3) and mutant derivatives. J6/H77NS2/JFH-(NS2-IRES-NS3) encodes a stop codon after NS2, an encephalomyocarditis virus (EMCV) internal ribosome entry site (IRES), a start codon, and the remainder of the JFH-1 polyprotein starting with NS3. Mutant derivatives of J6/H77NS2/JFH(NS2-IRES-NS3) were created by site-directed mutagenesis using the PmeI/MluI restriction sites.

(iii) J6/H77NS2/JFH(NS2-IRES-nsGluc2AUbi) and mutant derivatives. J6/H77NS2/JFH(NS2-IRES-nsGluc2AUbi) is similar to J6/H77NS2/JFH(NS2-IRES-NS3) but encodes a *Gaussia* luciferase gene followed by the foot and mouth disease virus 2A peptide and a ubiquitin monomer (nsGluc2AUbi cassette) between the EMCV IRES and NS3 (14). The N-terminal signal sequence of *Gaussia* luciferase has been deleted so that the reporter is not secreted. Mutant derivatives of J6/H77NS2/JFH(NS2-IRES-nsGluc2AUbi) were created by site-directed mutagenesis using the PmeI/MluI restriction sites. NS2 extensions into NS3 were subcloned using BbvCI/SpeI/KpnI restriction sites.

Cell culture. Huh-7.5 cells were cultured in Dulbecco's modified Eagle medium (Invitrogen) supplemented with 0.1 mM nonessential amino acids and 10% fetal bovine serum (complete medium). Cells were grown at 37°C in 5% CO_2.

RNA transcription. In vitro transcripts were generated as previously described (18). Briefly, plasmid DNA was linearized by XbaI and purified by using a Minelute column (Qiagen, Valencia, CA). RNA was transcribed from 1 μg of purified template by using the T7 Megascript kit (Ambion, Austin, TX) or the T7 RNA polymerase kit (Promega, Madison, WI). Reaction mixtures were incubated at 37°C for 3 h, followed by a 15-min digestion with 3 U of DNase I (Ambion). RNA was purified by using an RNeasy kit (Qiagen) with an additional on-column DNase treatment. RNA was quantified by absorbance at 260 nm and diluted to 0.5 μg/μl. Prior to storage at −80°C, RNA integrity was determined by agarose gel electrophoresis and visualization by ethidium bromide staining.

RNA electroporation. Huh-7.5 cells were electroporated with RNA as previously described (18). Briefly, Huh-7.5 cells were treated with trypsin, washed twice with ice-cold RNase-free AccuGene phosphate-buffered saline (PBS) (BioWhittaker, Rockland, ME), and resuspended at 1.75×10^7 cells/ml in PBS. Then, 2 μg of each RNA was combined with 0.4 ml of cell suspension and immediately pulsed using a BTX ElectroSquare Porator ECM 830 (820 V, 99 μs, five pulses). Electroporated cells were incubated at room temperature for 10 min prior to resuspension in 15 ml or 30 ml complete medium for nonreporter and reporter constructs, respectively. Resuspended cells were plated into 24-well, 6-well, and P100 tissue culture dishes.

Assays for RNA replication. At 4 or 8, 24, 48, and 72 h postelectroporation, cells in 24-well plates were washed with Dulbecco PBS and lysed by the addition of *Renilla* lysis buffer (Promega, Madison, WI) or RLT buffer (Qiagen) containing 1% β-mercaptoethanol for assay of replication by luciferase activity or quantitative reverse transcription-PCR (qRT-PCR), respectively. For luciferase assays, the lysates were thawed prior to the addition of *Renilla* substrate (Promega) according to the manufacturer's instructions. The luciferase activity was measured by using a Berthold Centro LB 960 96-well luminometer. For qRT-PCR analysis, prior to storage at −80°C, the lysates were homogenized by centrifugation through a QiaShredder column (Qiagen) for 2 min at $14,000 \times g$. Total RNA was isolated by RNeasy kit (Qiagen) and quantified by determining the absorbance at 260 nm. A total of 50 ng of total cellular RNA was used per reaction mixture. qRT-PCRs were performed on a LightCycler 480 (Roche, Basel, Switzerland) using the LightCycler amplification kit (Roche) with primers directed against the viral 3′ NTR. We assembled 20-μl reaction mixtures according to the manufacturer's instructions as previously described (14).

Assays for infectious virus production. At 4 or 8, 24, 48, and 72 h postelectroporation, the cell culture medium was harvested and replaced with fresh complete medium. Harvested cell culture supernatants were clarified by using a 0.45-μm-pore-size filter and stored in aliquots at −80°C. For detection of infectious virus production by qRT-PCR or luciferase assay, naïve cells were infected with clarified cell culture supernatants and incubated for 72 h prior to analysis. Determination of infectious virus production by limiting dilution assay was performed as described previously (14, 18). Briefly, clarified cell culture supernatants were serially diluted and used to infect approximately 3×10^3 cells plated in 96-well dishes. At 3 days postinfection, cells were washed with Dulbecco PBS, fixed with ice-cold methanol, and stained for the presence of NS5A expression as described previously. The 50% tissue culture infectious dose ($TCID_{50}$) was calculated using the Reed and Muench method (18).

Anti-NS2 MAb (6H6). The immunogen was a recombinant NS2 protease domain of strain H77 (residues 94 to 217 with an amino-terminal hexahistidine tag) expressed in *Escherichia coli* and purified by fast protein liquid chromatog-

raphy under denaturing conditions (6 M guanidinium hydrochloride) or in the presence of detergent (21). BALB/c mice were immunized three times intraperitoneally with 50 μg NS2 purified under denaturing conditions, followed by a final boost with 50 μg NS2 purified in the presence of detergent. The preimmune and test bleeds were assayed for the presence of NS2-specific polyclonal antibodies by a standard enzyme-linked immunosorbent assay, as well as by Western blotting. Screening of hybridoma supernatants produced 6H6, an isotype immunoglobulin G1 monoclonal antibody (MAb).

SDS-PAGE and immunoblotting. Cells were lysed at 72 h postelectroporation with RLT buffer (Qiagen) containing 1% β-mercaptoethanol and homogenized by centrifugation through a QiaShredder column (Qiagen) for 2 min at 14,000 × *g*. The lysates were separated by sodium dodecyl sulfate-polyacrylamide gel electrophoresis (SDS-PAGE). After transfer to nitrocellulose membrane, the blots were blocked for 1 h with 5% milk–PBS-T (PBS plus 0.1% Tween). For NS2 detection, MAb 6H6 (1.0 mg/ml), was diluted 1:1,000 in PBS-T. For NS5A detection, MAb 9E10 (18) was diluted 1:1,000 in PBS-T. For β-actin detection, mouse anti-β-actin MAb (Sigma, St. Louis, MO) was diluted 1:20,000 in PBS-T. After 1-h incubation at room temperature and extensive washing with PBS-T, horseradish peroxidase-conjugated rabbit anti-mouse immunoglobulin secondary antibody (Pierce, Rockford, IL) was added at 1:10,000 dilution in 5% milk–PBS-T for 45 min at room temperature. After additional washing, blots were developed with SuperSignal West Pico chemiluminescent substrate (Pierce).

RESULTS

Creation and characterization of triple chimeric HCV genomes. The crystal structure of $NS2^{pro}$ was solved using the H77 genotype 1a protein (21). In order to facilitate a structure-based mutational analysis of NS2, we created J6/JFH genomes encoding the H77 NS2 sequence. Three different full-length HCV genome constructs were used (Fig. 1A). J6/H77NS2/JFH is a monocistronic genome encoding J6 core through p7, H77 NS2, and JFH-1 NS3 through NS5B; the 5′ and 3′ NTRs of all the genomes are derived from JFH-1. J6/H77NS2/JFH replicated with kinetics similar to those of J6/JFH but released approximately 50-fold-less infectious virus (data not shown). By passaging transfected cells, we selected a single nucleotide change, G1145A (chimeric genome nucleotide numbering) encoding an A269T mutation in the J6 E1 protein. This substitution enhanced infectious particle production (data not shown) and was included in all genomes constructed. To study the functions of NS2 in infectious virus production independent of its autoproteolytic cleavage requirements, we created bicistronic genomes. J6/H77NS2/JFH(NS2-IRES-NS3) is identical to J6/H77NS2/JFH but with the addition of a stop codon after H77 NS2 and an encephalomyocarditis virus internal ribosome entry site upstream of NS3. This genome allows expression of the viral replicase independently of NS2-3 cleavage, and thus uncouples processing from replication and virus production. J6/H77NS2/JFH(NS2-IRES-nsGluc2AUbi) is identical to J6/H77NS2/JFH(NS2-IRES-NS3), but it encodes the reporter gene *Gaussia* luciferase immediately downstream of the EMCV IRES. Cleavage of the reporter protein from the viral polyprotein is mediated by the foot-and-mouth disease virus 2A peptide and cleavage after the C terminus of the ubiquitin monomer by host ubiquitin carboxy-terminal hydrolase (31). This generates nonsecreted *Gaussia* luciferase (nsGluc) and the proper N terminus of NS3. The triple chimeric genomes were tested for replication and infectious virus production at various times postelectroporation of Huh-7.5 cells with in vitro-transcribed RNA; 72-h time points are shown (Fig. 1). All chimeric genomes were viable, although RNA replication levels and infectious particle production were somewhat reduced compared to the parental J6/JFH. As ex-

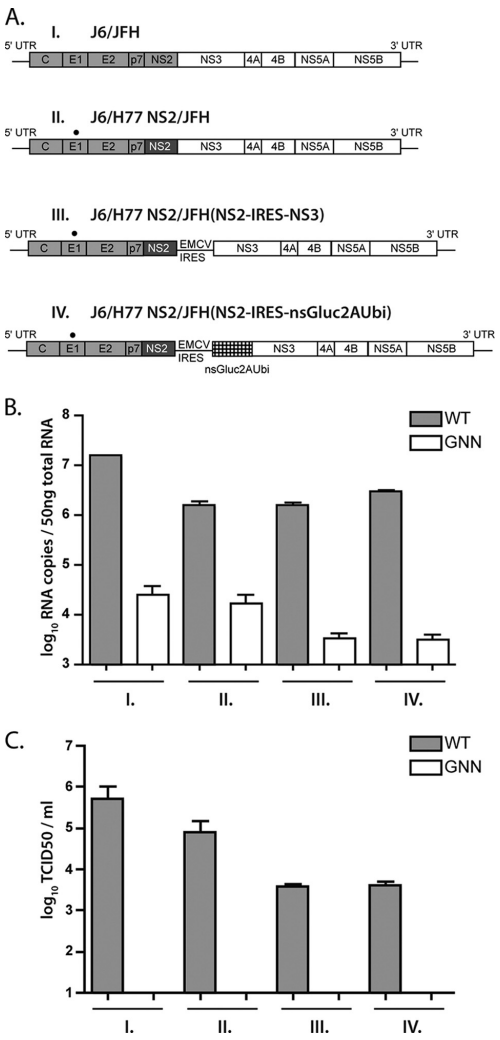

FIG. 1. HCV genomes used in this study. (A) Schematic representation of HCV genomes. (I) J6/JFH with J6 C-NS2 shown in gray and JFH NS3-NS5B in white. (II) J6/H77NS2/JFH with J6 (gray), H77 NS2 (dark gray), and JFH (white) with adaptive mutation in E1 (black dot). (III) Bicistronic construct similar to that shown for construct II but with an EMCV IRES between NS2 and NS3. (IV) Bicistronic reporter construct similar to construct III with EMCV IRES, plus nonsecreted *Gaussia* luciferase, foot and mouth disease virus 2A and ubiquitin cleavage sites (nsGluc2AUbi) between NS2 and NS3 (checkered box). 5′ UTR and 3′UTR, 5′ untranslated region and 3′ untranslated region, respectively. (B) RNA replication of J6/JFH and J6/H77/JFH genomes measured by quantitative RT-PCR at 72 h postelectroporation. HCV RNA copies normalized to 50 ng of total RNA. (C) Infectious virus production of bicistronic constructs at 72 h postelectroporation, as measured by limiting dilution assay ($TCID_{50}$). WT, wild type of each genome indicated; GNN, corresponding polymerase-defective control. The means plus standard errors of the means (error bars) of three independent experiments with two different RNA preparations are shown.

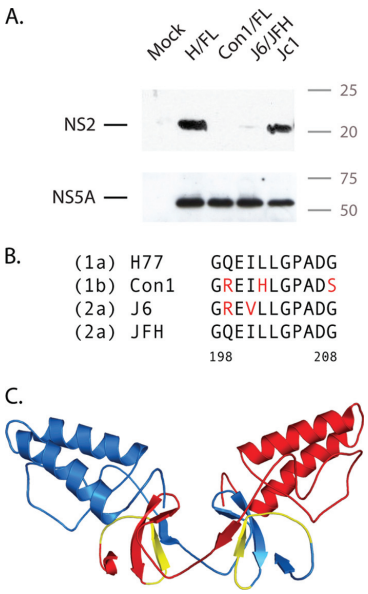

FIG. 2. Characterization of anti-NS2 antibody (6H6). (A) Western blot comparing the reactivity of the 6H6 anti-NS2 antibody and 9E10 anti-NS5A antibody against genotype 1a, 1b, and 2a proteins. Huh-7.5 cells were infected with a recombinant vaccinia helper virus expressing the T7 polymerase, followed by transfection with plasmids coding for a full-length HCV genomes under the control of a T7 promoter. The lysates were harvested 16 h posttransfection. The positions of molecular mass markers (in kilodaltons) are indicated to the right of the blot. (B) Amino acid sequence alignment of the 6H6 epitope region. Variation between protein sequences is indicated in red. (C) Crystal structure of the dimeric NS2 protease domain (21) with monomers shown in red and blue with the 6H6 antibody epitope shown in yellow.

pected, genomes containing a mutation of the NS5B RNA-dependent RNA polymerase motif GDD to GNN did not replicate (Fig. 1B and C).

The monoclonal antibody 6H6 recognizes a C-terminal epitope of NS2. In Western blot, MAb 6H6 strongly recognized NS2 from strains H77 (genotype 1a) and JFH-1 (Jc1 genome, genotype 2a) (16, 28) and showed a weak signal for strain J6 (J6/JFH genome, genotype 2a) (18); it did not react with Con1 (genotype 1b) (2) (Fig. 2A). Strain H77 NS2 is also recognized in an enzyme-linked immunosorbent assay, immunoprecipitation, and immunofluorescence (data not shown). Epitope mapping with an NS2 peptide library revealed that 6H6 binding occurs close to the NS2 C terminus (H77 NS2 amino acids 197 to 208, GQEILLGPADG). Sequence alignments in this region showed variability between NS2 genotypes that correlated with the Western blot results (Fig. 2B). The epitope of MAb 6H6 is shown on the NS2 crystal structure in Fig. 2C.

NS2 catalytic-cleft residues are required for NS2-3 cleavage. Previous studies have shown that the catalytic activity of the NS2-3 protease is not required for infectious virus production (14). To investigate whether residues surrounding the active site pocket were required for the generation of infectious progeny, we mutated individual residues in this region. Y141 and L144 are highly conserved amino acids surrounding the protease active site, H143 is part of the catalytic triad, and P164 is an unusual *cis*-proline residue important for active site geometry. We mutated these residues to alanine and/or to less conservative substitutions in the context of the monocistronic J6/H77NS2/JFH and bicistronic J6/H77NS2/JFH(NS2-IRES-NS3) genome, and assayed replication by quantitative RT-PCR for intracellular HCV RNA at 72 h postelectroporation. We confirmed that the active site mutation H143A abolished replication in the full-length monocistronic background (10), and we found that Y141A also severely impaired RNA accumulation; a Y141F substitution, which preserved the aromatic ring, did not have a dramatic effect (Fig. 3A). Replication was decreased by mutation of L144 to bulky residues (L144F, L144K) and by substitutions of P164 (P164A, P164G). Consistent with the requirement for NS2-3 cleavage, robustly replicating genomes showed processed NS2 by Western blotting (Fig. 3C).

To test the effects of NS2 active cleft mutations on infectious virus production, we engineered these substitutions into the bicistronic J6/H77NS2/JFH(NS2-IRES-NS3) genome. In this context, all mutants replicated as efficiently as the wild-type virus did; J6/H77NS2/JFH(NS2-IRES-NS3)/GNN did not replicate (Fig. 3B). Infectious virus production was measured by inoculating naïve Huh-7.5 cells with filtered culture supernatants harvested at 72 h postelectroporation and calculating the $TCID_{50}$/ml. Mutations Y141A, Y141F, H143A, L144F, and L144K were not impaired or only slightly impaired in terms of infectious titers compared to wild-type J6/H77NS2/JFH(NS2-IRES-NS3), whereas substitution of P164 mutated to Ala or Gly decreased infectious virus production by about 10-fold (Fig. 3D). Western blotting of cell lysates harvested at 72 h postelectroporation revealed that all of the mutants expressed readily detectable levels of NS2 (Fig. 3C).

These results indicate that mutations at the NS2 active cleft can inhibit replication of a monocistronic genome, likely by affecting NS2-3 processing, but that the catalytic activity is not required for infectious virus production of a bicistronic genome. The moderate deleterious effect of *cis*-proline 164 mutations on infectivity may indicate a more global impact of this unusual residue on NS2 architecture.

Residues in the NS2 dimer crossover region are important for infectious virus production. NS2 dimerization creates two composite active sites and has been shown to be essential for proteolytic cleavage at the NS2/NS3 junction (21). Although the critical residues for dimer formation and stabilization are not known, amino acids in the crossover region between the two monomers may be envisioned to participate. To test the effects of mutations in the dimer crossover region on replication and infectious virus production, we created several substitutions of highly conserved amino acids in the context of monocistronic and bicistronic genomes: a triple mutation with M170A, I175A, and W177A (M/I/W) and individual mutations M170A, I175S, W177A, and W177C. The single isoleucine-to-serine substitution was chosen in order to change a nonpolar residue to a polar residue, with predicted disruption to the dimer interface. In the monocistronic J6/H77NS2/JFH background, replication levels close to those of the wild type were observed for the M170A, I175S, and W177A mutants, whereas

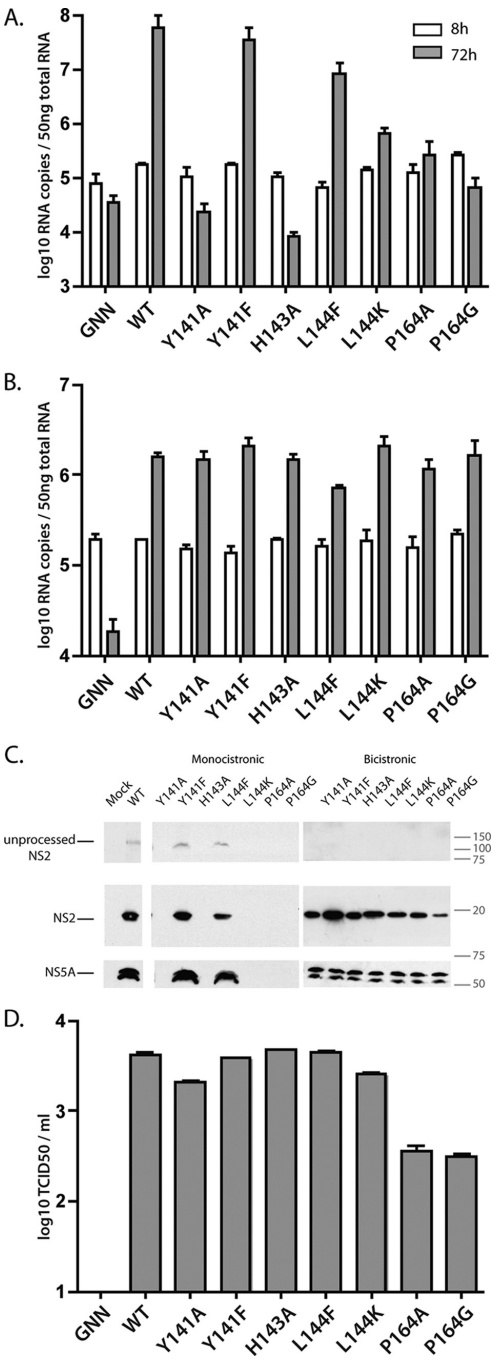

FIG. 3. Mutagenesis of the NS2 active site region. (A) RNA replication of GNN, the polymerase-defective control, wild-type (WT) and mutated monocistronic constructs at 8 h and 72 h postelectroporation. (B) RNA replication of GNN, wild-type and mutated bicistronic constructs at 8 h and 72 h postelectroporation. The numbers of HCV RNA copies per 50 ng of total cellular RNA are shown. (C) Polyprotein processing of monocistronic and bicistronic constructs. Huh-7.5 cells were lysed 72 h postelectroporation and analyzed by SDS-PAGE. Unprocessed and processed NS2 are shown in the top two panels (6H6 antibody). NS5A protein is shown in the bottom panel (9E10 antibody). The positions of molecular mass markers (in kilodaltons) are shown to the right of the immunoblots. (D) Infectious virus production by the bicistronic constructs at 72 h postelectroporation, as measured by limiting dilution assay ($TCID_{50}$). Mutated residues are indicated (H77 NS2 numbering). WT and GNN, parental monocistronic or bicistronic wild type and polymerase-defective control, respectively. The means plus standard errors of the means (error bars) for three independent experiments with two different RNA preparations are shown.

the W177C mutant and the genome with the M/I/W triple mutation exhibited impaired RNA accumulation by 10- to 100-fold (Fig. 4A). This somewhat surprisingly efficient replication may indicate that dimer formation, and thereby protease activity, is not disrupted by these substitutions. Western blot analysis confirmed that NS2 was properly processed for each of these genomes, although to a lower extent for the triple mutant M/I/W (Fig. 4C). To test the effects of these mutations on infectious virus production, they were engineered into the bicistronic genome J6/H77NS2/JFH(NS2-IRES-NS3). While replication in this context was not affected by any of the NS2 substitutions (Fig. 4B), infectious particle production was decreased close to 100-fold for all of the mutant genomes (Fig. 4D). Wild-type levels of NS2 were detected for all the bicistronic constructs, indicating that the mutations do not change protein stability (Fig. 4C). These results indicate that mutations in the dimer crossover region are deleterious to infectious virus production, although likely not as a result of dimer destabilization.

The C-terminal region of NS2 is essential for infectious virus production. The crossover residues position the NS2 C-terminal region of one monomer close to the N-terminal region of the other, leading to the formation of the composite active site. To investigate the importance of the C-terminal region of NS2 for infectious virus production, we generated truncations after residues Y124, G137, G178, W214, R215, and L216 (Fig. 5A). These deletions were engineered in the context of the bicistronic *Gaussia* luciferase reporter genome, J6/H77NS2/JFH(NS2-IRES-nsGluc2AUbi), which was used to facilitate mutant characterization. Truncations were created by introducing two in-frame stop codons after the designated residue without deletion of the downstream nucleotides. This strategy allowed replication and infectivity to be monitored with minimal effects on genome length or potential RNA secondary structures. RNA replication was measured by assaying Huh-7.5 cell lysates for luciferase activity at 72 h postelectroporation. All the C-terminal truncation mutants replicated, although with a slight reduction for mutants with stops after G137 and G178 compared to wild type; J6/H77NS2/JFH(NS2-IRES-nsGluc2AUbi)/GNN did not replicate (Fig. 5B). Infectious virus production was assayed at 72 h postelectroporation by measuring luciferase activity in infected Huh-7.5 cell lysates.

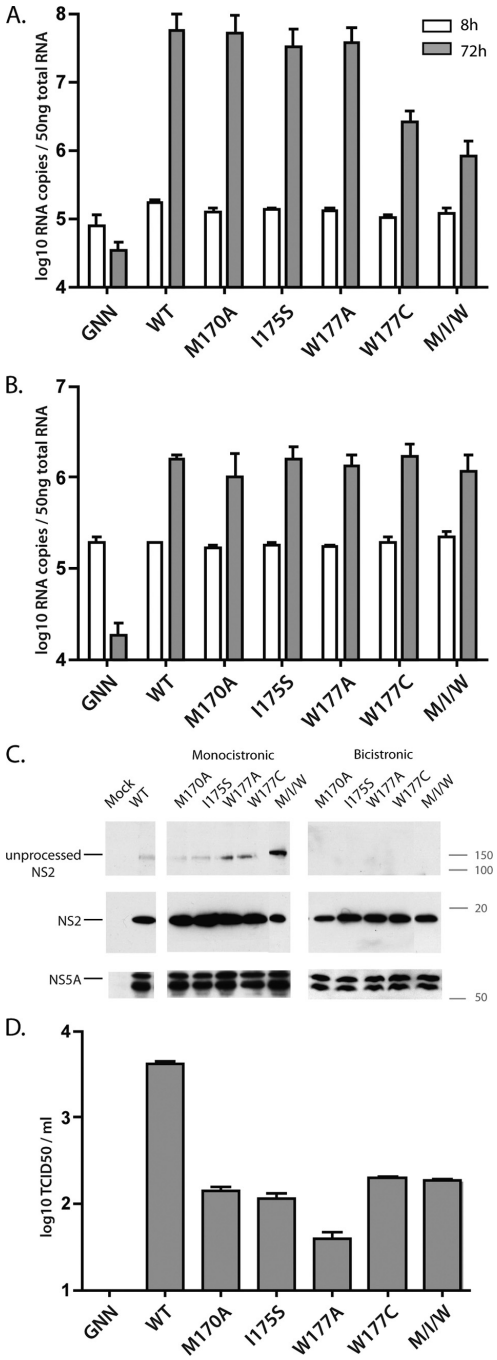

FIG. 4. Mutagenesis of the NS2 dimer crossover region. (A) RNA replication of GNN and wild-type and mutated monocistronic constructs at 8 h and 72 h postelectroporation. (B) RNA replication of bicistronic constructs at 8 h and 72 h postelectroporation. The numbers of HCV RNA copies per 50 ng of total cellular RNA are shown. (C) Polyprotein processing of monocistronic and bicistronic constructs. Huh-7.5 cells were lysed 72 h postelectroporation and analyzed by SDS-PAGE. Unprocessed and processed NS2 are shown in the top two panels (6H6 antibody). NS5A protein is shown in the bottom panel (9E10 antibody). The positions of molecular mass markers (in kilodaltons) are shown to the right of the immunoblots. (D) Infectious virus production by the bicistronic constructs at 72 h postelectroporation, as measured by limiting dilution assay ($TCID_{50}$). Mutated residues are indicated (H77 NS2 numbering). WT and GNN, parental monocistronic or bicistronic wild type and polymerase-defective control, respectively. The means plus standard errors of the means (error bars) for three independent experiments with two different RNA preparations are shown.

Consistent with our mutational analysis (Fig. 4), truncation of NS2 before the dimer crossover region (Y124 and G137) abolished infectivity (Fig. 5C). Similarly, deletion of the entire C-terminal region (G178) prevented progeny virus production (Fig. 5C). Surprisingly, more subtle deletions of three, two, or even one amino acid from the C terminus severely impaired infectivity (Fig. 5C). Western blot analysis showed detectable levels of NS2 expression for the W214, R215, and L216 truncations (Fig. 5D); the larger deletions were missing the 6H6 antibody epitope and could therefore not be tested.

To identify individual amino acids in the C-terminal region that were important for NS2 functions, we mutated highly conserved residues shown in the crystal structure to mediate contacts between NS2 monomers. These substitutions—nonpolar I188 mutated to a polar serine, changing N189, L191, and I201 to a small amino acid (alanine), and changing D207 to alanine or a bulky, charged arginine—were created in the monocistronic J6/H77NS2/JFH and bicistronic J6/H77NS2/JFH(NS2-IRES-NS3) genomes. In the monocistronic background, RNA replication of the I188S, D207A, and D207R mutants was detected but impaired (Fig. 6A). NS2-3 processing could be observed for I188S, N189A, and L191A mutants; processing of the I201 and D207 mutants could not be assessed since the epitope of the 6H6 antibody had been disrupted (Fig. 6C). In the context of the bicistronic genome [J6/H77NS2/JFH(NS2-IRES-NS3)], none of the mutations in the C-terminal region impaired RNA replication (Fig. 6B). Infectious virus production was decreased for I188S, I201, D207A, and D207R mutants but not affected by N189A and L191S substitutions (Fig. 6D). The decreased titers seen for the I188S mutant did not result from NS2 degradation, as close to wild-type levels of this protein were detected by Western blotting.

Taken together, these results indicate that the C-terminal region of NS2 is important for infectious virus production, although individual residues contribute to various degrees. Interestingly, the ability of the mutations to disrupt replication of the monocistronic genome correlated with the extent of virus titer reduction, suggesting that attributes of the C-terminal region, such as interactions with the partner monomer, may be important for both proteolytic activity and infectious particle production.

The C-terminal leucine of NS2 is critical for infectious virus production. Our deletion analysis had shown that removing a

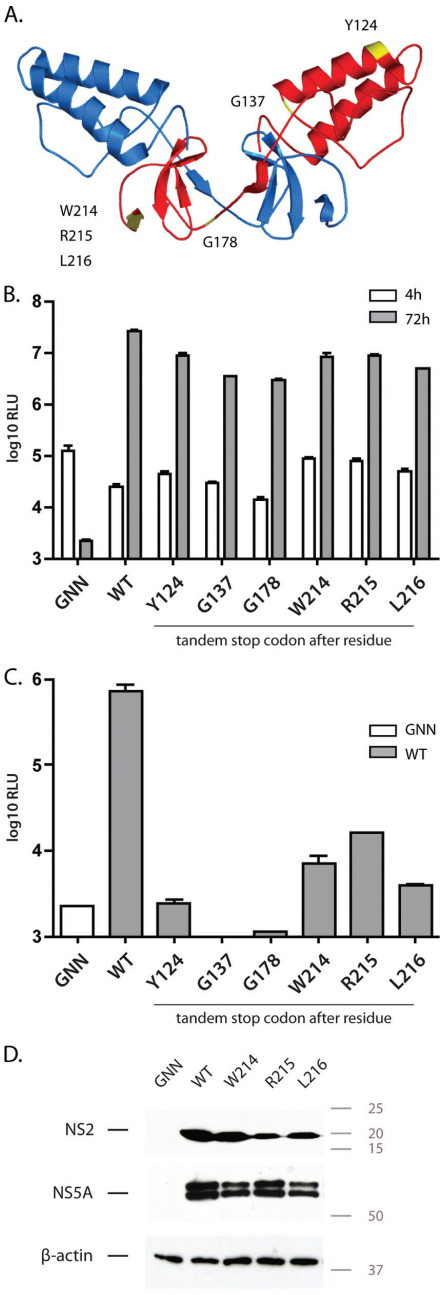

FIG. 5. Characterization of NS2 C-terminal truncations. (A) NS2^{pro} dimer with monomers shown in red and blue (21). The positions of the C-terminal truncations are indicated in yellow. (B) RNA replication at 4 h and 72 h postelectroporation of GNN, wild type, and C-terminal truncations in the bicistronic *Gaussia* luciferase reporter virus background, as measured by luciferase activity (in relative light units [RLU]). (C) Infectious virus production of NS2 C-terminal truncations at 72 h after infection of naïve Huh-7.5 cells with supernatants harvested 72 h postelectroporation. Truncation points are indicated (H77 NS2 numbering). WT, wild type [J6/H77NS2/JFH(NS2-IRES-nsGluc2AUbi)]; GNN, J6/H77NS2/JFH(NS2-IRES-nsGluc2AUbi)/GNN. The means plus standard errors of the means (error bars) for three independent experiments with two different RNA preparations are shown. (D) Polyprotein processing of NS2 truncations. Huh-7.5 cells lysed 72 h postelectroporation and analyzed by SDS-PAGE. NS2 expression is shown in the top panel (6H6 antibody), NS5A protein in the middle panel (9E10 antibody), and β-actin control in the bottom. The antibody epitope is not present in the NS2 truncations Y124, G137, and G178. The positions of molecular mass markers (in kilodaltons) are shown to the right of the immunoblots.

single NS2 residue, the C-terminal leucine 217, almost completely abolished infectious virus production. The crystal structure of the postcleavage form of NS2^{pro} shows that leucine 217 remains in the active site through hydrogen bond interactions with the catalytic triad, a conformation that is proposed to limit the enzyme to a single autoproteolytic cleavage (21). To investigate the importance of this C-terminal residue for infectivity, L217 was mutated to a variety of amino acids—isoleucine, valine, alanine, tryptophan, asparagine, or lysine—in the context of the bicistronic reporter virus, J6/H77NS2/JFH(NS2-IRES-nsGluc2AUbi). The L217 mutants replicated, although at levels somewhat reduced compared to that of the wild type (Fig. 7A). Infectious virus production was markedly impaired for all mutants tested apart from L217I, which showed a reduction of infectious titers of about 10-fold (Fig. 7B). These defects were not a result of NS2 instability, as the mutant proteins were readily detected by Western blotting (Fig. 7C). These data suggest that infectious virus production specifically requires a leucine at the C terminus of NS2, although an isoleucine can function to some degree.

Additional residues fused to the C terminus of NS2 abolish infectious virus production. NS2 requires residues 1 to 181 of NS3 for optimal proteolytic activity (30). Our finding of a critical role for the NS2 C-terminal leucine in infectivity suggested divergent requirements for infectious virus production and proteolysis. To investigate the effect of adding residues from NS3 on viral titers, we created J6/H77NS2/JFH bicistronic reporter genomes in which NS2 was followed by 1, 31, 40, 90, or 181 amino acids of NS3, a stop codon, the EMCV IRES, the *Gaussia* luciferase-2AUbi cassette, and full-length NS3 (Fig. 8A). These extensions were created in the context of wild-type H77 NS2, as well as in the context of the H143A active site mutation to prevent NS2-3 cleavage. At 72 h postelectroporation, the NS3 fusion constructs replicated, although extensions of 1, 31, 40, and 90 amino acids impaired this process up to 10-fold, in both the wild-type and H143A backgrounds. Mutant virus with the 181-amino-acid extension showed replication levels comparable to that of the parental genome in the wild-type background but more drastically impaired RNA replication in the H143A background; the reasons for this discrepancy are not known (Fig. 8B). Infectious virus production was severely impaired by uncleavable NS3 fusions of 31 to 181 amino acids (Fig. 8C). Even the addition of a single NS3 residue decreased infectivity by three- to fivefold. In

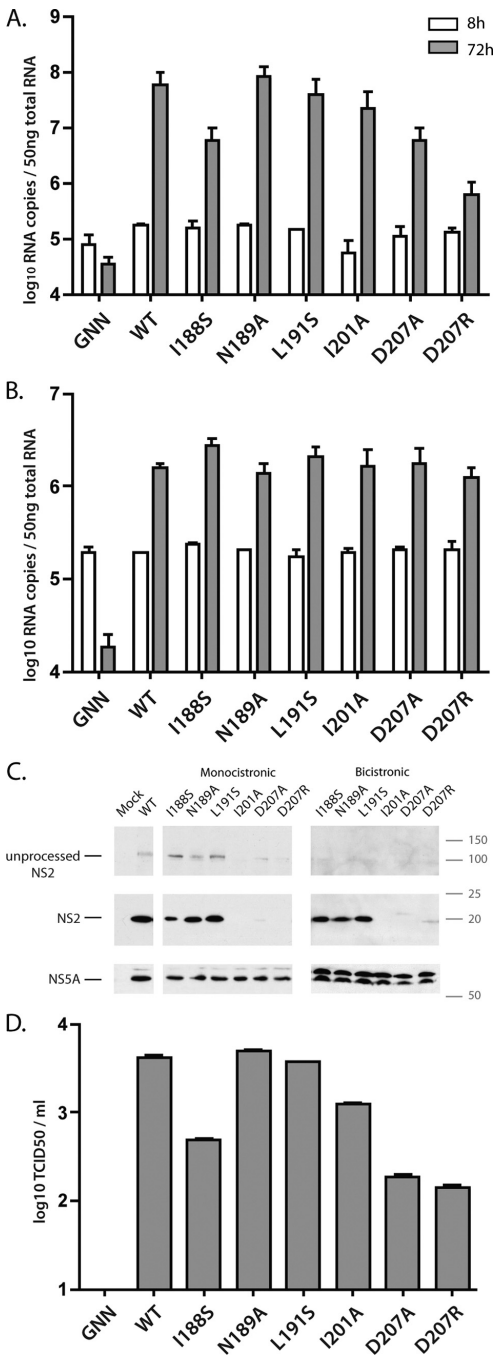

FIG. 6. Mutagenesis of the NS2 C-terminal region. (A) RNA replication of GNN and wild-type and mutated monocistronic constructs at 8 h and 72 h postelectroporation. (B) RNA replication of the bicistronic constructs at 8 h and 72 h postelectroporation. The numbers of HCV RNA copies per 50 ng of total cellular RNA are shown. (C) Polyprotein processing of monocistronic and bicistronic constructs. Huh-7.5 cells were lysed 72 h postelectroporation and analyzed by SDS-PAGE. Unprocessed and processed NS2 are shown in the top two panels (6H6 antibody). NS5A protein is shown in the bottom panel (9E10 antibody). The positions of molecular mass markers (in kilodaltons) are shown to the right of the immunoblots. (D) Infectious virus production at 72 h postelectroporation, as measured by limiting dilution assay ($TCID_{50}$). Mutated residues are indicated (H77 NS2 numbering). WT and GNN, parental monocistronic or bicistronic wild type and polymerase-defective control, respectively. The means plus standard errors of the means (error bars) for three independent experiments with two different RNA preparations are shown.

the context of wild-type, but not protease-defective NS2, fusion of 181 amino acids of NS3 produced infectious virus, suggesting that productive NS2-3 cleavage was required. Analysis of protein expression and processing by Western blotting indicated the presence of processed NS2 for those genomes producing significant levels of infectivity (Fig. 8D). Interestingly and consistent with the recent results of Schregel et al. (33), a small portion of processed NS2 could be detected for fusions expressing 31 and 40 amino acids of NS3. Taken together, these results further demonstrate the importance of the C-terminal residue of NS2 in infectious virus production and add to accumulating evidence that the multiple roles of NS2 in the viral life cycle have contrasting protein determinants.

DISCUSSION

NS2 has an essential but mechanistically undefined role in infectious HCV assembly (14, 28). The first set of determinants for this activity have been mapped; essential residues were identified in the N-terminal transmembrane domains, and a catalysis-independent role for the protease was found (13, 14). Here, we investigated the determinants of the NS2 protease domain that are required for infectious particle production. On the basis of the $NS2^{pro}$ crystal structure (21) and sequence alignments, conserved features of the various structural regions were analyzed. We found that most point mutations around the active site had little effect on infectious virus production but indirectly affected RNA replication in the context of a monocistronic genome, most likely by preventing NS2-3 cleavage. In contrast, mutations in the dimer crossover region and the C-terminal domain impaired or abolished infectious virus production. In addition, we showed the importance of a properly cleaved C terminus of NS2 with a free leucine 217.

The catalytic activity of the NS2 protease is required for NS2-3 processing (16, 38), but not for infectious virus assembly (14). In addition to the catalytic histidine, we identified several other residues important for NS2-3 processing and replication of a monocistronic genome. Mutation of Y141 to Ala abolished NS2-3 cleavage, whereas a more conservative change to Phe had little effect on processing or replication. The aromatic ring of position 141 acts as a support for the active site, a function that likely cannot tolerate a smaller side chain. Leucine 144 performs a similar role in creating the correct active site architecture, but we found that mutation of this

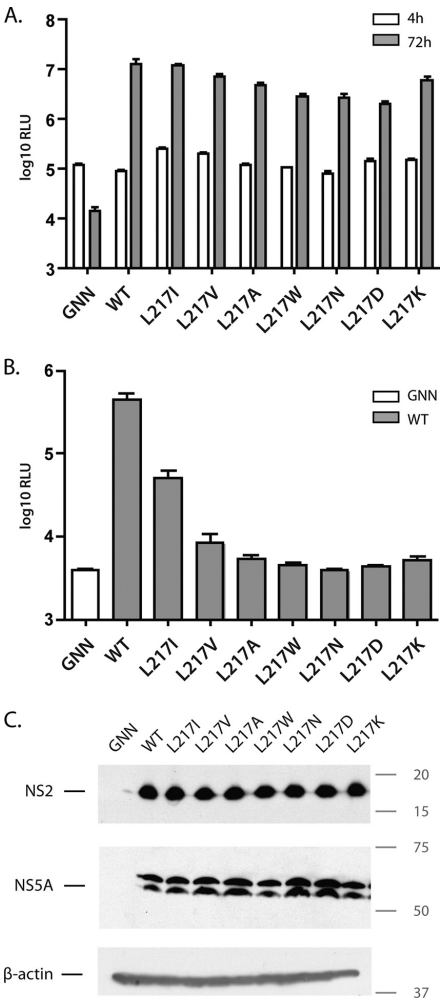

FIG. 7. Mutagenesis of the NS2 C-terminal leucine 217. (A) RNA replication at 4 h and 72 h postelectroporation of GNN, wild type, and C-terminal mutants in the context of the bicistronic *Gaussia* luciferase reporter virus, as measured by luciferase activity (in relative light units [RLU]). (B) Infectious virus production of genomes bearing Leu 217 mutations at 72 h after infection of naïve Huh-7.5 cells with supernatants harvested 72 h postelectroporation. WT, wild type [J6/H77NS2/JFH(NS2-IRES-nsGluc2AUbi)]; GNN, J6/H77NS2/JFH(NS2-IRES-nsGluc2AUbi)/GNN. The means plus standard errors of the means (error bars) for three independent experiments with two different RNA preparations are shown. (C) Polyprotein processing of 72 h postelectroporation. Huh-7.5 cells were lysed and analyzed by SDS-PAGE. NS2 expression is shown in the top panel (6H6 antibody), NS5A protein in the middle panel (9E10 antibody), and β-actin control in the bottom. The positions of molecular mass markers (in kilodaltons) are shown to the right of the immunoblots.

residue to Phe allowed detectable levels of NS2-3 processing, whereas Lys apparently abolished the function of the active site. Proline 164 has a *cis* conformation that is thought to bend the peptide backbone to establish the correct geometry of the Glu 163 side chain for catalysis; mutation of P164 to Ala or Gly prevented replication of a monocistronic genome. The majority of active site changes had little effect on infectious virus production in a bicistronic genome. Substitutions of P164, however, decreased infectious titers. It is possible that mutation of this *cis*-proline dramatically affects NS2 structure; indeed, the P164G substitution appeared to slightly destabilize the protein. It is also possible that mutations of P164 affect NS2 dimer formation, as this proline is important for positioning the linker between the N- and C-terminal subdomains. Alternatively, P164 may directly participate in infectious virus assembly independent of a role in catalysis. Studies of the NS2-3 protein of the distantly related pestivirus, classical swine fever virus, have similarly shown that the NS2 protease activity is dispensable for infectious virus production (23). However, a histidine-to-arginine mutation within the active site abolished infectivity without affecting NS2-3 expression (23).

The crystal structure of $NS2^{pro}$ shows a crossover region that positions the subdomains for creation of the composite active sites (21). We hypothesized that mutations in this region would disrupt dimer stability and NS2-3 processing. RNA replication of a monocistronic genome, however, was impaired only by substitution of W177 to Cys or by a triple mutation of M170A/I175A/W177A. This suggests that single point mutations do not have a drastic effect on dimer integrity; indeed, the significant buried surface area between the monomers indicates that the NS2 dimer is highly stable (21). Although NS2-3 processing was not greatly impacted by mutations in the crossover sequence, infectious virus production was impaired by all substitutions we tested in this region. A number of the crossover residues are exposed on the surface of the $NS2^{pro}$ dimer (Fig. 9). Mutations in this region may disrupt associations with viral or host proteins involved in infectious virus production. Indeed, NS2 has been suggested to participate in a number of genetic or physical interactions, including with structural proteins core and E2 as well as with nonstructural proteins p7, NS3, NS4A, and NS5A (15, 19, 25, 29, 34, 40). The A269T adaptive mutation identified here suggests a genetic interaction between NS2 and E1. Cellular kinase CKII also appears to associate with and phosphorylate NS2 (8), and NS2 may interact with additional host factors to influence apoptosis (6) and cellular gene expression (5).

In addition to mediating contacts between monomers, the C-terminal subdomain of NS2 contributes the catalytic cysteine to the composite active site. Deletion analysis revealed that even a single amino acid truncation at the C terminus severely impaired infectious virus production. Furthermore, the majority of substitutions at the terminal L217 were highly deleterious to infectivity. Interestingly, previous reports have shown that most modifications of L217 have little effect on NS2-3 processing (12, 30). Our finding of an essential role for L217 in infectious virus production helps explain its high level of conservation across all genotypes. The structure of the postcleavage form of $NS2^{pro}$ shows that L217 occupies the active site through contacts with H143 and C184 (13, 21). This conformation has been suggested to render the protease inactive

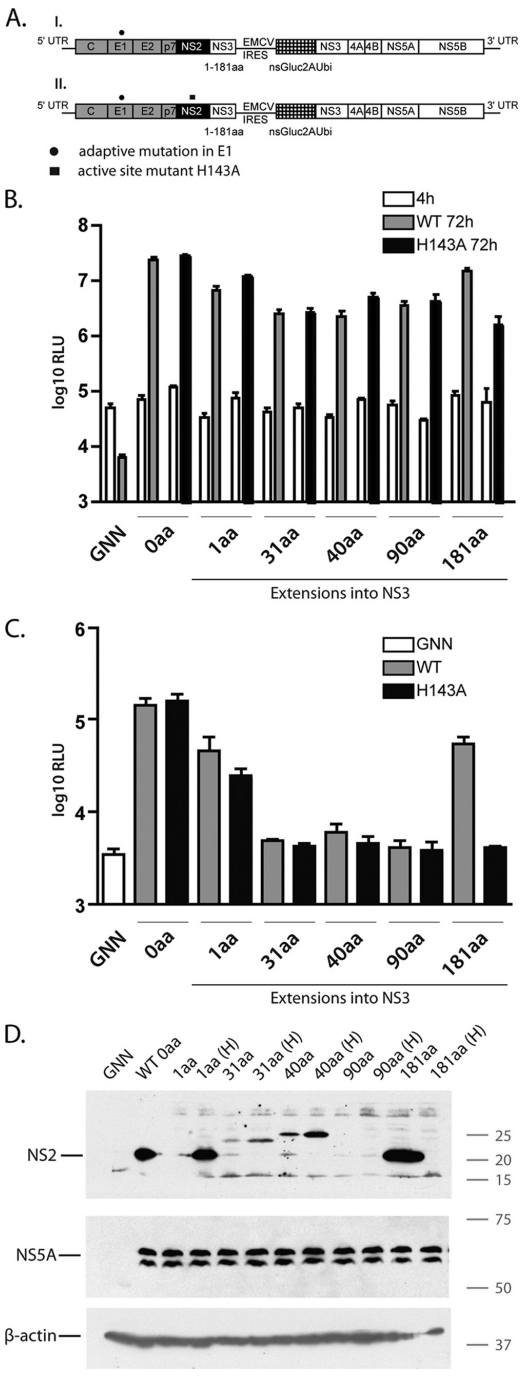

FIG. 8. Characterization of NS2 C-terminal extensions. (A) Schematic representation of J6/H77NS2/JFH(NS3*-IRES-nsGluc2AUbiNS3). Genes from J6 (core-p7) (gray boxes), H77 (NS2) (black boxes), and from JFH (white boxes) are indicated. This construct contains JFH NS3 extensions of 1, 31, 40, 90, or 181 amino acids, followed by an EMCV IRES, a *Gaussia* luciferase cassette (nsGluc2AUbi), and JFH nonstructural proteins NS3-NS5B. Wild-type H77 NS2 (I) and H77 NS2 encoding active-site mutation H143A (small solid square) (II). 5′ UTR and 3′UTR, 5′ untranslated region and 3′ untranslated region, respectively. (B) RNA replication at 4 h postelectroporation, 72 h postelectroporation for the wild type, and 72 h postelectroporation for H143A as measured by luciferase activity (in relative light units [RLU]). 0aa, 0 amino acid. (C) Infectious virus production at 72 h postelectroporation, as measured by luciferase activity in infected cells. GNN, replication-deficient control, WT, wild-type NS2 protease; H143A, cleavage-deficient NS2 protease. The means plus standard errors of the means (error bars) for three independent experiments with two different RNA preparations are shown. (D) NS2 protein expression at 72 h postelectroporation of either wild-type or cleavage-deficient (H) NS3 extension constructs. Top panel NS2 (6H6 antibody), NS5A protein in the middle panel (9E10 antibody), and β-actin control in the bottom. GNN, corresponding polymerase-defective control of wild-type NS2. The positions of molecular mass markers (in kilodaltons) are indicated to the right of the immunoblots.

after a single autoproteolytic processing event (21). Although NS2 expression and stability were not dramatically altered by most C-terminal substitutions, it is possible that deletion of L217 changes the structure of NS2 by liberating the C terminus from the active site. Releasing the C terminus might alter the position of the C-terminal subdomain, affecting surfaces required for essential interactions, such as dimerization or heterotypic associations with viral or host proteins. A similar function of a C-terminal residue is seen for the alphavirus capsid protein, which is also an autoprotease involved in infectious virus assembly. Analogous to NS2, the highly conserved C-terminal tryptophan of the alphavirus capsid occupies the active site postcleavage (4); in fact, distinct similarities have been noted in the catalytic cleft architecture of the two enzymes (21). Mutation of this C-terminal tryptophan to alanine or arginine in a system that uncoupled proteolysis from infectious alphavirus production almost completely abolished nucleocapsid assembly; substitution of the terminal tryptophan with phenylalanine, however, was tolerated (35). Similarly, mutations in the alphavirus capsid that displaced the terminal tryptophan from the active site pocket were found to be highly deleterious to its function (3). These observations suggest that the location of the C terminus, as well as the presence of a leucine or similar residue at position 217, may be critical to the structure and postcleavage functions of these viral proteases.

Further supporting the critical role for L217 in infectious virus production, we found that C-terminal extensions into NS3 were highly deleterious; even one additional amino acid reduced viral titers by three to fivefold. Similar results have been previously reported, where ubiquitin fused to the NS2 C terminus abolished infectious virus production (13). Interestingly, we observed that extensions shorter than the minimal functional NS3 protease domain (31, 40, and 90 amino acids) showed NS2-3 processing to some extent in the context of a functional NS2 active site; recent work from Schregel et al. has similarly demonstrated residual enzymatic activity of NS2 followed by only 2 amino acids of NS3 (33). Despite detectable

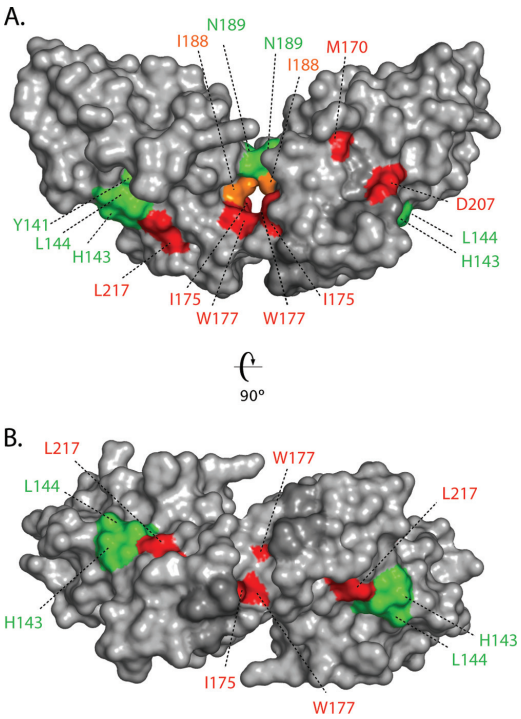

FIG. 9. Summary of critical NS2^{pro} residues. (A) Exposed surface rendering of the NS2^{pro} dimer. Mutations showing abolished infectious virus production are shown in red (M170, I175, W177, D207, and L217), mutations showing impaired infectious virus production are shown in orange (P164 and I188), and mutations with no significant effect on infectious virus production are shown in green (Y141, H143, L144, N189, and L191). (B) NS2^{pro} dimer rotated 90° around the horizontal axis as shown in panel A.

NS2-3 processing, however, genomes encoding NS3 extensions still did not support infectious virus production. This could indicate that insufficient quantities of mature NS2 are produced by suboptimal cleavage or that short fragments of NS3 impair infectivity, possibly by acting as dominant-negative inhibitors of interactions between NS2 and full-length NS3 (15). The finding that fused residues from NS3 are deleterious to the role of HCV NS2 infectivity contrasts with the related pestiviruses, in which the uncleaved NS2-3 precursor is essential for infectious virus production (1, 23). The possibility that NS2 and NS3 form functional associations during virion morphogenesis, however, suggests conserved strategies between HCV and other members of the family *Flaviviridae* (24).

Using monocistronic and bicistonic genomes, we were able to analyze the effects of NS2 mutations on protease activity and postcleavage functions. Our results add to accumulating evidence that the determinants of these two essential roles are divergent. Previous work has demonstrated that the transmembrane domains of NS2 play critical roles in infectivity (13) but are not absolutely required for protease activity (10, 26, 32, 37). Conversely, the active cleft is essential for the protease function but predominantly dispensable for infectivity (13, 14; this study). A number of substitutions in the dimer crossover region and C-terminal subdomain affected infectious titers, but not protease activity, and L217 was found to be dispensable for processing but critical for infectious virus production. Similarly, the finding that NS2 functions in assembly do not tolerate C-terminal extensions contrasts with the requirement for the NS3 protease domain for optimal NS2-3 cleavage. These differences highlight the two distinct functions of NS2 and suggest that further analysis of these roles may reveal important regulatory switches.

In conclusion, we dissected the determinants of the NS2 protease domain required for infectious virus production. We found critical roles for residues in the dimer crossover region and at the extreme C terminus of the protein, and we showed that C-terminal extensions into NS3 are deleterious to infectivity. These insights increase our understanding of the multifunctional NS2 protein and may facilitate exploiting this target for antiviral drug development.

ACKNOWLEDGMENTS

We thank Maryline Panis and Anesta Webson for laboratory support and technical assistance. We are grateful to Catherine L. Murray, Christopher T. Jones, Cynthia de la Fuente, and Kimberly D. Ritola for reagents, constructs, helpful discussions, and critical reading of the manuscript.

This study was supported by The Greenberg Medical Research Institute, NIH Public Health Service grant (AI075099), and the Starr Foundation. T.G.D. is supported by the Fonds National de la Recherche Luxembourg.

REFERENCES

1. **Agapov, E. V., C. L. Murray, I. Frolov, L. Qu, T. M. Myers, and C. M. Rice.** 2004. Uncleaved NS2-3 is required for production of infectious bovine viral diarrhea virus. J. Virol. **78:**2414–2425.
2. **Blight, K. J., J. A. McKeating, and C. M. Rice.** 2002. Highly permissive cell lines for subgenomic and genomic hepatitis C virus RNA replication. J. Virol. **76:**13001–13014.
3. **Choi, H. K., S. Lee, Y. P. Zhang, B. R. McKinney, G. Wengler, M. G. Rossmann, and R. J. Kuhn.** 1996. Structural analysis of Sindbis virus capsid mutants involving assembly and catalysis. J. Mol. Biol. **262:**151–167.
4. **Choi, H. K., L. Tong, W. Minor, P. Dumas, U. Boege, M. G. Rossmann, and G. Wengler.** 1991. Structure of Sindbis virus core protein reveals a chymotrypsin-like serine proteinase and the organization of the virion. Nature **354:**37–43.
5. **Dumoulin, F. L., A. von dem Bussche, J. Li, L. Khamzina, J. R. Wands, T. Sauerbruch, and U. Spengler.** 2003. Hepatitis C virus NS2 protein inhibits gene expression from different cellular and viral promoters in hepatic and nonhepatic cell lines. Virology **305:**260–266.
6. **Erdtmann, L., N. Franck, H. Lerat, J. Le Seyec, D. Gilot, I. Cannie, P. Gripon, U. Hibner, and C. Guguen-Guillouzo.** 2003. The hepatitis C virus NS2 protein is an inhibitor of CIDE-B-induced apoptosis. J. Biol. Chem. **278:**18256–18264.
7. **Everhart, J. E., Y. Wei, H. Eng, M. R. Charlton, D. H. Persing, R. H. Wiesner, J. J. Germer, J. R. Lake, R. K. Zetterman, and J. H. Hoofnagle.** 1999. Recurrent and new hepatitis C virus infection after liver transplantation. Hepatology **29:**1220–1226.
8. **Franck, N., J. Le Seyec, C. Guguen-Guillouzo, and L. Erdtmann.** 2005. Hepatitis C virus NS2 protein is phosphorylated by the protein kinase CK2 and targeted for degradation to the proteasome. J. Virol. **79:**2700–2708.
9. **Grakoui, A., D. W. McCourt, C. Wychowski, S. M. Feinstone, and C. M. Rice.** 1993. A second hepatitis C virus-encoded proteinase. Proc. Natl. Acad. Sci. USA **90:**10583–10587.
10. **Grakoui, A., D. W. McCourt, C. Wychowski, S. M. Feinstone, and C. M. Rice.** 1993. Characterization of the hepatitis C virus-encoded serine proteinase: determination of proteinase-dependent polyprotein cleavage sites. J. Virol. **67:**2832–2843.
11. **Hijikata, M., H. Mizushima, T. Akagi, S. Mori, N. Kakiuchi, N. Kato, T. Tanaka, K. Kimura, and K. Shimotohno.** 1993. Two distinct proteinase activities required for the processing of a putative nonstructural precursor protein of hepatitis C virus. J. Virol. **67:**4665–4675.

12. **Hirowatari, Y., M. Hijikata, Y. Tanji, H. Nyunoya, H. Mizushima, K. Kimura, T. Tanaka, N. Kato, and K. Shimotohno.** 1993. Two proteinase activities in HCV polypeptide expressed in insect cells using baculovirus vector. Arch. Virol. **133:**349–356.
13. **Jirasko, V., R. Montserret, N. Appel, A. Janvier, L. Eustachi, C. Brohm, E. Steinmann, T. Pietschmann, F. Penin, and R. Bartenschlager.** 2008. Structural and functional characterization of nonstructural protein 2 for its role in hepatitis C virus assembly. J. Biol. Chem. **283:**28546–28562.
14. **Jones, C. T., C. L. Murray, D. K. Eastman, J. Tassello, and C. M. Rice.** 2007. Hepatitis C virus p7 and NS2 proteins are essential for production of infectious virus. J. Virol. **81:**8374–8383.
15. **Kiiver, K., A. Merits, M. Ustav, and E. Zusinaite.** 2006. Complex formation between hepatitis C virus NS2 and NS3 proteins. Virus Res. **117:**264–272.
16. **Kolykhalov, A. A., E. V. Agapov, K. J. Blight, K. Mihalik, S. M. Feinstone, and C. M. Rice.** 1997. Transmission of hepatitis C by intrahepatic inoculation with transcribed RNA. Science **277:**570–574.
17. **Liang, T. J., B. Rehermann, L. B. Seeff, and J. H. Hoofnagle.** 2000. Pathogenesis, natural history, treatment, and prevention of hepatitis C. Ann. Intern. Med. **132:**296–305.
18. **Lindenbach, B. D., M. J. Evans, A. J. Syder, B. Wolk, T. L. Tellinghuisen, C. C. Liu, T. Maruyama, R. O. Hynes, D. R. Burton, J. A. McKeating, and C. M. Rice.** 2005. Complete replication of hepatitis C virus in cell culture. Science **309:**623–626.
19. **Liu, Q., R. A. Bhat, A. M. Prince, and P. Zhang.** 1999. The hepatitis C virus NS2 protein generated by NS2-3 autocleavage is required for NS5A phosphorylation. Biochem. Biophys. Res. Commun. **254:**572–577.
20. **Lohmann, V., F. Korner, J. Koch, U. Herian, L. Theilmann, and R. Bartenschlager.** 1999. Replication of subgenomic hepatitis C virus RNAs in a hepatoma cell line. Science **285:**110–113.
21. **Lorenz, I. C., J. Marcotrigiano, T. G. Dentzer, and C. M. Rice.** 2006. Structure of the catalytic domain of the hepatitis C virus NS2-3 protease. Nature **442:**831–835.
22. **Moradpour, D., F. Penin, and C. M. Rice.** 2007. Replication of hepatitis C virus. Nat. Rev. Microbiol. **5:**453–463.
23. **Moulin, H. R., T. Seuberlich, O. Bauhofer, L. C. Bennett, J. D. Tratschin, M. A. Hofmann, and N. Ruggli.** 2007. Nonstructural proteins NS2-3 and NS4A of classical swine fever virus: essential features for infectious particle formation. Virology **365:**376–389.
24. **Murray, C. L., C. T. Jones, and C. M. Rice.** 2008. Architects of assembly: roles of Flaviviridae non-structural proteins in virion morphogenesis. Nat. Rev. Microbiol. **6:**699–708.
25. **Murray, C. L., C. T. Jones, J. Tassello, and C. M. Rice.** 2007. Alanine scanning of the hepatitis C virus core protein reveals numerous residues essential for production of infectious virus. J. Virol. **81:**10220–10231.
26. **Pallaoro, M., A. Lahm, G. Biasiol, M. Brunetti, C. Nardella, L. Orsatti, F. Bonelli, S. Orru, F. Narjes, and C. Steinkuhler.** 2001. Characterization of the hepatitis C virus NS2/3 processing reaction by using a purified precursor protein. J. Virol. **75:**9939–9946.
27. **Penin, F., J. Dubuisson, F. A. Rey, D. Moradpour, and J. M. Pawlotsky.** 2004. Structural biology of hepatitis C virus. Hepatology **39:**5–19.
28. **Pietschmann, T., A. Kaul, G. Koutsoudakis, A. Shavinskaya, S. Kallis, E. Steinmann, K. Abid, F. Negro, M. Dreux, F. L. Cosset, and R. Bartenschlager.** 2006. Construction and characterization of infectious intragenotypic and intergenotypic hepatitis C virus chimeras. Proc. Natl. Acad. Sci. USA **103:**7408–7413.
29. **Pietschmann, T., V. Lohmann, A. Kaul, N. Krieger, G. Rinck, G. Rutter, D. Strand, and R. Bartenschlager.** 2002. Persistent and transient replication of full-length hepatitis C virus genomes in cell culture. J. Virol. **76:**4008–4021.
30. **Reed, K. E., A. Grakoui, and C. M. Rice.** 1995. Hepatitis C virus-encoded NS2-3 protease: cleavage-site mutagenesis and requirements for bimolecular cleavage. J. Virol. **69:**4127–4136.
31. **Ryan, M. D., A. M. King, and G. P. Thomas.** 1991. Cleavage of foot-and-mouth disease virus polyprotein is mediated by residues located within a 19 amino acid sequence. J. Gen. Virol. **72:**2727–2732.
32. **Santolini, E., L. Pacini, C. Fipaldini, G. Migliaccio, and N. Monica.** 1995. The NS2 protein of hepatitis C virus is a transmembrane polypeptide. J. Virol. **69:**7461–7471.
33. **Schregel, V., S. Jacobi, F. Penin, and N. Tautz.** 2009. Hepatitis C virus NS2 is a protease stimulated by cofactor domains in NS3. Proc. Natl. Acad. Sci. USA **106:**5342–5347.
34. **Selby, M. J., E. Glazer, F. Masiarz, and M. Houghton.** 1994. Complex processing and protein:protein interactions in the E2:NS2 region of HCV. Virology **204:**114–122.
35. **Skoging, U., and P. Liljestrom.** 1998. Role of the C-terminal tryptophan residue for the structure-function of the alphavirus capsid protein. J. Mol. Biol. **279:**865–872.
36. **Steinmann, E., F. Penin, S. Kallis, A. H. Patel, R. Bartenschlager, and T. Pietschmann.** 2007. Hepatitis C virus p7 protein is crucial for assembly and release of infectious virions. PLoS Pathog. **3:**e103.
37. **Thibeault, D., R. Maurice, L. Pilote, D. Lamarre, and A. Pause.** 2001. In vitro characterization of a purified NS2/3 protease variant of hepatitis C virus. J. Biol. Chem. **276:**46678–46684.
38. **Welbourn, S., R. Green, I. Gamache, S. Dandache, V. Lohmann, R. Bartenschlager, K. Meerovitch, and A. Pause.** 2005. Hepatitis C virus NS2/3 processing is required for NS3 stability and viral RNA replication. J. Biol. Chem. **280:**29604–29611.
39. **Yamaga, A. K., and J. H. Ou.** 2002. Membrane topology of the hepatitis C virus NS2 protein. J. Biol. Chem. **277:**33228–33234.
40. **Yi, M., Y. Ma, J. Yates, and S. M. Lemon.** 2007. Compensatory mutations in E1, p7, NS2, and NS3 enhance yields of cell culture-infectious intergenotypic chimeric hepatitis C virus. J. Virol. **81:**629–638.

10 Chapter 4: NS2 dimerization

Structural data revealed that NS2 is present as a dimer in order to create the two composite active sites to mediate cleavage. With the help of various assays, we tried to detect NS2 oligomers.

10.1 Chemical crosslinking of NS2

The classical biochemical approach of isolation and characterization of protein components does not always reveal transient interactions or migratory behavior of proteins, which occur in the natural environment of the cell. Crosslinking technology is the exploitation of homo- and heterobifunctional reagents to identify ligand-binding components in complex biological systems. The covalent linkage of a ligand to a specific protein provides a strategy for visualizing this behavior.

10.1.1 *In vitro* dimerization: purified $NS2^{pro}$

To identify possible binding sites of a specific crosslinker, the distances between side chains of various amino acids lying on the surface of the $NS2^{pro}$ dimer were measured. A set of crosslinker was then chosen based on the arm spacer length and its physical properties. These reagents were predicted to bind two NS2 molecules by a covalent bond (Table 1).

In a first screen, crosslinker were tested with purified $NS2^{pro}$ protein. This was the same protein we used to determine the $NS2^{pro}$ crystal structure. $NS2^{pro}$ allowed us to identify crosslinker that react with purified NS2 protein, without the interference of other proteins or factors present in a cell. The purified HCV NS2 protein used for these experiments spans amino acids 94-217 and is thus smaller (14.5 kDa) than NS2 generated by the virus (~23 kDa). Crosslinker were added to purified NS2 protein at various molar ratios of crosslinker:protein at a pH of 7.5. Three different crosslinker concentrations were used, corresponding to a molar excess of 1x, 10x and 50x of the protein concentration. After 90 min of incubation at room temperature, the samples were subjected to SDS-PAGE (4 to 20% gradient gel), and proteins were visualized by staining with Coomassie Blue.

The screens on purified NS2 protein revealed that the two similar crosslinker DSS (Disuccinimidyl suberate), molecular weight of 368.35 with an 11.4 Å spacer arm and EGS [Ethylene glycolbis(succinimidylsuccinate)] with a molecular weight of 456.36 and a 16.1 Å spacer arm efficiently crosslinked $NS2^{pro}$, thus showing a dimer. Supplementary experiments, described below, confirmed the ability of DSS and EGS as a potent crosslinker.

DSS is a water-insoluble, homobifunctional N-hydroxysuccinimide ester (NHS ester). NHS esters react efficiently with primary amino groups (-NH2) in pH 7-9 buffers to form stable amide bonds. The reaction results in the release of N-hydroxysuccinimide. Proteins generally have several primary amines in the side chain of lysine (K) residues and the N terminus of each polypeptide that are available as targets for NHS-ester reagents. DSS does not possess a charged group and is lipophilic and membrane-permeable, which makes it useful for intracellular and intramembrane conjugations (Fig. 4-1).

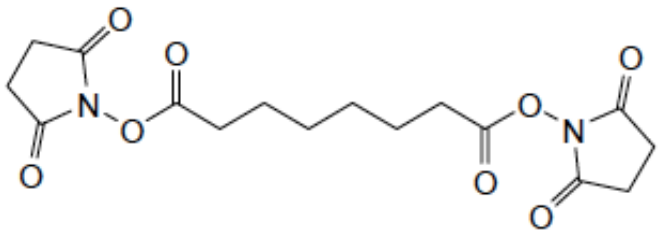

Fig. 4-1. Chemical structure of Disuccinimidyl suberate (DSS).

In order to find the optimal crosslinker concentration, DSS was added in a more narrow range of molar ratios of crosslinker:protein, as shown in (Fig. 4-2). The dimer was already visible at low concentrations of added crosslinker and levels gradually increased with higher crosslinker concentrations. In addition, trimeric and even tetrameric $NS2^{pro}$ was detected at high crosslinker concentrations. Complete crosslinking of the monomer could be achieved at a 16x concentration.

To prove that the dimerization seen in Fig. 4-2 is not due to high protein concentrations, we repeated the same experiment with different protein concentrations, and constant DSS

crosslinker concentration, as shown in Fig. 4-2, B. Crosslinking occurs at protein concentrations from 100 to 10μM. We were unable to detect $NS2^{pro}$ at lower protein concentrations in a coomassie gel. This demonstrates clearly that the dimerization is not due to high protein concentrations. The same experiments were done under different temperatures, 4, 20, and 60 °C. No protein and no crosslinking could be detected at 60 degrees Celsius, while there was no difference between 4 and 20 °C (data not shown).

Crosslinker	size in A	reactive groups	reactive towards	water-soluble	membrane permeable	cleavable	M.W.
AMAS	4.4	maleimide and NHS-ester	sulfhydryl and amino groups	no	n/a	no	252.18
BS3	11.4	sulfo-NHS-ester (homobifunctional)	amino groups	yes	no	no	572.43
DMA	8.3	imidoester (homobifunctional)	amino groups	yes	yes	no	245.15
DMS	11	imidoester (homobifunctional)	amino groups	yes	yes	no	273.2
DSP	12	NHS-ester (homobifunctional)	amino groups	no	yes	yes	404.42
DSS	11.4	NHS-ester (homobifunctional)	amino groups	no	yes	no	368.35
DTBP	11.9	imidoester (homobifunctional)	amino groups	yes	yes	yes	309.28
DTSSP	12	sulfo-NHS-ester (homobifunctional)	amino groups	yes	no	yes	608.51
EGS	16.1	NHS-ester (homobifunctional)	amino groups	no	n/a	yes	456.36
SADP	13.9	phenyl azide and NHS-ester	amino groups	no	n/a	yes	352.39
SANPAH	18.2	nitrophenyl azide and NHS-ester	amino groups	no	n/a	n/a	390.35
SATA	2.8	NHS-ester and thioacetyl-protected sulfhydryl	amino and maleimide/iodoacetyl or vinyl sulfone	n/a	n/a	yes	231.23
SATP	4.1	NHS-ester and thioacetyl-protected sulfhydryl	amino and maleimide/iodoacetyl or vinyl sulfone	n/a	n/a	yes	245.25
SIAB	10.6	iodoacetyl and NHS-ester	sulfhydryl and amino groups	no	n/a	n/a	402.14
SMPH	14.3	maleimide and NHS-ester	sulfhydryl and amino groups	no	n/a	no	379.36
Sulfo-DST	6.4	sulfo-NHS-ester (homobifunctional)	amino groups	yes	n/a	yes	548.32
Sulfo-SADP	13.9	phenyl azide and sulfo-NHS-ester	amino groups	yes	n/a	yes	454.44

Table 4-1: Chemical crosslinker. List of crosslinker that potentially link two HCV NS2 monomers via covalent binding.

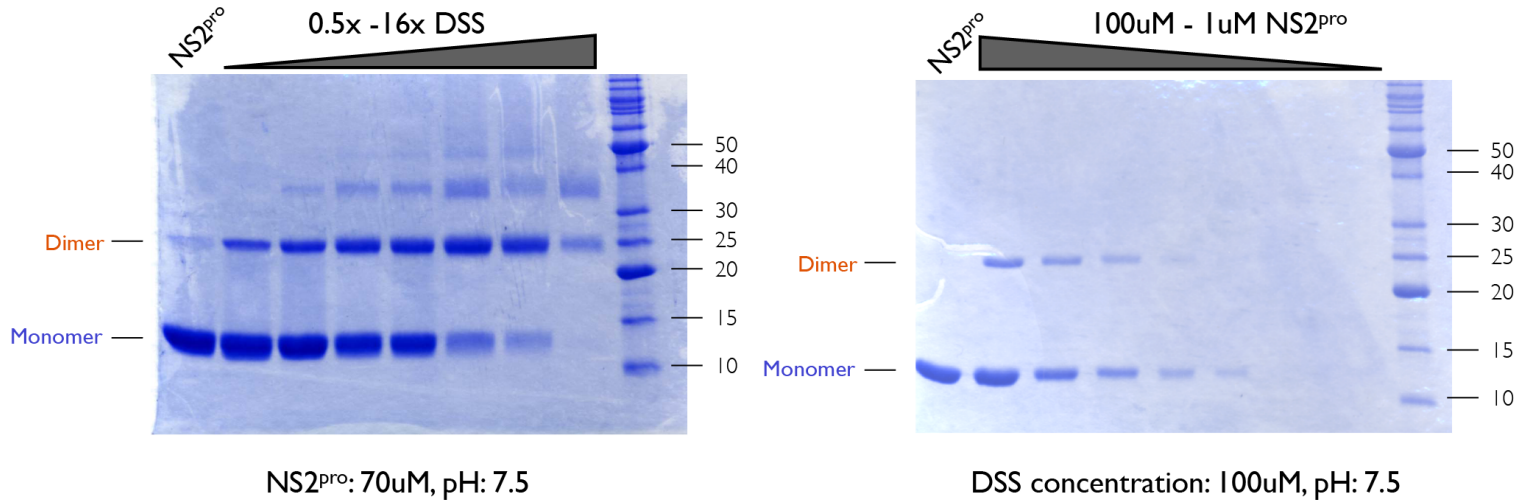

Fig. 4-2. Crosslinking of NS2^{pro} with DSS. **A.** DSS concentration range. DSS was added to purified NS2 at various molar ratios of crosslinker:protein, followed by separation of the proteins by SDS-PAGE. Lane 1, no crosslinker added. **B.** NS2 concentration range. Various concentrations of purified NS2 were incubated with a constant 100 uM concentration of DSS, followed by separation of the protein by SDS-PAGE. Lane 1, no crosslinker added.

10.1.2 Dimerization in mammalian cells expressing HCV NS2-NS3

Based on the results from previous crosslinking experiments with purified $NS2^{pro}$ protein, a crosslinking assay in U2OS and Huh-7.5 cells was established to test whether NS2 expressed in tissue culture was able to form dimers.

A vaccinia virus (vTF7-3) T7 polymerase system was used to express NS2-NS3 constructs in mammalian cells. These constructs contained the NS2 protease domain (aa 94-217) and the N-terminal region of NS3 (aa 1-181). Cells were infected with the vTF7-3 vaccinia helper virus, followed by transfection of the cells with the NS2-NS3 expressing construct. Twenty-four hours later, the cells were washed and crosslinked either before or after lysis, depending on the crosslinker properties. Proteins were then resolved by SDS-PAGE and analyzed by immunoblotting.

DSS and EGS crosslinker that efficiently crosslinked the purified protein, also showed the best results in transfected HuH-7.5 cells in a crosslinker screen. A wider range of DSS crosslinker concentrations determined the best protein:crosslinker ratio for dimerization shown in Fig. 4-3.

Dimerization could be detected in U2OS cells at concentrations as low as 0.05 and 0.5 mM DSS, while a 0.5 mM concentration showed better crosslinking and higher order oligomerization. NS2 crosslinking in Huh-7.5 cells occurred at a concentration of 0.05 mM DSS and efficiency increased with the amount of DSS added, ranging from 0.05 to 5 mM (Fig. 4-3).

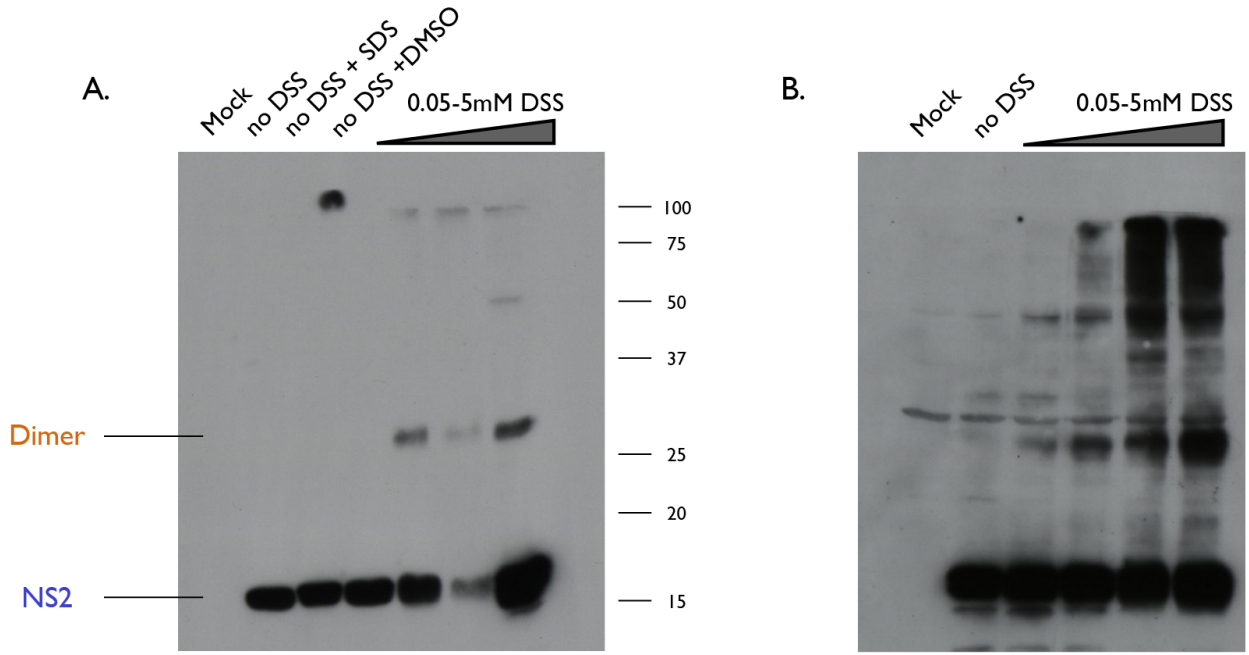

Fig. 4-3. NS2 crosslinking in cells. Immunoblot with an anti-NS2 antibody (Wu107). **A.** U2OS cells. 0.05 to 5mM of DSS was added 30 h post-transfection of NS2/NS3 constructs. **B.** HuH7.5 cells. NS2/NS3 constructs were transfected into Huh-7.5 cells and crosslinked 30 h later with 0.05 mM to 5 mM DSS. Monomeric NS2 (blue) and its dimeric form (orange) are indicated in color.

10.1.3 Dimerization in mammalian cells expressing HCV full-length genomes

After successful crosslinking of over-expressed NS2-NS3, a full length J6/H77/JFH genome was expressed in Huh-7.5 cells with a vTF7-3 vaccinia helper virus.

Fig. 4-13 shows a time dependent crosslinking experiment. The reaction was stopped after 5, 10, 20, or 30 min of incubation with the crosslinker at a concentration of 0.5mM. Control lanes 1 and 2 without DSS showed no NS2 dimer, while an NS2 dimer could be detected after 5 min, and up to 30 min in lanes 3 to 6 respectively.

In Fig. 4-4, samples were all crosslinked for 30 min with increasing amounts of DSS crosslinker. All DSS containing samples showed detectable NS2 dimer. A DSS concentration of 0.4 mM gave a more pronounced band while higher concentrations (0.5, and 0.6 mM) showed weaker bands than lower concentrations.

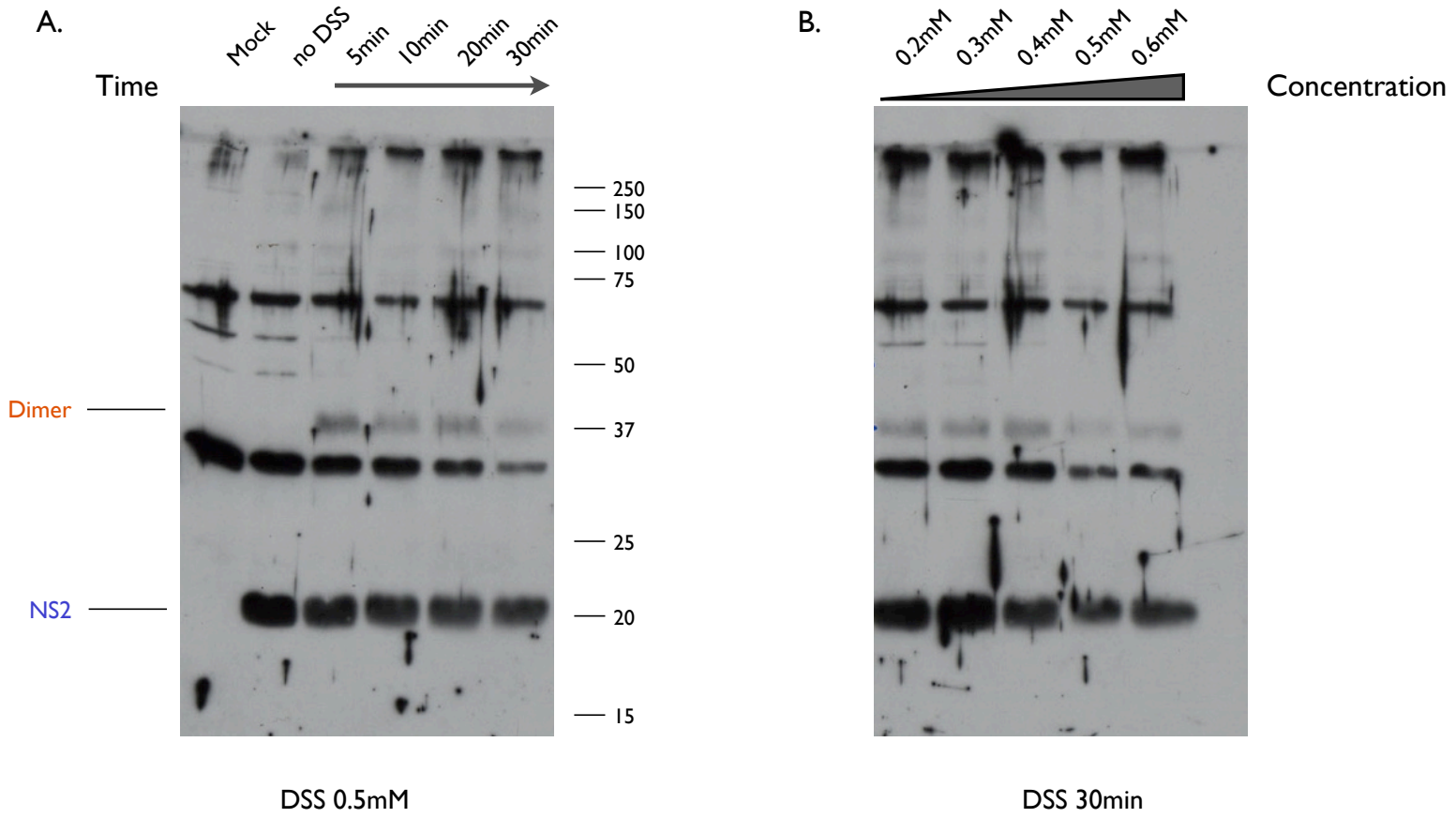

Fig. 4-4. Full length HCV crosslinking. A. Time dependent crosslinking. A full length HCV genome was incubated for 30 min in the presence of 0.5 mM DSS, followed by separation of the proteins by SDS-PAGE and detection of NS2. **B**. Various DSS concentrations (0.2-0.6 mM) were incubated with the lysates for 30 min, followed by separation of the proteins by SDS-PAGE and detection of NS2. Monomeric NS2 (blue) and its dimeric form (orange) are indicated in color.

10.2 Fluorescence resonance energy transfer (FRET) dimerization assay

We have shown that residues at the NS2 protease domain are involved in polyprotein processing and infectious virus production. Several mutations revealed a deficiency in RNA replication in the monocistronic background, which could be overcome in the bicistronic system. Focusing on the NS2 residues around the active site, tyrosine 141 and the cis-proline 164, we wanted to investigate the cause of this effect.
Based on previously described findings, it is thought that NS2 acts as a dimer and that the C-terminus stays bound to the active site allowing only one cleavage event to happen. A possible explanation for the non-replicating mutant viruses could be the destabilization of the dimer or complete failure of dimerization by the introduced mutation.

A functional interaction between two NS2 monomers, dimerization, seems to be critical to the production of infectious progeny. We developed an assay to analyze these interactions under physiologically relevant conditions. Fluorescence resonance energy transfer (FRET) can be used to detect close co-localization of proteins within a cell. We have created constructs expressing NS2 fused to a FRET acceptor and a FRET donor fluorescent proteins (Fig. 4-5).
NS2 could be expressed as a C-terminal fusion with EGFP or mCherry by incorporating a flexible linker and six residues of NS3 following NS2. To increase our signal to noise ratio, we engineered our NS2 mutations and wild type into a different pair of acceptor and donor, Venus and Cerulean.

Expression of Venus and Cerulean versions were comparable (Fig. 4-6), but only the NS2(1-6) containing the C-terminus of p7, full length NS2, and six amino acids from NS3 before the flexible linker produced a robust FRET signal. Constructs containing a linker and forty residues of NS3, a signal sequence before the fluorophore followed by NS2, and the Sig CTR construct without NS2 did not produce FRET (Fig. 4-7). Evaluation of the various modified wild type constructs showed only 29% signal for NS2(1-40), 16% for Sig CTR and 22% for Sig NS2. The critical distance between the protein and the fluorophore to produce a FRET signal is six residues plus a flexible linker, whereas 40 amino acids have proven to be too long (Fig. 4-7).

A. pCMV-p7-NS2-NS3 (aa1-6)-VEN

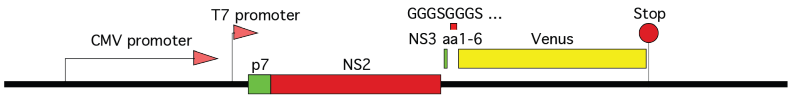

B. pCMV-p7-NS2-NS3 (aa1-40)-VEN

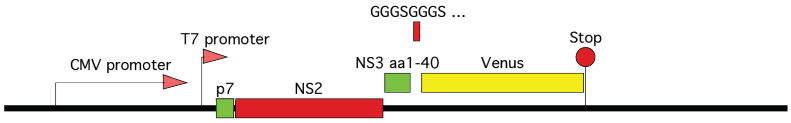

C. pCMV-Sig-VEN-CTR

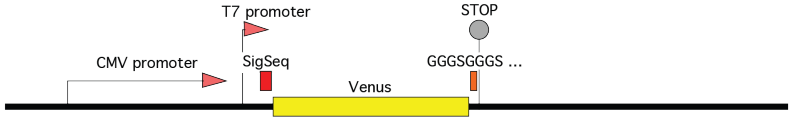

D. pCMV-Sig-VEN-NS2

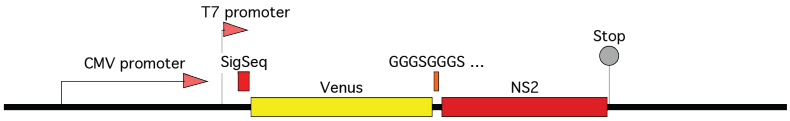

Fig. 4-5: FRET pair constructs Venus/Cerulean. In the background of a pCMV, driven by a CMV or alternatively a T7 promoter, NS2 constructs were engineered containing the C-terminal of p7, full length NS2, and either the first six residues of NS3 (A), or the first forty amino acids of NS3 (B). Venus or Cerulean fused to the NS3 residues via a flexible linker followed by a stop codon. (C) pCMV-Sig-VEN-CTR is a control construct that doesn't express NS2 and pCMV-Sig-VEN-NS2 contains a signal sequence before Venus, then the linker and NS2, followed by a stop codon (D).

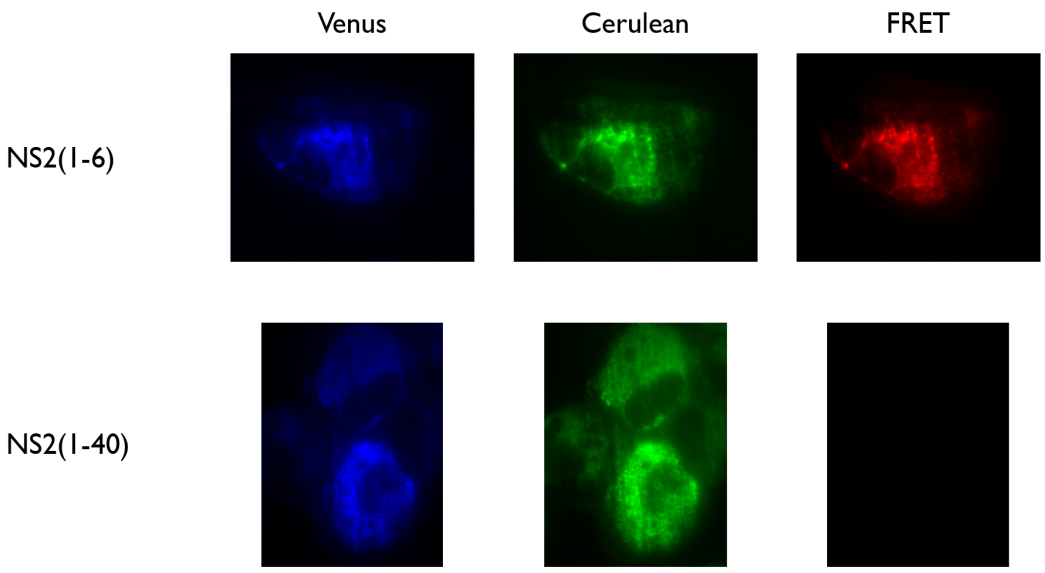

Fig. 4-6. NS2 Venus and Cerulean expression with FRET signal. Top: Expression of the Venus NS2(1-6) (blue) and the Cerulean NS2(1-6) construct (green). FRET signal is shown in red. Bottom: Expression of the negative control Venus NS2(1-40) (blue) and the Cerulean NS2(1-40) construct (green) with corresponding FRET signal.

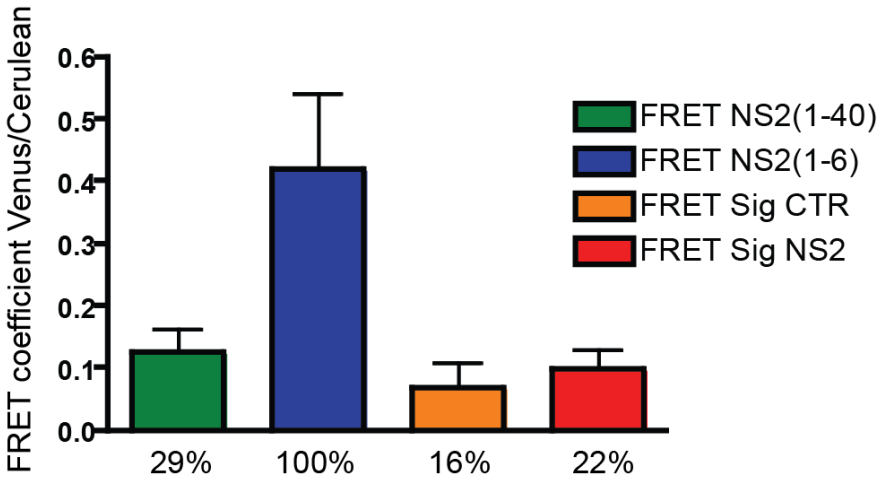

Fig. 4-7. Comparison of various FRET pair constructs. NS2 followed by forty residues of NS3 and a flexible linker (green), NS2 with six residues of NS3 and a flexible linker (blue). Sig NS2 CTR with a signal sequence in front of Venus or Cerulean, then a flexible linker and a stop codon (orange). Sig NS2 containing a signal sequence, Venus or Cerulean, and the linker that connects to the N-terminus of NS2 followed by a stop codon at the C-terminus of NS2 (red).

We analyzed mutations in the background of the NS2(1-6) construct while using the NS2(1-40) construct as a no FRET control. Two different residues around the active site with four different mutations showed distinctive effects on RNA replication and therefore also virus production. The first residue, tyrosine 141 is located next to the active site residue histidine 143. The dimerization assay showed a strong signal (107%) for Y141F compared to wild type whereas Y141A demonstrated only 40% FRET signal. These results correlate well with our RNA replication data where Y141 in a monocistronic background did not replicate when mutated to an alanine while a phenylalanine substitution behaved like wild type (55). This may indicate that the defect is actually caused by low dimerization levels of the mutant NS2 or even complete inhibition of dimer formation. The cis-proline 164 presents a similar effect (Figs. 4-8 and 4-9). An alanine substitution gave up to 67% of FRET signal, while P164G only up to 50% compared to wild type. Neither of these mutations replicated in the monocistronic background, possibly by preventing NS2 dimer formation. Interestingly, Infectious virus production was still impaired in the bicistronic background, which may hint to an NS2 dimer function in infectious particle production.

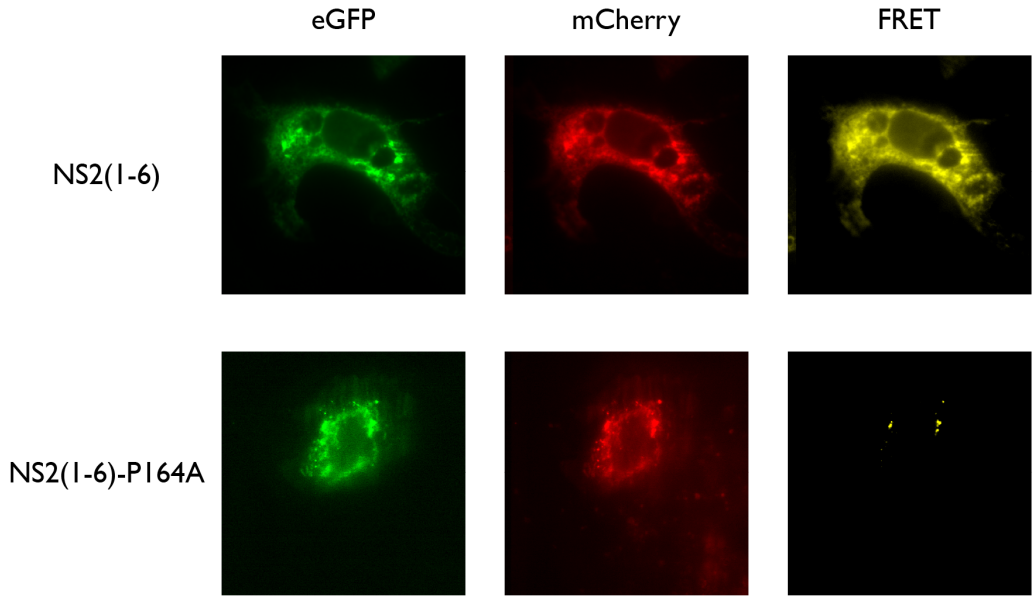

Fig. 4-8. NS2 wild type and P164A FRET. Expression of the eGFP NS2(1-6) (green) and mCherry NS2(1-6) construct (red). FRET signal is shown in yellow. Top shows wild type NS2, while the bottom represents the NS2 P164A mutation.

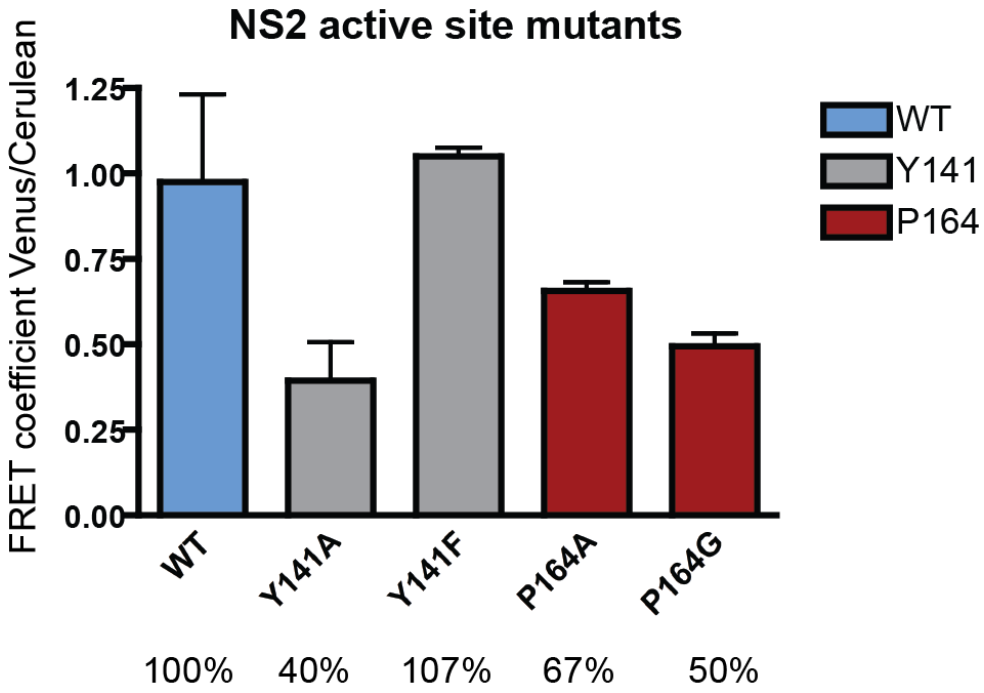

Fig. 4-9. FRET signal of NS2 active site mutations. 24 hours post-transfection with NS2 constructs; Huh7.5 cells were excited with a 480 nm laser to determine FRET. Results represent means of three different regions with 50 spots/cell. Wild type NS2 (blue), Mutation Y141 (grey), Mutations P164A (red).

11 Chapter 5: Additional functions of the NS2/NS3 cleavage site

11.1 Introduction

NS2/NS3 interactions as well as NS2/NS3 processing of the polyprotein represent important steps in the viral life cycle. We found that the NS2/NS3 cleavage site fulfills additional important roles, notably in infectious virus production. Further we were able to establish an NS2-NS3 structural model of interactions and found genetic evidence and of NS2-E1 and NS2-NS3 interactions. The results of our study will be submitted for publication to the journal of virology with the title:

11.2 "Importance of NS2 and NS3 interplay in infectious hepatitis C virus production" (Publication 2)

Importance of NS2 and NS3 interplay in infectious hepatitis C virus production

Thomas G. Dentzer[1, 2], Meigang Gu[1], and Charles M. Rice[1*]

[1]Center for the Study of Hepatitis C, Laboratory of Virology and Infectious Disease, The Rockefeller University, 1230 York Avenue, New York, New York 10065,
[2]Laboratoire de Rétrovirologie, Centre de Recherche Public-Santé, 84 rue Val Fleuri, L-1526 Luxembourg

Running title: NS2/3 cleavage site and interaction residues

*To whom correspondence should be addressed: Laboratory of Virology and Infectious Disease, Center for the Study of Hepatitis C, The Rockefeller University, 1230 York Ave., New York, NY 10065. Phone: (212) 327-7046. Fax: (212) 327-7048. E-mail: ricec@rockefeller.edu

Introduction

The hepatitis C virus (HCV), a member of the Flaviviridae, has become a major global health problem over the last two decades with close to 3% of the human population infected (1, 9). The disease is primarily transmitted via blood but other routes, such as non-injection drug use, have been proposed. The virus typically establishes a chronic infection, which can consequently lead to liver cirrhosis, HCC, and end-stage liver disease (56, 57). In the Western world, HCV is a leading indicator for liver transplantation, although this procedure is not curative as reinfection of the graft occurs universally (69). There is no vaccine for HCV and current therapy -pegylated interferon-α in combination with ribavirin - leads to a sustained response in only about half of genotype 1-infected patients (183).

The HCV genome consists of a positive-stranded RNA of 9.6 kb, which encodes a single open reading frame flanked by a 5' and 3' untranslated regions (UTR) (204, 223). Translation, which is driven by an internal ribosomal entry site (IRES) within the 5' UTR, produces a polyprotein that is co- and post-translationally cleaved into ten distinct viral proteins. The structural proteins core, E1, and E2 are followed by the NS proteins p7, NS2, NS3, NS4A, NS4B, NS5A, NS5B, which are responsible for viral RNA synthesis and virion assembly (15, 55, 112, 114, 117, 175, 256).

NS2 (23 kDa) is a hydrophobic protein containing one to three TM

segments in the N-terminal region and protease activity in the C-terminal domain (112). The protease domain of NS2 ($NS2^{pro}$) and the N-terminal third of NS3 form the NS2-3 protease, which responsible for the single intramolecular cleavage between the two proteins. While 181 residues of NS3 are required for optimal NS2-3 protease activity, basal levels of cleavage could be detected with as little as 2 amino acids of NS3 (58, 99, 245). In vitro studies have shown that purified NS2-3 protease is active in the absence of additional cofactors (99, 245, 268). The crystal structure of $NS2^{pro}$ revealed a dimeric cysteine protease containing two composite active sites; the C terminus stays bound to the active site after cleavage, rendering $NS2^{pro}$ inactive (167). NS2 is not required for the replication of subgenomic replicons, which span NS3 to NS5B (164). However, cleavage at the NS2/3 junction is necessary for replication in chimpanzees (131), the full-length replicon (292), and in cell culture (114). NS2 has been described to interact with every HCV NS protein and various cellular partners (58, 66, 78, 100). Co-immunoprecipitation experiments have shown a direct interaction between NS2 and NS3 (58, 99, 126).

A second protease, NS3-4A, cleaves the remainder of the viral polyprotein in the NS region (84, 99, 245). NS3 (70 kDa) encodes a serine protease activity in the N-terminal one third of the protein, which acts together with its co-factor NS4A (84, 86, 272). The C-terminal region of NS3 possesses RNA helicase and nucleoside triphosphatase (NTPase) activities (185, 260, 288). The NS3 helicase, together with the RNA-dependent RNA polymerase (NS5B) participate in viral RNA genome replication, with coordinated activation of NS3 and NS5B (311).

NS proteins were once thought to be involved exclusively in viral RNA replication or polyprotein processing, but recent findings have shown essential roles in infectious particle production. The NS2 TM domains and its C terminus have been reported to play a crucial role progeny production (55, 112) and deletion of the entire NS2 protein in the context of a bicistronic HCV genome results in loss of intracellular infectious virus assembly, while RNA replication is unaltered (114). NS3 has been implicated in virus infectivity through titer enhancing adaptive mutations that map to its helicase domain (305). Here we analyzed the NS2-3 region to investigate the potential interplay of these proteins in infectious virus production. We tried to find structural and genetic evidence for a post-cleavage association between these proteins. We fitted the $NS2^{pro}$ and NS3 crystal structures into an

NS2-3 model to investigate the possibility of post-cleavage interactions and analyzed potential interacting residues in the context of a cell culture infectious genome.

Materials and Methods

Plasmid constructs. The parental mono- and bicistronic reporter genomes were generated from Jc1 (228) using site directed mutagenesis. The newly generated constructs were verified by restriction enzyme digest and sequencing of PCR-amplified segments.

(i) Jc1(5'C19nsGluc2AUbi) was subcloned using a *Gaussia* luciferase construct J6/JFH(5'C19Gluc2AUbi) (274) as backbone while inserting the BsaBI/BbvCI fragment from Jc1. Monocistronic mutant derivatives were created by site directed mutagenesis using the same BsaBI/BbvCI restrictions sites.

(ii) Jc1(NS2-IRES-nsGluc2AUbi) was created by site directed mutagenesis inserting a stop codon and a PmeI site into Jc1, which was then digested with BsaBI/PmeI and inserted into the opened vector J6/JFH(NS2-IRES-nsGluc2AUbi) (114). Bicistronic mutant derivatives were created by site directed mutagenesis using NotI/SpeI restrictions sites.

Cell culture. Huh-7.5 cells were cultured in Dulbecco's modified Eagle medium (Invitrogen) supplemented with 0.1 mM non-essential amino acids and 10% fetal bovine serum (complete medium). Cells were grown at 37 °C in 5% CO_2.

RNA transcription. *In vitro* transcripts were generated as previously described (150). Briefly, plasmid DNA was linearized by XbaI and purified by using a Minelute column (QIAGEN, Valencia, CA). RNA was transcribed from 10 µg of purified template by using the T7 Megascript kit (Ambion, Austin, TX) or the T7 RNA polymerase kit (Promega, Madison, WI). Reactions were incubated at 37 °C for 3 h, followed by a 15 min digestion with 3 U of DNase I (Ambion). RNA was purified by using an RNeasy kit (QIAGEN) with an additional on-column DNase treatment. RNA was quantified by absorbance at 260 nm and diluted to 0.5 µg/µl. Prior to storage at -80 °C, RNA integrity was determined by agarose gel electrophoresis and visualization by ethidium bromide staining.

RNA electroporation. Huh-7.5 cells were electroporated with RNA as previously described (150). Briefly, Huh-7.5 cells were treated with trypsin, washed twice with ice-cold RNase-free AccuGene phosphate-buffered saline (PBS; Bio-Whittaker, Rockland ME), and resuspended at 1.75 x 107 cells/ml in

PBS. Then, 2 µg of each RNA was combined with 0.4 ml of cell suspension and immediately pulsed using a BTX ElectroSquare Porator ECM 830 (820 V, 99 µs, five pulses). Electroporated cells were incubated at room temperature for 10 min prior to resuspension in 15 ml or 30 ml complete medium for non-reporter and reporter constructs, respectively. Resuspended cells were plated into 24-well, 6-well and P100 tissue culture dishes.

Assays for RNA replication. At 4, 8, 24, 48, and 72 h post-electroporation, cells in 24-well plates were washed with Dulbecco PBS (DPBS) and lysed by the addition of Renilla lysis buffer (Promega, Madison WI) or RLT buffer (QIAGEN) containing 10% ß-mercaptoethanol for assay of replication by luciferase activity or quantitative reverse transcription-PCR (qRT-PCR), respectively. For luciferase assays, lysates were thawed prior to addition of Renilla substrate (Promega) according to the manufacturer's instructions. The luciferase activity was measured by using a Berthold Centro LB 960 96-well luminometer. For qRT-PCR analysis, prior to storage at -80°C, lysates were homogenized by centrifugation through a QiaShredder column (QIAGEN) for 2 min at 14,000 x g. Total RNA was isolated by RNeasy kit (QIAGEN) and quantified by determining the absorbance at 260 nm. A total of 50 ng of total cellular RNA was used per reaction. qRT-PCRs were performed on a LightCycler 480 (Roche, Basel Switzerland) using the LightCycler amplification kit (Roche) with primers directed against the viral 3' NTR. We assembled 20 µl reactions according to the manufacturer's instructions as previously described (114).

Assays for infectious virus production. At 4, 8, 24, 48, and 72 h post-electroporation, the cell culture media was harvested and replaced with fresh complete medium. Harvested cell culture supernatants were clarified by using a 0.45-µm pore-size filter and stored in aliquots at -80 °C. For detection of infectious virus production by qRT-PCR or luciferase assay, naive cells were infected with clarified cell culture supernatants and incubated for 72 h prior to analysis. Determination of infectious virus production by limiting dilution assay was performed as described previously (114, 150). Briefly, clarified cell culture supernatants were serially diluted and used to infect approximately 3 x 10^3 cells plated in 96-well dishes. At 3 days post-infection, cells were washed with DPBS, fixed with ice-cold methanol, and stained for the presence of NS5A expression as described previously. The 50% tissue

culture infectious dose (TCID50) was calculated using the Reed & Muench method (150).

SDS-PAGE and Immunoblot. Cells were lysed at 72 h post-electroporation with RLT buffer (QIAGEN) containing 1% ß-mercaptoethanol and homogenized by centrifugation through a QiaShredder column (QIAGEN) for 2 min at 14,000 x g. Lysates were separated by SDS-polyacrylamide gel electrophoresis (PAGE). After transfer to nitrocellulose membrane, blots were blocked for 1 h with 5% milk/PBS-T (phosphate buffered saline, 0.1% Tween). For NS2 detection, mAb 6H6 (1.0 mg/ml), was diluted 1:1000 in PBS-T. For NS5A detection mAb 9E10 (17) was diluted 1:1000 in PBS-T. For β-actin detection mouse-anti-β-actin mAb (Sigma, St Louis, MO) was diluted 1:20000 in PBS-T. After 1 h incubation at room temperature, and extensive washing with PBS-T, rabbit-anti-mouse immunoglobulin-horseradish peroxidase (HRP) secondary antibody (Pierce, Rockford, IL) was added at 1:10000 dilution in 5% milk/PBS-T for 45 min at RT. After additional washing, blots were developed with SuperSignal West Pico chemiluminescent substrate (Pierce).

Passaging for revertants. Jc1 reporter constructs were electroporated into Huh-7.5 cells and 72 h post-electroporation, supernatant was transferred to naïve Huh-7.5 cells. Cells were split upon confluency, passaged for a total of seven passages and samples of each passage were stored at -80°C. Lysates were thawed prior to addition of Renilla substrate (Promega) according to the manufacturer's instructions. The luciferase activity was measured by using a Berthold Centro LB 960 96-well luminometer.

Reverse transcription (RT) PCR. Total RNA was isolated by RNeasy kit (QIAGEN) and quantified by determining the absorbance at 260 nm. A total of 2 ug of total cellular RNA was used per reaction of the SuperScript III First-Strand Synthesis System for RT-PCR (Invitrogen) according to the manufacturer's instructions. 1ul of the RT mix (RNA/primer/dNTP mix) was used to amplify the Jc1 genome. The amplified fragments were then sequenced and analyzed for revertants or second site mutations.

Results

Creation and characterization of HCV constructs. We previously found the NS2 C-terminus (leucine 217) has an important function in infectious virus production (55). We therefore decided to analyze the role

of the entire NS2-3 cleavage site in the HCV life cycle. Mono- and bicistronic reporter versions of the Jc1 genome (228) were constructed for this analysis (Fig. 1A). The monocistronic Jc1(5'C19nsGluc2AUbi) (Fig. 1A-II.) is identical to the Jc1 (Fig. 1A-I.) but contains a non-secreted *Gaussia* luciferase (nsGluc) reporter followed by foot and mouth disease virus (FMDV) 2A and a ubiquitin (Ubi) monomer upstream of core. Cleavage of the reporter from the viral polyprotein is mediated by two heterologous cleavages, the FMDV 2A autoproteolytic peptide and removal of Ubi by host ubiquitin carboxylyase. The bicistronic genome Jc1(NS2-IRES-nsGluc2AUbi) (Fig. 1A-III.) includes an encephalomyocarditis virus internal ribosome entry site (EMCV IRES) downstream of NS2, followed by the nsGluc2AUbi cassette and NS3 to NS5B.

RNA replication complete kinetics (data not shown) and at 72 h post-electroporation of the reporter and non-reporter monocistronic constructs were comparable, whereas the bicistronic reporter virus showed a drop of RNA replication of about half a log (Fig1B). The corresponding genomes with mutation of the NS5B motif GDD to GNN did not replicate. The three constructs produced infectious particles, although the titers were reduced almost ten-fold for the reporter constructs (Fig. 1C).

NS2 cleavage site residue leucine 217 (P1). We have previously shown that non-conservative mutations of L217 impair infectious virus production by a bicistronic genome (55). To investigate the importance of L217 for NS2-3 cleavage, we engineered the L217 (cleavage site position P1) mutations into the monocistronic reporter genome, Jc1(5'C19nsGluc2AUbi). Mutations of NS2 L217 to alanine resulted in impaired RNA replication, whereas mutation to isoleucine, proline or lysine abolished RNA replication completely (Fig. 2A). This correlates with protein expression data (Fig. 2C) where NS2, NS3 and NS5A could only be detected for wild type and L217A. Further, infectious particle production was not detected for any of the NS2 C-terminal mutations, supporting the findings in the bicistronic context (55).

NS3 cleavage site residues P1', P2', P3', P4' in a monocistronic background. To investigate the importance of NS3 residues for cleavage, we introduced mutations into the P1' to P4' positions (NS3 residues 1-4, APIT). Substitution of alanine at position P1' to lysine (A1K) impaired replication, whereas changes to leucine, proline or aspartic acid

abolished RNA accumulation (Fig. 3A). Mutation of NS3 A1K also resulted in low amounts of infectious particles, about two log less than wild type. No other tested mutation at this position showed infectivity (Fig. 3B). Position P2' (proline) showed more tolerance for substitutions, as mutations to alanine and lysine resulted in replication at close to wild type levels and detectable titers of infectious virus; mutation P2L, however, severely impaired replication (Fig. 3A, B). Substitution of the isoleucine at position P3' with alanine, glutamic acid, or proline resulted in no RNA replication or infectious virus production (Fig. 3A, B). An alanine substitution of the threonine at position P4' was tolerated for replication, whereas a proline at this position abolished RNA accumulation (Fig. 3A). Neither of these changes allowed the production of infectious particles (Fig. 3B). Protein expression of NS2, NS3, and NS5A could only be detected for mutants that replicated robustly at 72 h post-electroporation, for example A1K, P2A, P2K, and T4A (Fig. 3C). In these cases NS2-3 appeared to be correctly processed.

NS3 cleavage site residues P1', P2', P3', P4' in a bicistronic background. To investigate potential additional effects of the NS2-3 cleavage site mutations independent from polyprotein processing, the bicistronic genome Jc1(NS2-IRES-nsGluc2AUbi) was used. We had previously shown that the P1 residue (NS2 L217) is essential for infectious progeny production, but not RNA replication, in the bicistronic context. Substitutions at the P1' position (A1K, A1L, A1P, and A1D) were also tolerated for replication, although RNA accumulation of mutants A1P and A1D was impaired compared to wild type (Fig. 4A). Infectious particles could only be detected for A1K and A1L (Fig. 4B). Mutation of position P2' to alanine or leucine allowed close to wild-type levels of RNA replication, while P2K was impaired. Interestingly, P2A was defective in infectious virus production despite robust RNA replication. Moderately (I3A, and I3P) and severely (I3E) impaired RNA replication was detected for genomes with mutations at position P3'; none of these mutants were infectious (Fig. 4A,B). Changes at position P4' (T4A and T4P) allowed replication, but only T4P produced low infectious particles (Fig. 4A, B). Protein expression levels correlated with the 72 h post-electroporation RNA replication data (Fig. 4A).

A model of NS2 and NS3 interactions. Crystal structures for both $NS2^{pro}$ and NS3 have been solved. The structure of $NS2^{pro}$ represents the protease domain in the

post-cleavage form, which is presumed to be the state active in infectious virus assembly. We used computer modeling to fit the $NS2^{pro}$ dimer into the NS3 structure with respect to charges and spatial arrangements of the residues. $NS2^{pro}$ is represented in red and blue (one monomer in red, the other in blue) whereas NS3 is shown in grey (Fig. 5A).

Based on this model, we chose several residues that seemed to be important for an NS2-NS3 interaction and mutated them to alanine. Targeted NS2 residues are shown in yellow (D207A, and S211A) while NS3 mutations are shown in green (Q9A, Q29A, Q34A, Q41A, D81A, K136A, S139A, R155A, R161A, K165A, D168A) (Fig. 5B). Further, we found three NS3 loops that fit well into the NS2 structure. Loop residues were replaced by alanine in combination in attempts to disrupt this potential interaction. Loop T38-F43 is shown in yellow, Y51-F43 in green, and S77-D81 in orange (Fig. 5C).

NS2-NS3 model interaction residues in a monocistronic background. Mutations potentially disrupting NS2-NS3 interactions were engineered into the Jc1(5'C19nsGluc2AUbi) monocistronic genome. In this context, the two NS2 mutations (D207A and S211A) showed impaired RNA replication compared to wild type (Fig. 6A). Alanine substitutions at NS3 positions Q9, Q29, Q34, Q41, R155A, R161A, and D168A had no effect on RNA replication, while mutants S139A and K165A were heavily impaired. NS3 mutants D81A, K136A and loop mutants T38A-F43A, Y56A-F43A, S77A-D81A did not replicate (Fig. 6A).

In keeping with a role for the NS2 C-terminal domain in infectivity, NS2 mutations D207A, and S211A completely abolished infectious particle production (Fig. 6B). The glutamine substitutions in NS3 had only a moderate effect on infectious titers, while the R155A, R161A and D168A mutants showed a drop of more than one log compared to wild type. D81A, K136A, S139A, K165A and T38A-F43A, Y56A-F43A, S77A-D81A, the loop depletion constructs did not produce any infectious particles (Fig. 6B).

NS2 expression was detected for the two NS2 mutants; weak detection probably reflects the impaired RNA replication, and the location of the 6H6 antibody epitope just upstream of these mutations. All viral proteins tested were expressed at similar levels to wild type for mutants Q9A, Q29A, Q34A, Q41A, R155A, R161A, and D168A. D81A, K136A, S139A, K165A and the three loop mutants did not show viral protein expression because of their impaired replication (Fig. 6C).

NS2-NS3 model interaction residues in a bicistronic background. Each of the potential interaction-disrupting mutants was engineered into the bicistronic genome Jc1(NS2-nsGluc2AUbi). As expected, RNA replication was similar to wild type for the NS2 mutations D207A, S211A. NS3 glutamine mutations (Q9A, Q29A, Q34A, Q41A), as well as S139A, R155A, K161A, and D168A also showed robust RNA accumulation. NS3 mutants D81A, K136A, K165A and the loop depletions, T38A-F43A, Y56A-F43A, S77A-D81A, however, did not replicate (Fig. 7A).

Consistent with previous results (55) the infectivity NS2 mutations D207A and S211A was reduced by about one log compared to wild type. Interestingly, several of the replication-competant NS3 mutants also showed defects in infectious virus production (S139A, R155A, R161A, and D168A). In keeping with the replication phenotypes, the NS3 glutamine mutations produced close to wild-type levels of infectious virus, while D81A, K136A, K165A and the loop depletions, T38A-F43A, Y56A-F43A, S77A-D81A, did not produce infectious particles (Fig. 7B).

All the constructs expressed the viral proteins at levels similar to wild type, except D81A, K136A, S139A, K165A and the loop depletions, which showed no protein expression, and D207A, which showed a reduced expression probably due to the proximity of the antibody epitope (Fig. 7C).

Genetic evidence of intra- and intermolecular HCV protein interactions. HCV genomes containing NS2 or NS3 mutations allowing robust RNA replication but a disrupting infectious particle production were passaged to analyze the appearance of enhancing second site mutations. We chose following mutants for passage: monocistronic genomes NS2 L217K, D207A and NS3 A1K, P2K, P2L, T4A, T4P, S139A, R155A, and R161A and bicistronic genomes NS2 D207A, L217I, L217A, L217V, and L217K. RNA replication of each construct was determined after every passage for up to seven passages (Fig. 8A), after which HCV RNA was isolated by RT-PCR and population sequencing. We could identify two mutations in E2 (A192G, A263G) for the monocistronic P2K construct while monocistronic R155A, and R161A did not show any other residue changes (Fig. 8B). The remaining monocistronic constructs reverted back to wild type. Sequencing of the bicistronic D207A construct revealed an additional mutation in NS3 (Q221L). L217A showed two changes in NS3 (Q221H, T478P) with residue Q221 at the same position as for construct D207A. Both bicistronic L217V and L217I

presented the same E1 (A78T) changes after sequencing (Fig. 8C).

Discussion

NS2 is essential for the HCV life cycle due to its protease function that, together with the N-terminal region of NS3, cleaves itself from the polyprotein (114, 228). More recently, NS2 has been found to be critical for the production of infectious particles (55, 112, 226). There is growing evidence that NS2 and NS3 work together, as post-cleavage interactions of the proteins have been detected in co-localization and co-immunoprecipitation studies (58, 99, 126). Here, we investigated the importance of the NS2/3 cleavage site residues for replication and infectious particle production in the Jc1 context. Further, we built a structural model of how NS2 might interact with NS3 in the post-cleavage form (Fig. 5A).

The importance of the NS2/3 junction residues in polyprotein processing and other lifecycle events had not been investigated in the context of the cell culture infectious system. Here we found that the P1 position (NS2 L217) tolerated only a leucine to alanine substitution (Fig. 1A, C). Consistent with our results, work in polyprotein overexpression systems found 69% cleavage efficiency for a L217A change, whereas a proline substitution completely prevented cleavage (236). Although replication was preserved, the L217A mutant was unable to produce infectious particles in a mono- or bicistronic context (55). In fact, only an isoleucine at this position produces infectious particles in a bicistronic construct (55). Position P1 of the NS3 cleavage site is highly conserved across genotypes, supporting its important role in HCV propagation.

The alanine at the N-terminus of NS3, position P1' of the cleavage site, tolerates a lysine, but not leucine, proline or aspartic acid for cleavage and RNA accumulation, whereas replication in the bicistronic was close to wild type. (Fig. 3 A, C and Fig. 4 A, C). The lysine is the only residue allowing NS2/3 cleavage, replication and infectious virus production, while other mutants supported only some functions. Proline and aspartic acid at this position had previously been shown to be cleavage deficient at 11% for A1D and 0% for A1P (236). Changes in P1 and P1' affecting the conformation severely inhibit cleavage, and therefore RNA replication and virus production (102).

Alanine and lysine substitutions at position P2' can replicate and produce virus which is in accordance to Reed et al, who found a 70% efficiency for P2A but did not analyze P2K (236). Interestingly a leucine at this position abolishes NS2/3

cleavage and by consequence inhibits RNA replication and infectivity. Leucine seems to be the preferred residue for infectious virus production alone as the bicistronic construct showed increased replication and infectivity (Fig. 4A,B). The isoleucine at position P3' is highly important for cleavage, as changes to alanine, glutamic acid, and proline inhibit NS2/3 processing. These results coincide with data showing that overexpression of NS2/3 mutants I3A and I3E allowed up 70% cleavage efficiency (236), indicating that the P3' residue might not be essential for processing but affects other aspects of RNA replication. Isoleucine P3' also plays a crucial role in infectious virus production, as all the mutants were lacking infectivity in the bicistronic background. Position P4' tolerated an alanine but not a proline for cleavage and, although replication of T4A was similar to wild type, but neither mutants were infectious.

In addition to interplay between the terminal residues during cleavage, NS2 and NS3 are thought to associate after processing to accomplish further roles in the life cycle. We therefore tried to establish an NS2-3 interaction model based on the solved $NS2^{pro}$ and NS3 crystal structures and assessed the importance of proximal residues for viral propagation. Potential interacting residues NS2 S211 and NS3 D168 were important for replication, which was disrupted by substituting either to an alanine. Previous research showed that the NS3 protease activity requires a catalytic triad (S139, H57 and D81) and an oxyanion hole (backbone amides of G137 and S139). Mutation of D81 abolished replication completely in an NS2/3 cleavage independent manner, while substitution of S139 heavily impaired RNA replication but allowed reduced infectious virus production in a bicistronic background. Necessary interactions for assembly and release are therefore still possible, including potentially an NS2-NS3 contact. Not surprisingly, substituting entire NS3 loops completely eliminated RNA replication. Interestingly, mutation of a residue involved in HCV inhibitor resistance (R155), which potentially interacts with NS2 residues W214 and R161, showed impaired infectious virus production in the bicistronic background.

The analysis of passaged NS3 mutations revealed a genetic interaction of NS3 with E2, NS4B and NS5A (Fig. 8B). Second site mutations from NS2 constructs exposed NS3 and E1 as genetic targets. Interestingly, sequence analysis of NS2 mutations L217V and L217I presented the same E1 mutation A269T, which has previously been described to enhance release of infectious particle production for a J6/H77NS2/JFH,

a J6/JFH construct with a full length H77 NS2 (55). These data add to our understanding of the interactions of NS2, NS3 and additional viral proteins required for cleavage, replication and infectivity and may promote the development of peptide-based inhibitors of these associations.

Acknowledgements

We thank Maryline Panis and Anesta Webson for laboratory support and technical assistance. We are grateful to Catherine L. Murray, Christopher T. Jones, Cynthia de la Fuente and Kimberly D. Ritola for reagents, constructs, helpful discussions, and critical reading of the manuscript. This study was supported by The Greenberg Medical Research Institute, NIH Public Health Service Grant (AI075099), and the Starr Foundation. TGD is supported by the Fonds National de la Recherche Luxembourg.

References

1. 2004. Global burden of disease (GBD) for hepatitis C. J Clin Pharmacol **44:**20-9.
2. **Alter, M. J.** 2007. Epidemiology of hepatitis C virus infection. World J Gastroenterol **13:**2436-41.
3. **Appel, N., M. Zayas, S. Miller, J. Krijnse-Locker, T. Schaller, P. Friebe, S. Kallis, U. Engel, and R. Bartenschlager.** 2008. Essential role of domain III of nonstructural protein 5A for hepatitis C virus infectious particle assembly. PLoS Pathog **4:**e1000035.
4. **Dentzer, T. G., I. C. Lorenz, M. J. Evans, and C. M. Rice.** 2009. Determinants of hepatitis C virus nonstructural protein 2 protease domain required for production of infectious virus. J Virol.
5. **Di Bisceglie, A. M.** 1997. Hepatitis C and hepatocellular carcinoma. Hepatology **26:**34S-38S.
6. **Di Bisceglie, A. M., R. L. Carithers, Jr., and G. J. Gores.** 1998. Hepatocellular carcinoma. Hepatology **28:**1161-5.
7. **Dimitrova, M., I. Imbert, M. P. Kieny, and C. Schuster.** 2003. Protein-protein interactions between hepatitis C virus nonstructural proteins. J Virol **77:**5401-14.
8. **Erdtmann, L., N. Franck, H. Lerat, J. Le Seyec, D. Gilot, I. Cannie, P. Gripon, U. Hibner, and C. Guguen-Guillouzo.** 2003. The hepatitis C virus NS2 protein is an inhibitor of CIDE-B-induced apoptosis. J Biol Chem **278:**18256-64.
9. **Everhart, J. E., Y. Wei, H. Eng, M. R. Charlton, D. H. Persing, R. H. Wiesner, J. J. Germer, J. R. Lake, R. K. Zetterman, and J. H. Hoofnagle.** 1999. Recurrent and new hepatitis C virus infection after liver transplantation. Hepatology **29:**1220-6.

10. **Franck, N., J. Le Seyec, C. Guguen-Guillouzo, and L. Erdtmann.** 2005. Hepatitis C virus NS2 protein is phosphorylated by the protein kinase CK2 and targeted for degradation to the proteasome. J Virol **79:**2700-8.
11. **Grakoui, A., D. W. McCourt, C. Wychowski, S. M. Feinstone, and C. M. Rice.** 1993. Characterization of the hepatitis C virus-encoded serine proteinase: determination of proteinase-dependent polyprotein cleavage sites. J Virol **67:**2832-43.
12. **Grakoui, A., C. Wychowski, C. Lin, S. M. Feinstone, and C. M. Rice.** 1993. Expression and identification of hepatitis C virus polyprotein cleavage products. J Virol **67:**1385-95.
13. **Hijikata, M., H. Mizushima, T. Akagi, S. Mori, N. Kakiuchi, N. Kato, T. Tanaka, K. Kimura, and K. Shimotohno.** 1993. Two distinct proteinase activities required for the processing of a putative nonstructural precursor protein of hepatitis C virus. J Virol **67:**4665-75.
14. **Hijikata, M., H. Mizushima, Y. Tanji, Y. Komoda, Y. Hirowatari, T. Akagi, N. Kato, K. Kimura, and K. Shimotohno.** 1993. Proteolytic processing and membrane association of putative nonstructural proteins of hepatitis C virus. Proc Natl Acad Sci U S A **90:**10773-7.
15. **Hirowatari, Y., M. Hijikata, Y. Tanji, H. Nyunoya, H. Mizushima, K. Kimura, T. Tanaka, N. Kato, and K. Shimotohno.** 1993. Two proteinase activities in HCV polypeptide expressed in insect cells using baculovirus vector. Arch Virol **133:**349-56.
16. **Jirasko, V., R. Montserret, N. Appel, A. Janvier, L. Eustachi, C. Brohm, E. Steinmann, T. Pietschmann, F. Penin, and R. Bartenschlager.** 2008. Structural and functional characterization of non-structural protein 2 for its role in hepatitis C virus assembly. J Biol Chem.
17. **Jones, C. T., C. L. Murray, D. K. Eastman, J. Tassello, and C. M. Rice.** 2007. Hepatitis C Virus p7 and NS2 Proteins Are Essential for Production of Infectious Virus. J Virol **81:**8374-83.
18. **Jones, D. M., A. H. Patel, P. Targett-Adams, and J. McLauchlan.** 2009. The hepatitis C virus NS4B protein can trans-complement viral RNA replication and modulates production of infectious virus. J Virol **83:**2163-77.
19. **Kiiver, K., A. Merits, M. Ustav, and E. Zusinaite.** 2006. Complex formation between hepatitis C virus NS2 and NS3 proteins. Virus Res **117:**264-72.
20. **Kolykhalov, A. A., E. V. Agapov, K. J. Blight, K. Mihalik, S. M. Feinstone, and C. M. Rice.** 1997. Transmission of hepatitis C by intrahepatic inoculation with transcribed RNA. Science **277:**570-4.

21. **Lindenbach, B. D., M. J. Evans, A. J. Syder, B. Wolk, T. L. Tellinghuisen, C. C. Liu, T. Maruyama, R. O. Hynes, D. R. Burton, J. A. McKeating, and C. M. Rice.** 2005. Complete replication of hepatitis C virus in cell culture. Science **309:**623-6.

22. **Lohmann, V., F. Korner, J. Koch, U. Herian, L. Theilmann, and R. Bartenschlager.** 1999. Replication of subgenomic hepatitis C virus RNAs in a hepatoma cell line. Science **285:**110-3.

23. **Lorenz, I. C., J. Marcotrigiano, T. G. Dentzer, and C. M. Rice.** 2006. Structure of the catalytic domain of the hepatitis C virus NS2-3 protease. Nature **442:**831-5.

24. **Ma, Y., J. Yates, Y. Liang, S. M. Lemon, and M. Yi.** 2008. NS3 helicase domains involved in infectious intracellular hepatitis C virus particle assembly. J Virol **82:**7624-39.

25. **Manns, M. P., J. G. McHutchison, S. C. Gordon, V. K. Rustgi, M. Shiffman, R. Reindollar, Z. D. Goodman, K. Koury, M. Ling, and J. K. Albrecht.** 2001. Peginterferon alfa-2b plus ribavirin compared with interferon alfa-2b plus ribavirin for initial treatment of chronic hepatitis C: a randomised trial. Lancet **358:**958-65.

26. **Matusan, A. E., M. J. Pryor, A. D. Davidson, and P. J. Wright.** 2001. Mutagenesis of the Dengue virus type 2 NS3 protein within and outside helicase motifs: effects on enzyme activity and virus replication. J Virol **75:**9633-43.

27. **Moradpour, D., F. Penin, and C. M. Rice.** 2007. Replication of hepatitis C virus. Nat Rev Microbiol **5:**453-63.

28. **Penin, F., J. Dubuisson, F. A. Rey, D. Moradpour, and J. M. Pawlotsky.** 2004. Structural biology of hepatitis C virus. Hepatology **39:**5-19.

29. **Phan, T., R. K. Beran, C. Peters, I. C. Lorenz, and B. D. Lindenbach.** 2009. Hepatitis C virus NS2 protein contributes to virus particle assembly via opposing epistatic interactions with the E1-E2 glycoprotein and NS3-NS4A enzyme complexes. J Virol **83:**8379-95.

30. **Pietschmann, T., A. Kaul, G. Koutsoudakis, A. Shavinskaya, S. Kallis, E. Steinmann, K. Abid, F. Negro, M. Dreux, F. L. Cosset, and R. Bartenschlager.** 2006. Construction and characterization of infectious intragenotypic and intergenotypic hepatitis C virus chimeras. Proc Natl Acad Sci U S A **103:**7408-13.

31. **Reed, K. E., A. Grakoui, and C. M. Rice.** 1995. Hepatitis C virus-encoded NS2-3 protease: cleavage-site mutagenesis and requirements for bimolecular cleavage. J Virol **69:**4127-36.

32. **Schregel, V., S. Jacobi, F. Penin, and N. Tautz.** 2009. Hepatitis C virus NS2 is a protease stimulated by

cofactor domains in NS3. Proc Natl Acad Sci USA **106:**5342-7.

33. **Steinmann, E., F. Penin, S. Kallis, A. H. Patel, R. Bartenschlager, and T. Pietschmann.** 2007. Hepatitis C virus p7 protein is crucial for assembly and release of infectious virions. PLoS Pathog **3:**e103.

34. **Suzich, J. A., J. K. Tamura, F. Palmer-Hill, P. Warrener, A. Grakoui, C. M. Rice, S. M. Feinstone, and M. S. Collett.** 1993. Hepatitis C virus NS3 protein polynucleotide-stimulated nucleoside triphosphatase and comparison with the related pestivirus and flavivirus enzymes. J Virol **67:**6152-8.

35. **Thibeault, D., R. Maurice, L. Pilote, D. Lamarre, and A. Pause.** 2001. In vitro characterization of a purified NS2/3 protease variant of hepatitis C virus. J Biol Chem **276:**46678-84.

36. **Tomei, L., C. Failla, E. Santolini, R. De Francesco, and N. La Monica.** 1993. NS3 is a serine protease required for processing of hepatitis C virus polyprotein. J Virol **67:**4017-26.

37. **Tscherne, D. M., C. T. Jones, M. J. Evans, B. D. Lindenbach, J. A. McKeating, and C. M. Rice.** 2006. Time- and temperature-dependent activation of hepatitis C virus for low-pH-triggered entry. J Virol **80:**1734-41.

38. **Warrener, P., and M. S. Collett.** 1995. Pestivirus NS3 (p80) protein possesses RNA helicase activity. J Virol **69:**1720-6.

39. **Welbourn, S., R. Green, I. Gamache, S. Dandache, V. Lohmann, R. Bartenschlager, K. Meerovitch, and A. Pause.** 2005. Hepatitis C virus NS2/3 processing is required for NS3 stability and viral RNA replication. J Biol Chem **280:**29604-11.

40. **Yi, M., Y. Ma, J. Yates, and S. M. Lemon.** 2007. Compensatory mutations in E1, p7, NS2, and NS3 enhance yields of cell culture-infectious intergenotypic chimeric hepatitis C virus. J Virol **81:**629-38.

41. **Zhang, C., Z. Cai, Y. C. Kim, R. Kumar, F. Yuan, P. Y. Shi, C. Kao, and G. Luo.** 2005. Stimulation of hepatitis C virus (HCV) nonstructural protein 3 (NS3) helicase activity by the NS3 protease domain and by HCV RNA-dependent RNA polymerase. J Virol **79:**8687-97.

Fig. 1. HCV Jc1 J6/JFH constructs. A. Schematic representation of HCV genomes. (I) Jc1 J6/JFH with J6 Core to the N-terminal third of NS2 in grey, JFH NS2-NS5B in white. (II) Jc1 J6/JFH(5'C19nsGluc2AUbi) monocistronic reporter virus with non-secreted *Gaussia luciferase*, FMDV 2A and ubiquitin cleavage sites (nsGluc2AUbi) at the 5' end preceding the core protein. (III) Jc1 J6/JFH(NS2-IRES-nsGluc2AUbi) bicistronic reporter construct with EMCV IRES, followed by non-secreted *Gaussia luciferase*, FMDV 2A and ubiquitin cleavage sites (nsGluc2AUbi) between NS2 and NS3. **B.** RNA replication of Jc1 J6/JFH, Jc1 J6/JFH(5'C19nsGluc2AUbi) and Jc1 J6/JFH(NS2-IRES-nsGluc2AUbi) genomes measured by RT-qPCR at 72 h post-electroporation. HCV RNA copies normalized to 50ng of total RNA. **C.** Production of infectious virus of Jc1 J6/JFH, Jc1 J6/JFH(5'C19nsGluc2AUbi), and Jc1 J6/JFH(NS2-IRES-nsGluc2AUbi)constructs as determined by RT-qPCR at 72h after infection of naïve Huh-7.5 cells with supernatants collected 72 h post-electroporation. WT, wild type of each genome indicated (grey, texture, lines); GNN, corresponding polymerase-defective control (white). Means and SEM of three independent experiments with two different RNA preparations are shown.

Fig. 2. Monocistronic NS2 C-terminal P1 mutagenesis. A. RNA replication of GNN, polymerase-defective control (white), wild-type (grey) and mutated (dark grey) monocistronic constructs at 72h post-electroporation. HCV RNA copies per 50ng total cellular RNA are shown. **B.** Infectious virus production of monocistronic constructs at 72 h post-electroporation, as measured by limiting dilution assay (TCID50). Means and SEM of three independent experiments with two different RNA preparations are shown. **C.** Polyprotein processing of monocistronic and bicistronic constructs 72 h post-electroporation. Huh-7.5 cells lysed 72 h post-electroporation and analyzed by SDS-PAGE. NS2 (6H6 antibody) is shown in the top panel, NS3 (1878 antibody), NS5A (9E10 antibody) in the middle and ß-actin in the bottom panel.

Fig. 3. Monocistronic NS3 N-terminal P1', P2', P3' and P4' mutagenesis. A. RNA replication at 72 h post-electroporation of GNN, wild type, and N-terminal NS3 mutations in the monocistronic reporter virus background, as measured by luciferase activity. **B.** Infectious virus production of NS3 N-terminal monocistronic constructs at 72 h post-electroporation, as measured by limiting dilution assay (TCID50). Means and SEM of three independent experiments with two different RNA preparations are shown. **C.** Polyprotein processing of monocistronic and bicistronic constructs 72 h post-electroporation. Huh-7.5 cells lysed 72 h post-electroporation and analyzed by SDS-PAGE. NS2 (6H6 antibody) is shown in the top panel, NS3 (1878 antibody), NS5A (9E10 antibody) in the middle and ß-actin in the bottom panel.

Fig. 4. Bicistronic NS3 N-terminal P1', P2', P3' and P4' mutagenesis. A. RNA replication at 72 h post-electroporation of GNN, wild type,

and N-terminal NS3 mutations in the bicistronic *Gaussia luciferase* reporter virus background, as measured by luciferase activity. **B.** Infectious virus production of NS3 N-terminal bicistronic constructs at 72 h post-electroporation, as measured by limiting dilution assay (TCID50). Means and SEM of three independent experiments with two different RNA preparations are shown. **C.** Polyprotein processing of monocistronic and bicistronic constructs 72 h post-electroporation. Huh-7.5 cells lysed 72 h post-electroporation and analyzed by SDS-PAGE. NS2 (6H6 antibody) is shown in the top panel, NS3 (1878 antibody), NS5A (9E10 antibody) in the middle and ß-actin in the bottom panel.

Fig. 5. Structural model of NS2 and NS3 interactions. A. $NS2^{pro}$ structure fitted into the NS3 structure, showing a possible post-cleavage interaction. $NS2^{pro}$ dimer in red and blue and NS3 in grey. **B.** NS2 and NS3 residues involved in contacts. NS2 mutations illustrated in yellow, NS3 mutations in green. Zinc represented in purple. **C.** Three distinct NS3 loops (yellow, green and orange) pointing into NS2 (Fig. 5C).

Fig. 6. Monocistronic NS2-3 model mutations. A. RNA replication at 72 h post-electroporation of GNN, wild type, and mutations in the monocistronic reporter virus background, as measured by luciferase activity. **B.** Infectious virus production of NS2 and NS3 monocistronic constructs at 72 h post-electroporation, as measured by limiting dilution assay (TCID50). Means and SEM of three independent experiments with two different RNA preparations are shown. **C.** Polyprotein processing of monocistronic constructs 72 h post-electroporation. Huh-7.5 cells lysed 72 h post-electroporation and analyzed by SDS-PAGE. NS2 (6H6 antibody) is shown in the top panel, NS3 (1878 antibody), NS5A (9E10 antibody) in the middle and ß-actin in the bottom panel.

Fig. 7. Bicistronic NS2-3 model mutations. A. RNA replication at 72 h post-electroporation of GNN, wild type, and mutations in the bicistronic *Gaussia luciferase* reporter virus background, as measured by luciferase activity. **B.** Infectious virus production of NS2 and NS3 bicistronic constructs at 72 h post-electroporation, as measured by limiting dilution assay (TCID50). Means and SEM of three independent experiments with two different RNA preparations are shown. **C.** Polyprotein processing of bicistronic constructs 72 h post-electroporation. Huh-7.5 cells lysed 72 h post-electroporation and analyzed by SDS-PAGE. NS2 (6H6 antibody) is shown in the top panel, NS3 (1878 antibody), NS5A (9E10 antibody) in the middle and ß-actin in the bottom panel.

Fig. 8. Passaging of NS2 and NS3 mutations for revertants. A. RNA replication as a read out for enhanced adaptation measured by luciferase activity after every passage for the *Gaussia luciferase* reporter virus. **B.** Identified second site mutations in the monocistronic Jc1 J6/JFH(5'C19nsGluc2AUbi) background. (I) NS3 P2K construct with two

adaptive mutations in E2 (A192G, A263G). **C.** Detected second site mutations in the bicistronic background Jc1 J6/JFH(NS2-IRES-nsGluc2AUbi). (I) NS2 D207A construct with an adaptive mutation in NS3 (Q221L). (II) NS2 L217A construct with two mutations in NS3 (Q221H, T478P). (III) NS2 L217V construct with one E1 mutation (A78T). (IV) NS2 L217I construct with one E1 mutation (A78T). * represents a new mutations whereas the original introduced mutation is represented by º.

Fig. 1

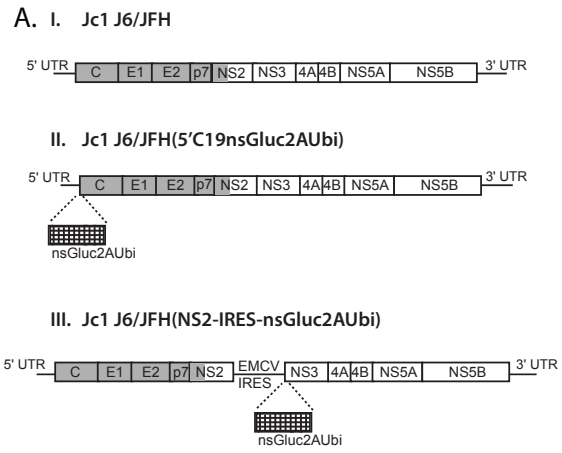
A. I. Jc1 J6/JFH
5' UTR
C
E1
E2
p7
NS2
NS3
4A
4B
NS5A
NS5B
3' UTR
II. Jc1 J6/JFH(5'C19nsGluc2AUbi)
nsGluc2AUbi
III. Jc1 J6/JFH(NS2-IRES-nsGluc2AUbi)
EMCV
IRES

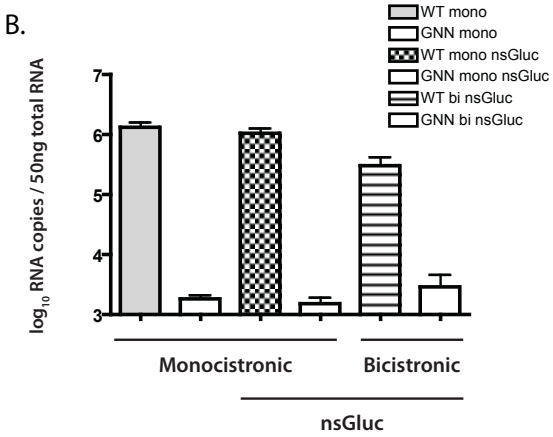
B.
WT mono
GNN mono
WT mono nsGluc
GNN mono nsGluc
WT bi nsGluc
GNN bi nsGluc
log10 RNA copies / 50ng total RNA
7
6
5
4
3
Monocistronic
Bicistronic
nsGluc

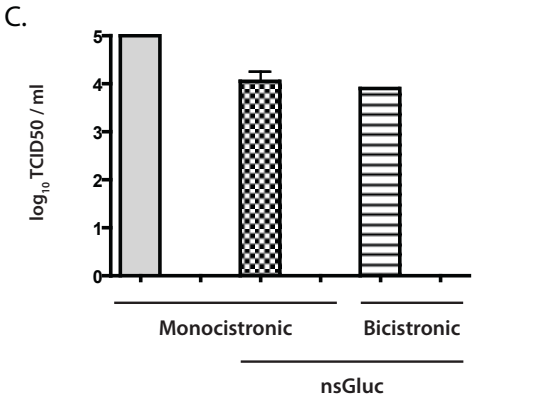
C.
log10 TCID50 / ml
5
4
3
2
1
0
Monocistronic
Bicistronic
nsGluc

Fig. 2

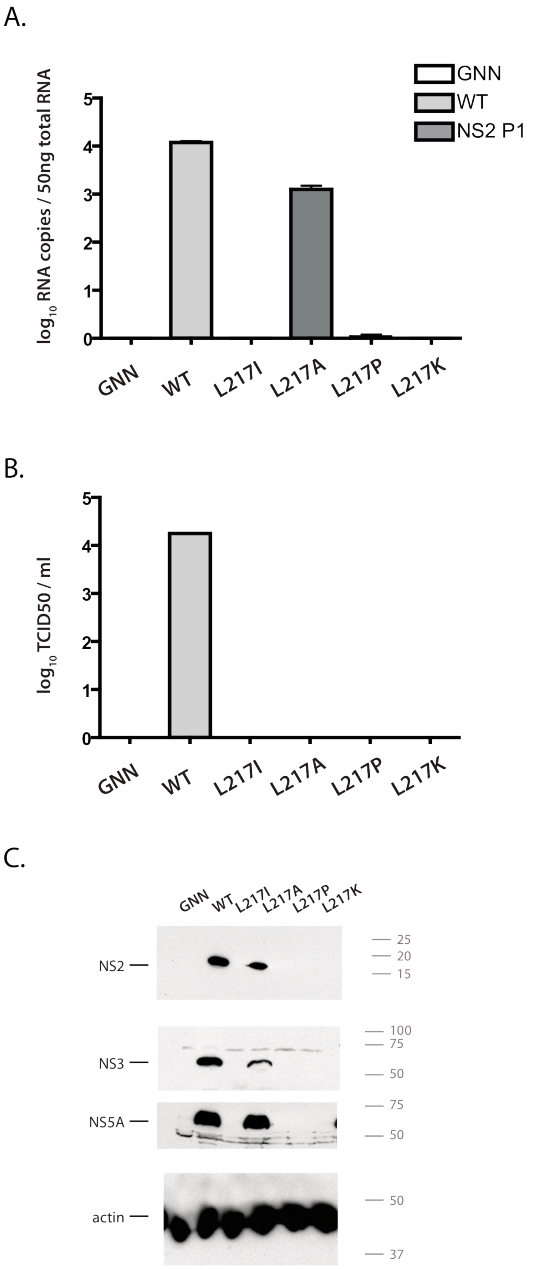
A.
GNN
WT
NS2 P1
log10 RNA copies / 50ng total RNA
0
1
2
3
4
5
GNN
WT
L217I
L217A
L217P
L217K
B.
log10 TCID50 / ml
0
1
2
3
4
5
GNN
WT
L217I
L217A
L217P
L217K
C.
GNN
WT
L217I
L217A
L217P
L217K
NS2
NS3
NS5A
actin
25
20
15
100
75
50
75
50
50
37

Fig. 3

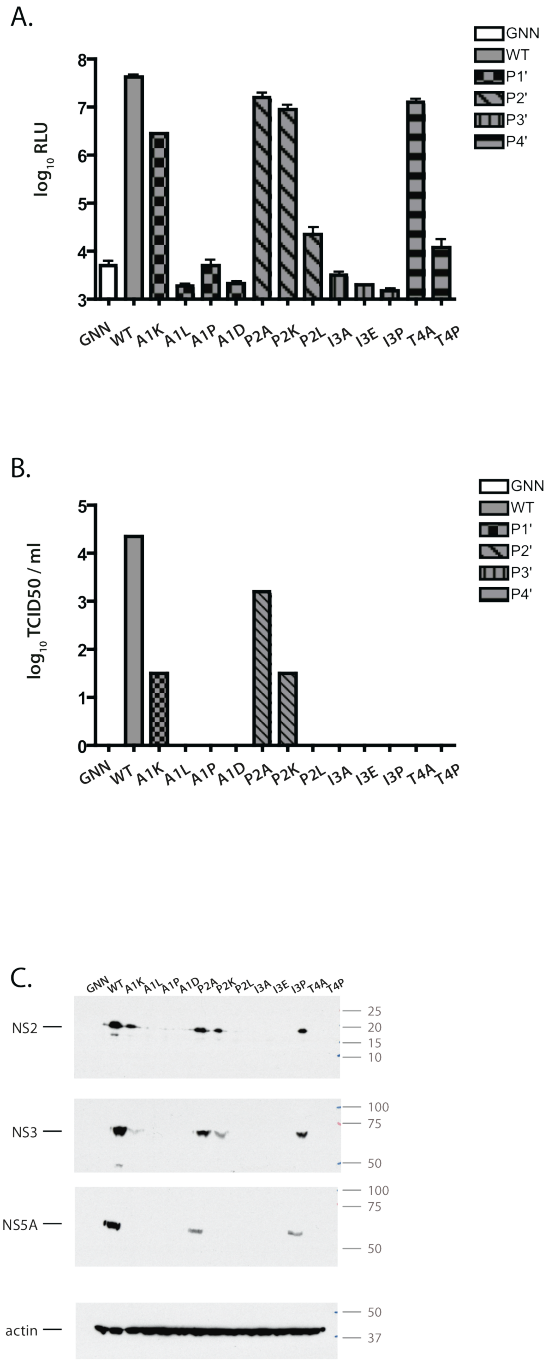
A.
log10 RLU
GNN
WT
P1'
P2'
P3'
P4'
GNN WT A1K A1L A1P A1D P2A P2K P2L I3A I3E I3P T4A T4P
B.
log10 TCID50 / ml
GNN
WT
P1'
P2'
P3'
P4'
GNN WT A1K A1L A1P A1D P2A P2K P2L I3A I3E I3P T4A T4P
C.
GNN WT A1K A1L A1P A1D P2A P2K P2L I3A I3E I3P T4A T4P
NS2
NS3
NS5A
actin
25
20
15
10
100
75
50
100
75
50
50
37

Fig. 4

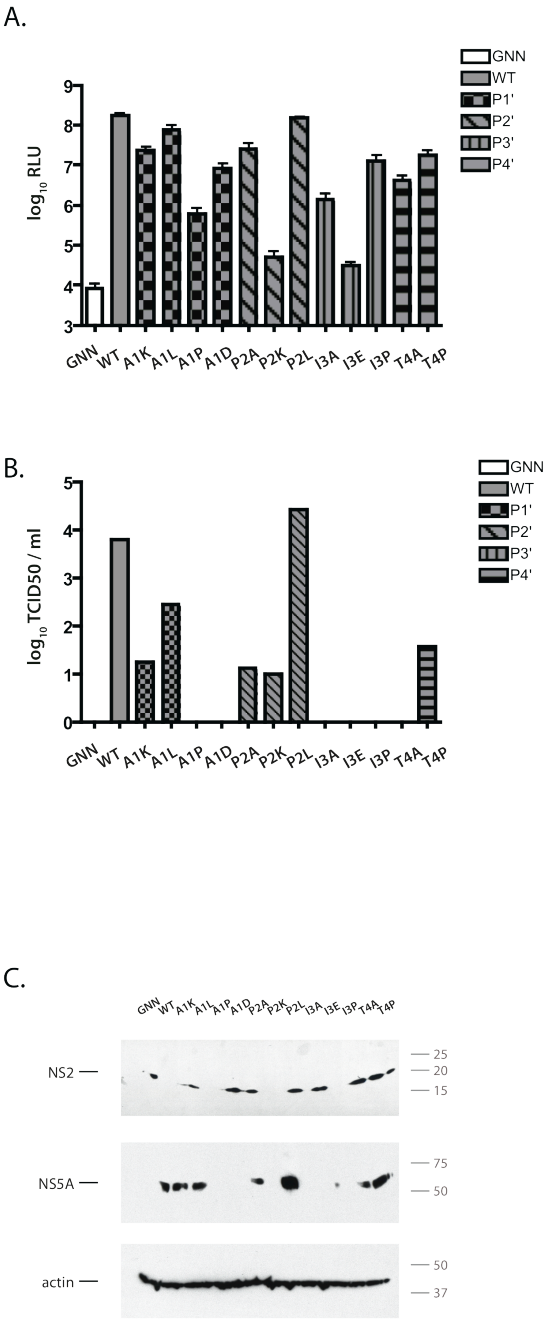
A.
GNN
WT
P1'
P2'
P3'
P4'
log10 RLU
9
8
7
6
5
4
3
GNN WT A1K A1L A1P A1D P2A P2K P2L I3A I3E I3P T4A T4P
B.
GNN
WT
P1'
P2'
P3'
P4'
log10 TCID50 / ml
5
4
3
2
1
0
GNN WT A1K A1L A1P A1D P2A P2K P2L I3A I3E I3P T4A T4P
C.
GNN WT A1K A1L A1P A1D P2A P2K P2L I3A I3E I3P T4A T4P
NS2
25
20
15
NS5A
75
50
actin
50
37

Fig. 5

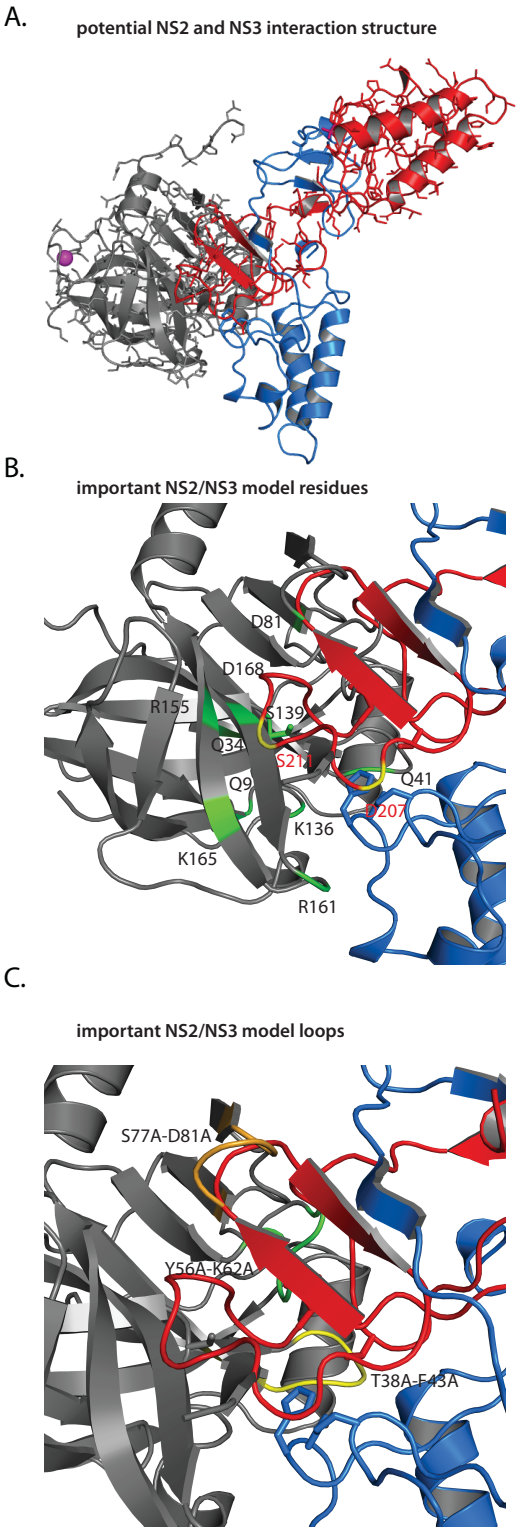
A.
potential NS2 and NS3 interaction structure
B.
important NS2/NS3 model residues
D81
D168
R155
S139
Q34
S217
Q41
Q9
D207
K136
K165
R161
C.
important NS2/NS3 model loops
S77A-D81A
Y56A-K62A
T38A-E43A

Fig. 6

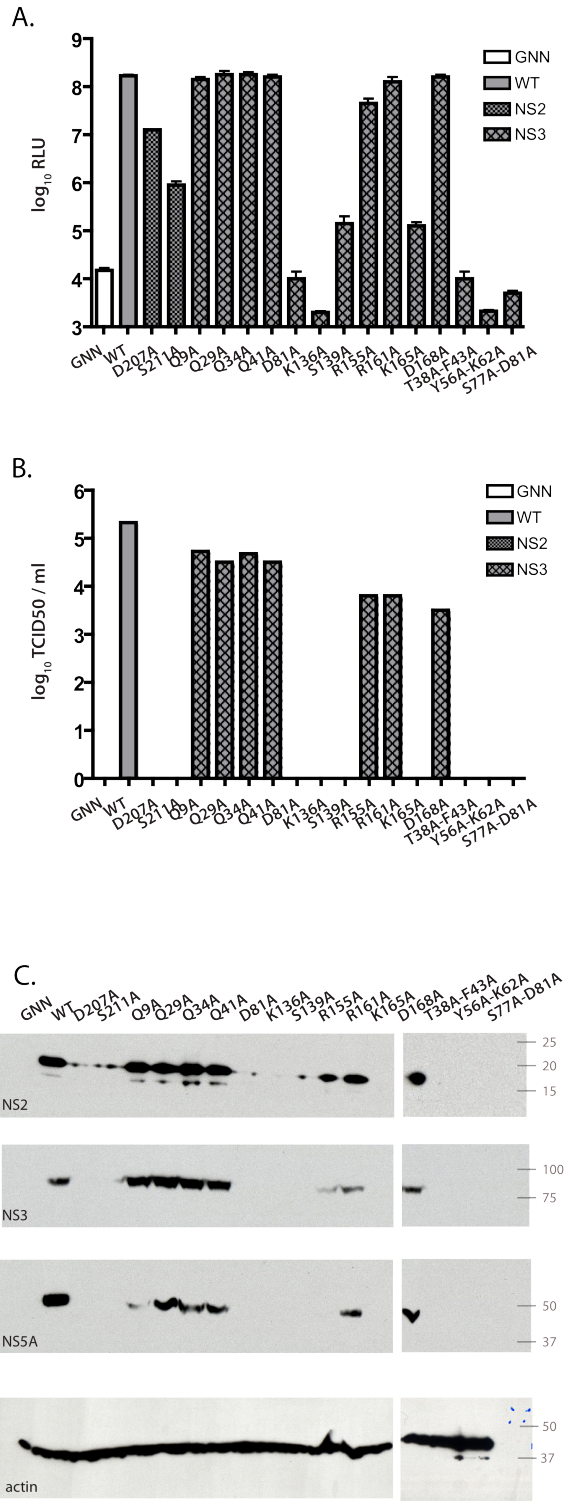
A.
log10 RLU
GNN
WT
NS2
NS3
GNN WT D207A S211A Q9A Q29A Q34A Q41A D81A K136A S139A R155A R161A K165A D168A T38A-F43A Y56A-K62A S77A-D81A
B.
log10 TCID50 / ml
GNN
WT
NS2
NS3
GNN WT D207A S211A Q9A Q29A Q34A Q41A D81A K136A S139A R155A R161A K165A D168A T38A-F43A Y56A-K62A S77A-D81A
C.
GNN WT D207A S211A Q9A Q29A Q34A Q41A D81A K136A S139A R155A R161A K165A D168A T38A-F43A Y56A-K62A S77A-D81A
NS2
NS3
NS5A
actin

Fig. 7

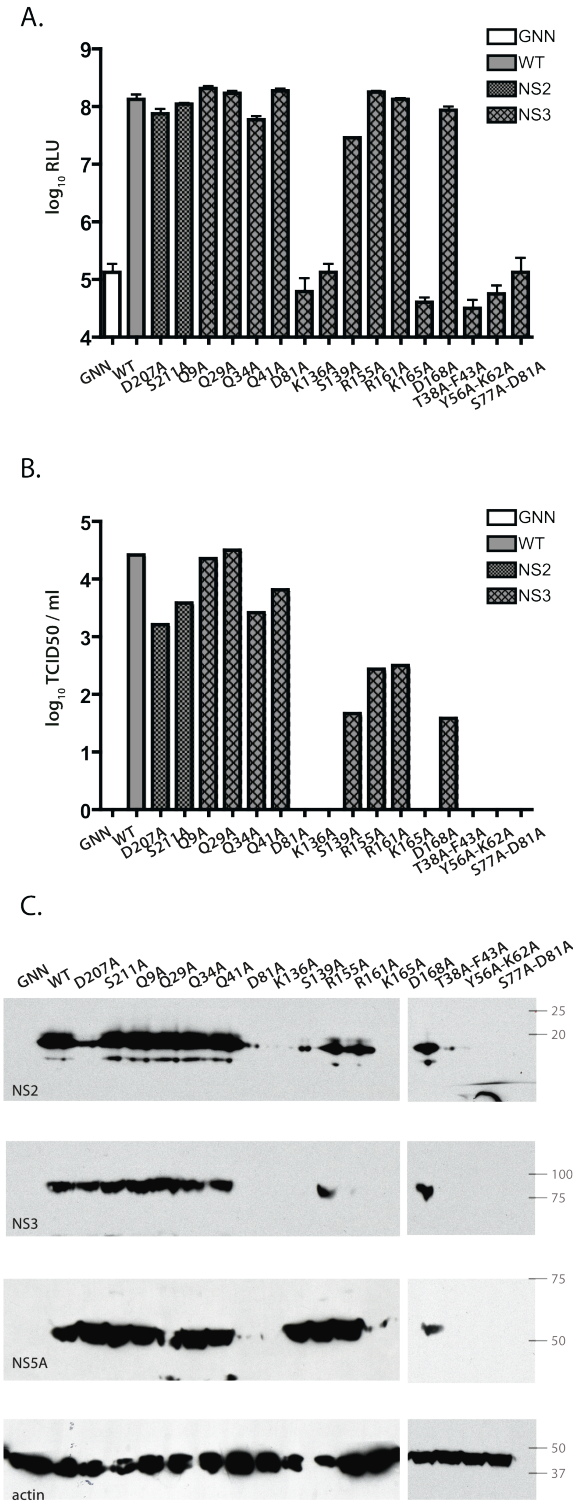
A.
GNN
WT
NS2
NS3
log10 RLU
9
8
7
6
5
4
GNN WT D207A S211A Q9A Q29A Q34A Q41A D81A K136A S139A R155A R161A K165A D168A T38A-F43A Y56A-K62A S77A-D81A
B.
GNN
WT
NS2
NS3
log10 TCID50 / ml
5
4
3
2
1
0
GNN WT D207A S211A Q9A Q29A Q34A Q41A D81A K136A S139A R155A R161A K165A D168A T38A-F43A Y56A-K62A S77A-D81A
C.
GNN WT D207A S211A Q9A Q29A Q34A Q41A D81A K136A S139A R155A R161A K165A D168A T38A-F43A Y56A-K62A S77A-D81A
NS2
25
20
NS3
100
75
NS5A
75
50
actin
50
37

Fig. 8

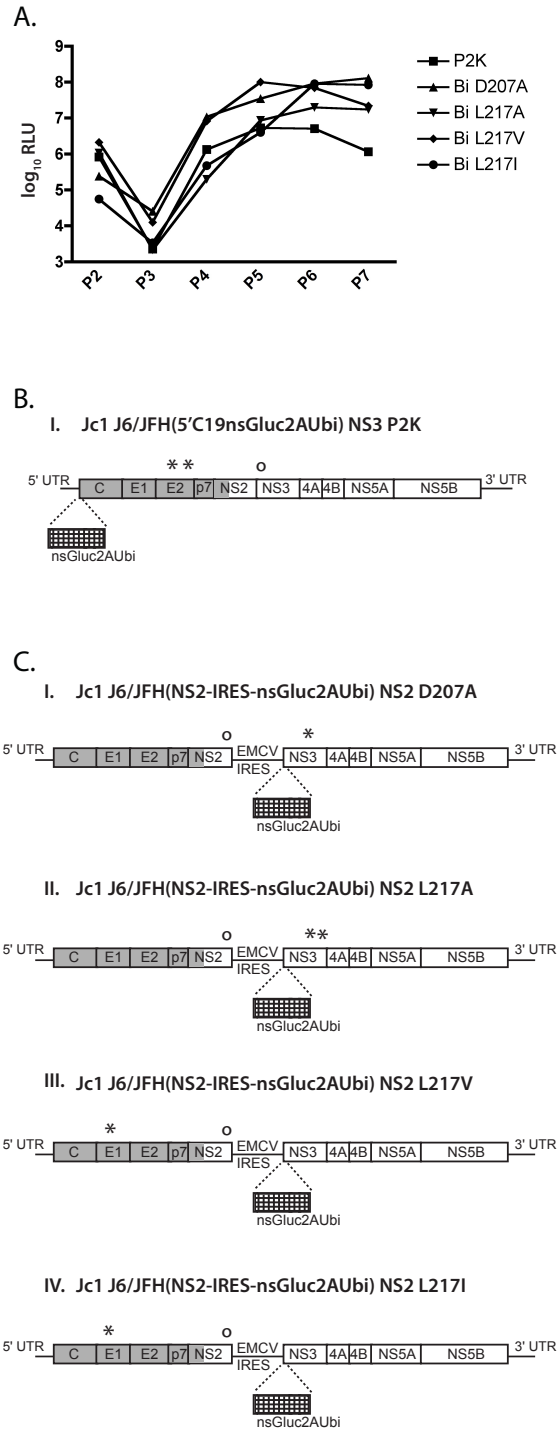
A.
log10 RLU
P2K
Bi D207A
Bi L217A
Bi L217V
Bi L217I
P2
P3
P4
P5
P6
P7
B.
I. Jc1 J6/JFH(5'C19nsGluc2AUbi) NS3 P2K
5' UTR
C
E1
E2
p7
NS2
NS3
4A
4B
NS5A
NS5B
3' UTR
nsGluc2AUbi
C.
I. Jc1 J6/JFH(NS2-IRES-nsGluc2AUbi) NS2 D207A
EMCV IRES
II. Jc1 J6/JFH(NS2-IRES-nsGluc2AUbi) NS2 L217A
III. Jc1 J6/JFH(NS2-IRES-nsGluc2AUbi) NS2 L217V
IV. Jc1 J6/JFH(NS2-IRES-nsGluc2AUbi) NS2 L217I

12 Chapter 6: Identification of NS2 interactions with host proteins

12.1 Introduction

NS2 has many roles in the viral life cycle but its mechanism of action has yet to be determined. We wanted to investigate essential NS2 interactions between viral and host proteins. Mapping NS2 interactions important for its multiple functions in the HCV life cycle may reveal mechanistic details of its activity as well as uncover new targets for anti-viral therapeutics. To identify biologically significant associations, we were pursuing a pull-down approach to precipitate NS2, along with viral and cellular interaction partners, from functional complexes.

12.2 Insertion of NS2 OST tag

Based on previously generated data as well as functional NS2 profiling a small epitope tag (OST strep tag) has been inserted at various positions in NS2 in the context of the full-length Jc1 J6/JFH infectious genome (Fig. 6-1).

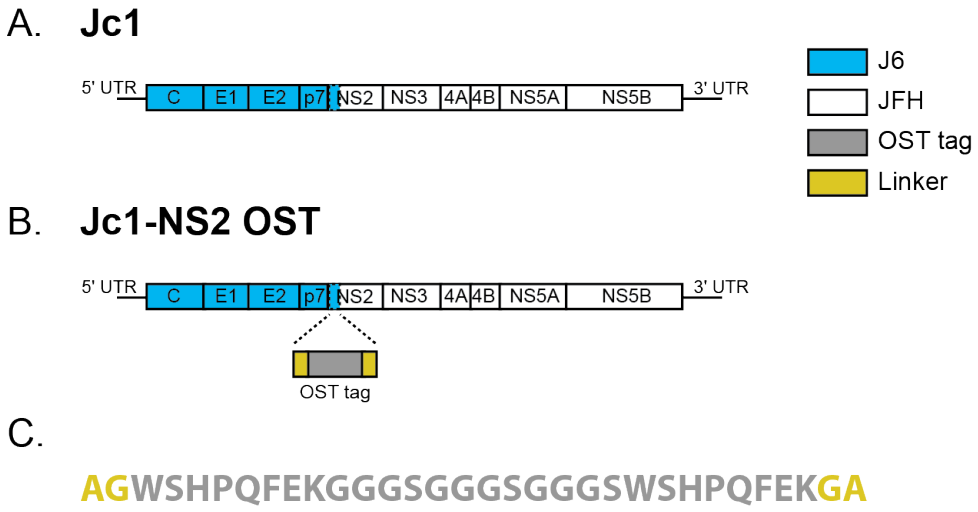

Fig. 6-1: Jc1 J6/JFH NS2 OST. Jc1, an intergenotypic J6/JFH chimera encoding wild type (A) or 2x OST-tagged NS2 (B). Genotype 2a J6 is shown in blue, and 2a JFH in white. The 2x OST tag is represented in grey, with its N and C-terminal linker in yellow (C).

We chose multiple locations close to the N-terminus of NS2 as our previous data showed the necessity of a free NS2 C-terminus that does not allow additional residues (55). The first insertion site was after amino acid one of NS2 (2783), the second after residue four of NS2 (2791) (Fig. 6-2).

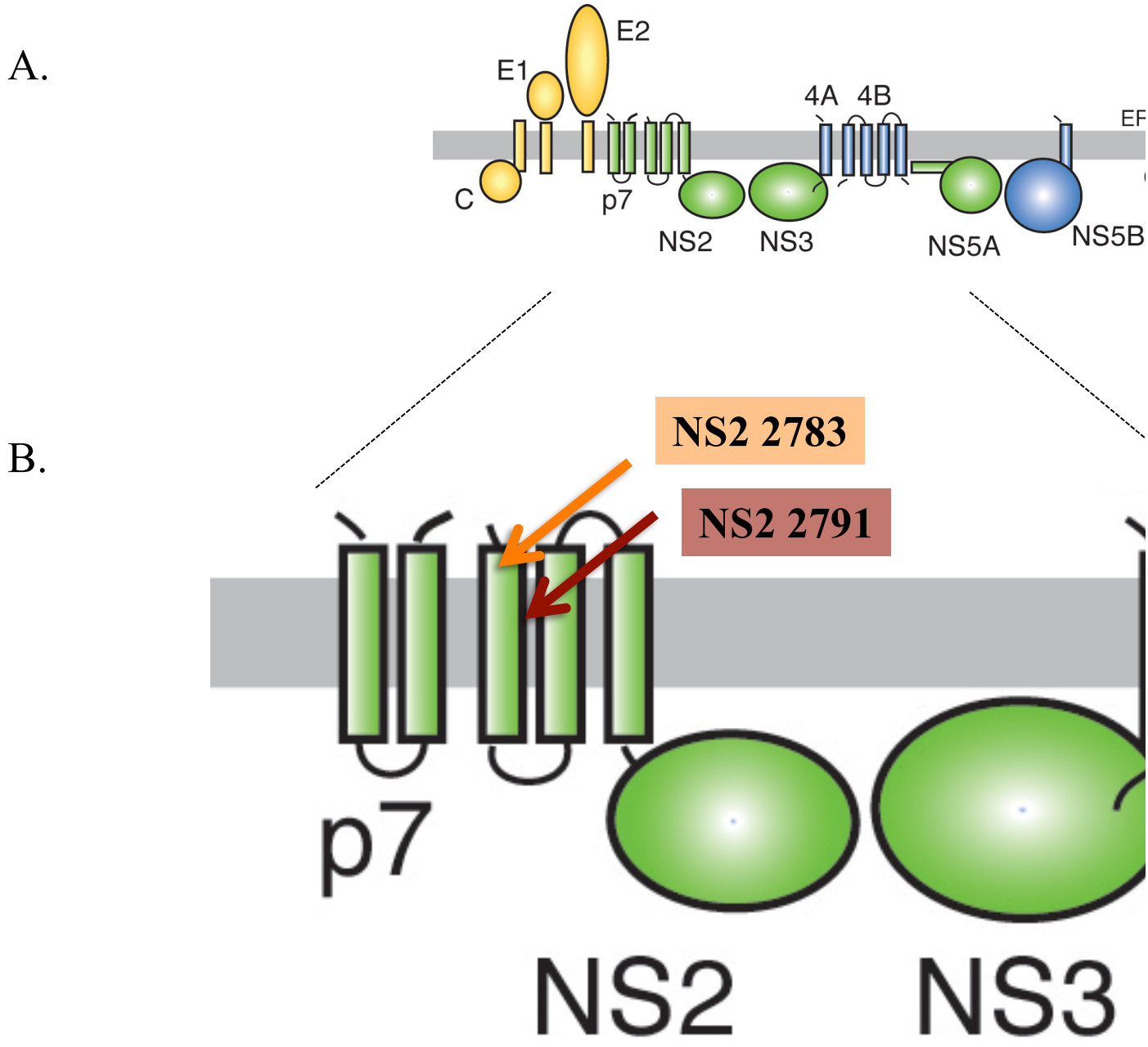

Fig. 6-2: **NS2 OST tag location.** HCV polyprotein schematic of N-terminal OST tag insertion into NS2 in a full-length Jc1 background. HCV polyprotein (A), NS2 N-terminal OST tag positions (B) ((210) modified).

12.3 Characterization of OST tagged NS2

We identified two locations that tolerate insertion of a strep tag while maintaining near wild-type levels and kinetics of replication and infectious virus production (Fig. 6-3, 6-4).

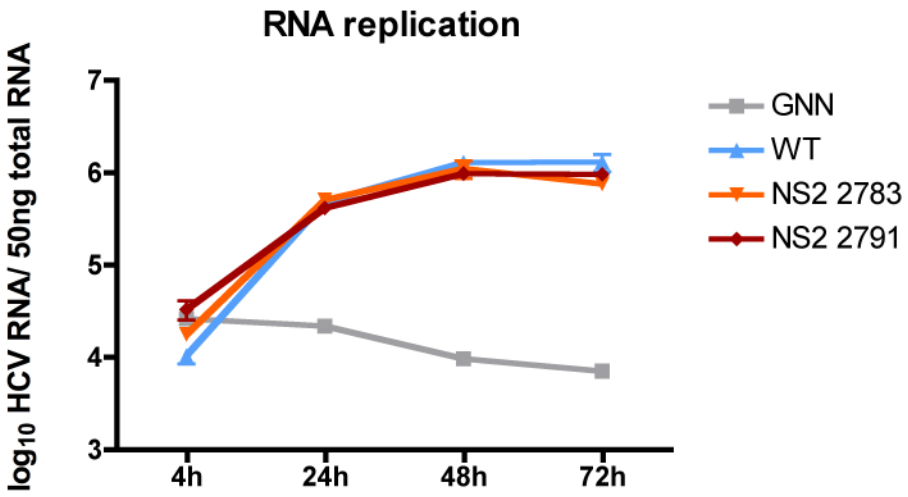

Fig. 6-3: Jc1 J6/JFH OST RNA replication. RNA replication of OST tagged NS2 determined by HCV-specific qRT-PCR of total RNA purified from Huh-7.5 cells harvested at 4, 24, 48, and 72 h post-electroporation. Polymerase defective Jc1/GNN shown in grey, wild type Jc1 in blue and two different tagged NS2 constructs in orange (NS2 2783), and red (NS2 2791).

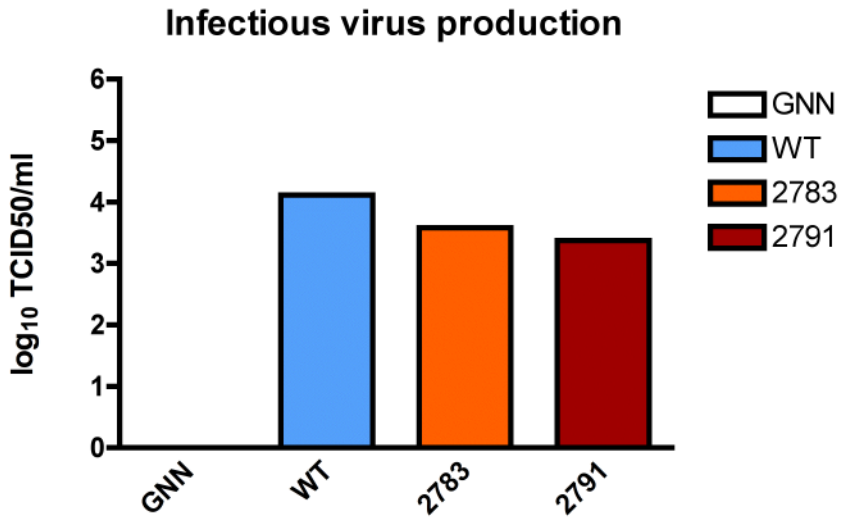

Fig. 6-4: Jc1 J6/JFH infectious particle production. Intracellular infectious virus production. Infectious titers determined by TCID50 assay at 72 h post-infection. Polymerase defective GNN shown in grey, wild type in blue and two different tagged NS2 constructs in orange (NS2 2783) and red (NS2 2791).

Proper polyprotein processing could be observed for the tagged genomes, and tagged NS2 protein remained stable. The shift of NS2 tagged protein in figure 6-5 shows that the tag remains bound to NS2 after cleavage.

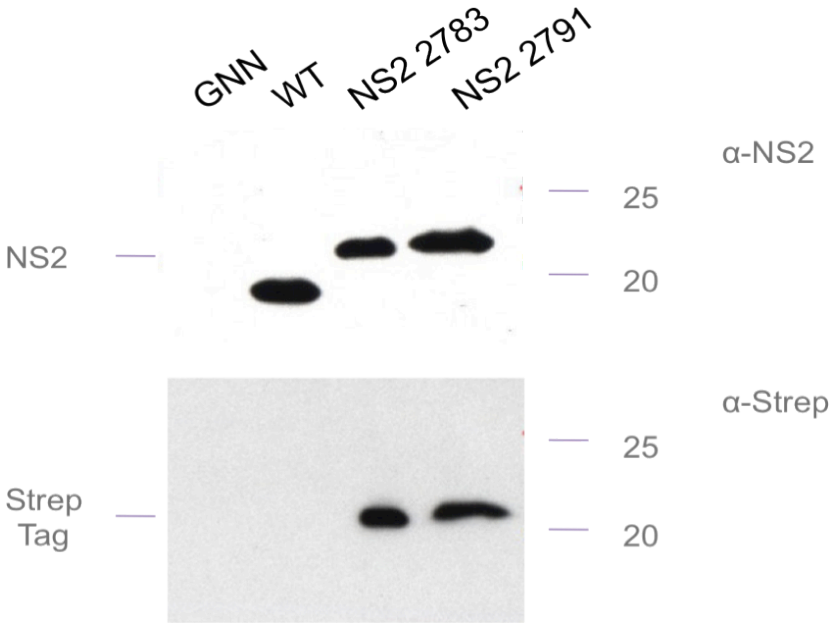

Fig. 6-5: NS2 OST expression. Immunoblot, using α-NS2 (6H6 1:500) top panel, and α-Strep mAb (1:500) bottom panel, reveals that 2x OST-tag is retained in NS2.

12.4 Scheme of NS2 OST pull down assay

After the validation and characterization of the tagged NS2 constructs, we were able to look for NS2 interactions in a pull down assay, followed by mass spectrometry. The scheme of the NS2 pull down assay is shown in Fig. 6-6. NS2 construct 2783 was electroporated into Huh-7.5 cells. Cells were lysed 72 h post-electroporation and incubated with Strep-tactin beads. After seven washes, proteins were separated on a 4-20% Tris-glycine gel followed by mass spectrometry analysis.

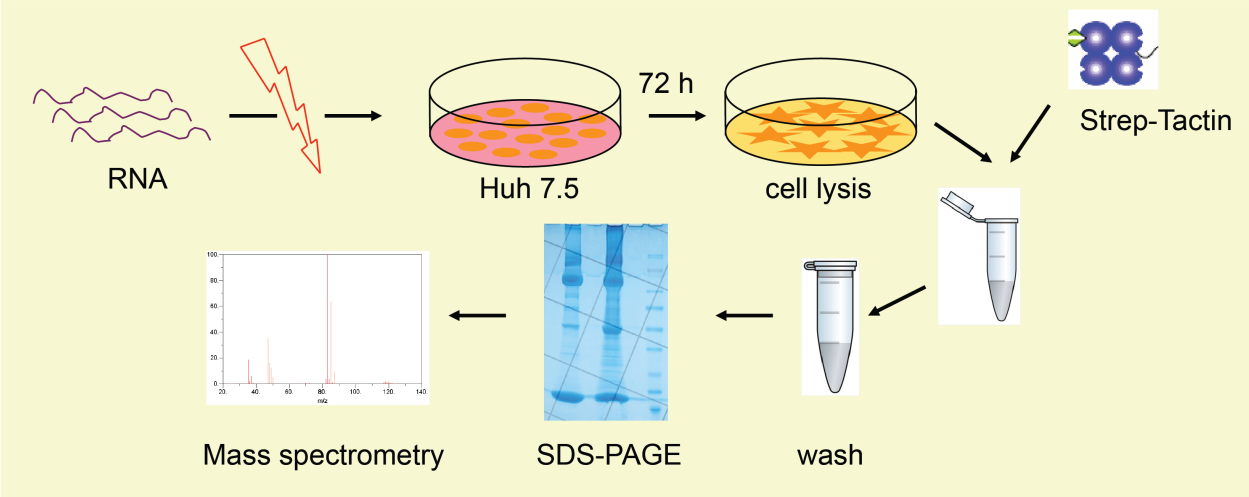

Fig. 6-6. NS2 OST pull-down scheme. Huh-7.5 cells were harvested 72 h post-electroporation and incubated with Strep-tactin. Proteins were separated by Tris-Glycine SDS-PAGE, and then stained with colloidal blue. Mass spectrometry revealed numerous known and unknown cellular and viral protein hits.

The colloidal blue stained 4-20% Tris-glycine gel revealed differences between the wild type (WT) and the OST tag NS2. The NS2 tag lane shows additional and more prominent bands than the control lane, indicating a successful pull-down of more relevant factors, bound to NS2 (Fig. 6-7).

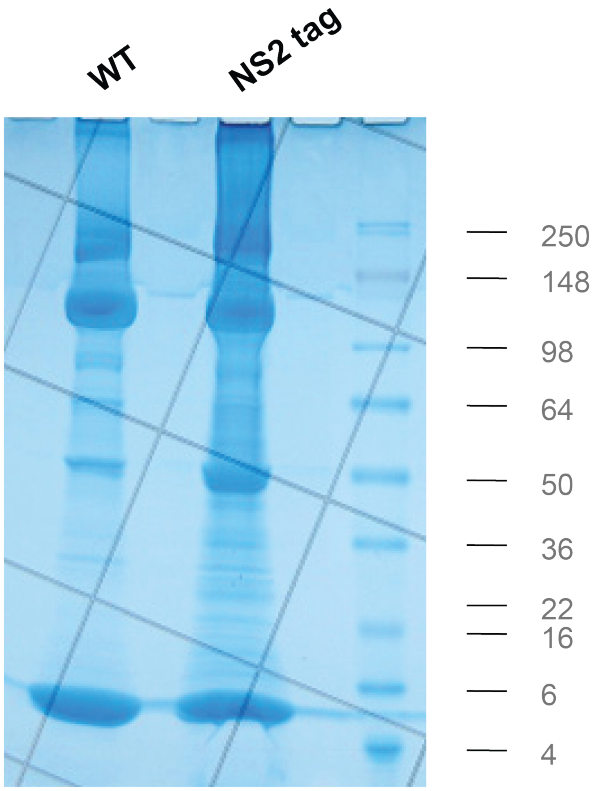

Fig. 6-7. Pull-down of wild type and OST-tagged NS2. 4-20% Tris-Glycine gradient gel with wild type Jc1 (WT) and NS2 2783 OST tag (NS2 tag) after pull down with Strep-tactin resin. SeeBlue Plus2 Pre-stained standard is shown on the right.

12.5 Identification of potential NS2 interacting partners

The mass spectrometry data revealed many proteins potentially interacting with NS2. Pathways involved in NS2 interactions included signaling pathways, hemostasis and lipid metabolism (Fig. 6-8). Many hits pointed to an interaction with actin, myosin and tubilin or vesicle transport. Chaperones (Calnexin) and heat shock proteins (HSP) could also be identified. Factors involved in apoptosis, RNA elongation, G-proteins and cell cycle/division were less abundant. Beclin-I was the only protein identified with known anti-viral activity. An example of a top ten hit list can be seen in Fig. 6-9. In addition to many cellular factors, we could determine physical viral protein interactions between NS2 and E2, as well as NS2 and NS3.

The importance of candidate interactions is currently validated and mechanistic studies are carried out to verify these results. The characterization of these important HCV factors will provide new insights into the NS2 mechanism in virus assembly, and establish new targets for the development of antivirals leading to improved HCV therapies.

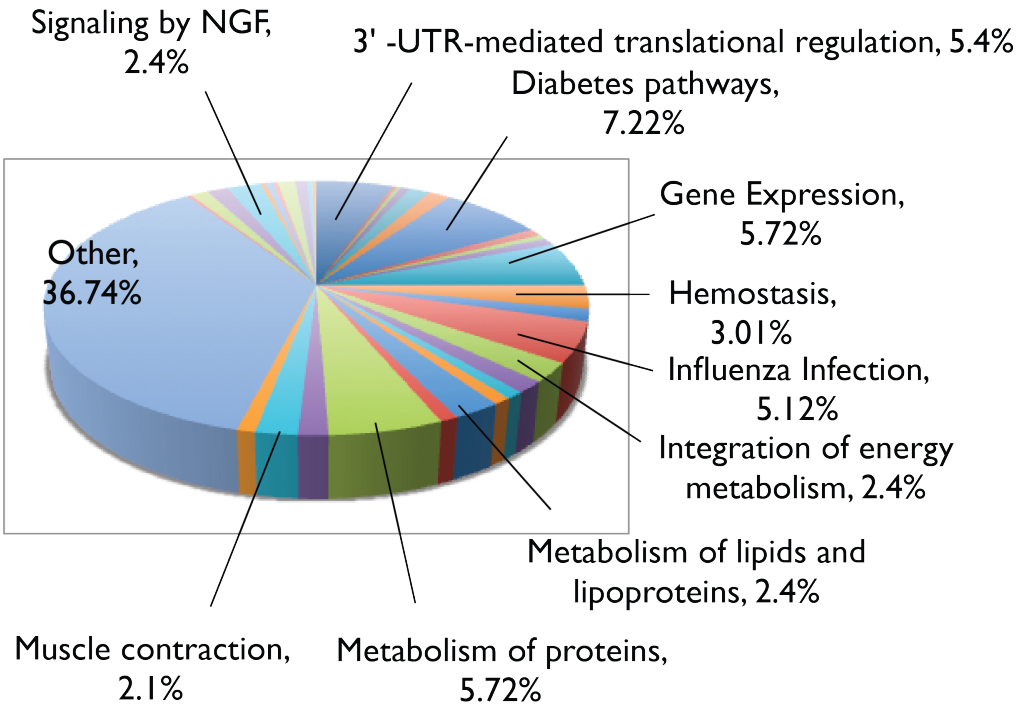

Fig. 6-8. Discovered NS2 interactions and their pathways. Mass spectrometry data from NS2 OST tag pull downs. Overview of the various pathways affected by NS2.

Hits

Accession	Description	Score	Matches	Band
MLRM_HUMAN	Myosin regulatory light chain 2, nonsarcomeric (Myosin RLC) - Homo sapiens (Human)	7154	247	17
ACTN4_HUMAN	Alpha-actinin-4 (Non-muscle alpha-actinin 4) (F-actin cross-linking protein) - Homo sapiens (Human) • Hemostasis	3502	170	7
RL13_HUMAN	60S ribosomal protein L13 (Breast basic conserved protein 1) - Homo sapiens (Human) • Diabetes pathways • Metabolism of proteins • Influenza Infection • Gene Expression • 3' -UTR-mediated translational regulation	1417	139	15
CLH2_HUMAN	Clathrin heavy chain 2 (CLH-22) - Homo sapiens (Human) • Gap junction trafficking and regulation	1875	121	5
RL7A_HUMAN	60S ribosomal protein L7a (Surfeit locus protein 3) (PLA-X polypeptide) - Homo sapiens (Human) • Diabetes pathways • Metabolism of proteins • Influenza Infection • Gene Expression • 3' -UTR-mediated translational regulation	1972	119	14
RL10A_HUMAN	60S ribosomal protein L10a (CSA-19) - Homo sapiens (Human) • Diabetes pathways • Metabolism of proteins • Influenza Infection • Gene Expression • 3' -UTR-mediated translational regulation	2057	112	15
AHNK_HUMAN	Neuroblast differentiation-associated protein AHNAK (Desmoyokin) (Fragments) - Homo sapiens (Human)	1377	97	1
RL6_HUMAN	60S ribosomal protein L6 (TAX-responsive enhancer element-binding protein 107) (TAXREB107) (Neoplasm-related protein C140) - Homo sapiens (Human)	1394	91	13
TBA6_HUMAN	Tubulin alpha-6 chain (Alpha-tubulin 6) - Homo sapiens (Human)	1945	83	11
RL4_HUMAN	60S ribosomal protein L4 (L1) - Homo sapiens (Human)	1274	75	11

Fig. 6-9. Cellular NS2 interaction partners. Example of a top ten hit list of NS2 interacting cellular proteins based score and matches from mass spectrometry. Hits were defined by: score >40, and matches >2.

It has become evident that NS2 is crucial in virus assembly, also via viral protein:protein interactions. Essential protein:protein interactions, indirectly affecting NS2 are core-NS5A, core-E1, and E1-E2. We were able to show an NS2-NS2 interaction via dimerization and genetic analysis of NS2 and NS3 mutations pointed towards E1 and NS3. In accordance to these results, a physical interaction could be identified between NS2-E2, NS2-NS2, and NS2-NS3 through an NS2 pull-down. Combining results from studies conducted with chimeric constructs and our data lead to a map of NS2 networks (Fig. 6-10, black and grey arrows).

12.6 Mechanisms of NS2 protein interactions

It has become evident that NS2 is crucial in virus assembly, also via viral protein:protein interactions. Essential protein:protein interactions, indirectly affecting NS2 are core-NS5A, core-E1, and E1-E2. We were able to show an NS2-NS2 interaction via dimerization and genetic analysis of NS2 and NS3 mutations pointed towards E1 and NS3. In accordance to these results, a physical interaction could be identified between NS2-E2, NS2-NS2, and NS2-NS3 through an NS2 pull-down. Combining results from studies conducted with chimeric constructs and our data lead to a map of NS2 networks (Fig. 6-10, black and grey arrows).

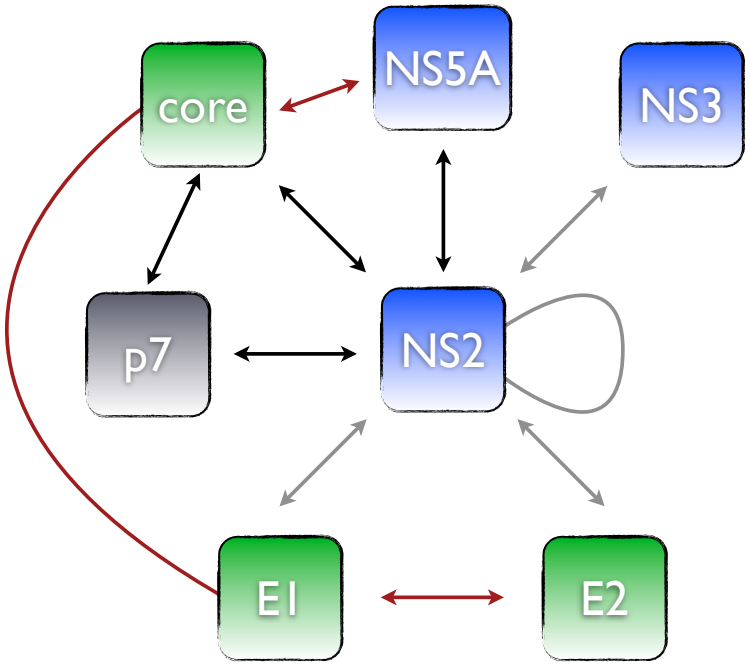

Fig. 6-10. NS2 assembly interaction map. Red arrows show experimentally determined viral interactions. Genetic interactions are shown in black while genetic and physical interactions identified in this study are shown in grey. Structural proteins are shown in green, NS proteins in blue, and p7 in grey ((116) modified).

13 Chapter 7: Discussion

13.1 The NS2 protease domain

The crystal structure of the post-cleavage form of the NS2 protease domain revealed that NS2 is active as a dimer and the C-terminus of NS2 restricts this activity to a one time event by binding to the active site (167). We investigated the role of this understudied protein which only determined function had been its proteolytic activity. Our preliminary data as well as other published data suggested that NS2 is essential for infectious particle production and that it is not involved in RNA replication.

Based on structural data (167) and sequence alignments, we investigated the importance of several residues within the protease domain to determine their function and importance in polyprotein processing, RNA replication and infectious virus production.

Residues of the NS2 protease domain were grouped into three different areas; the active site and its surroundings, the crossover region and the C-terminal domain.

The majority of residue substitutions around the active site had little effect on infectious virus production but indirectly affected RNA replication in the context of a monocistronic genome, by preventing NS2-3 cleavage.

His 143, Glu 163 and Cys 184 have been identified as essential active site residues required for NS2-3 processing (131, 268), but not for infectious virus assembly (114). In addition, we identified several other residues important for NS2-3 processing and replication. Mutation of residue Tyr 141 to an alanine abolished NS2-3 cleavage, whereas a more conservative change to Phe had little effect on processing or replication. The aromatic ring at position 141 probably acts as a support for the active site, a function that likely cannot tolerate a smaller side chain. Mutation of Pro 164 to alanine or glycine prevented replication of a monocistronic genome while substitutions in a bicistronic background, however, decreased infectious titers. It is possible that mutation of this cis-proline dramatically affects the overall NS2 structure; indeed, the P164G substitution appeared to slightly destabilize the protein. P164 may directly participate in infectious virus assembly independent of a role in catalysis. Combining the RNA replication and infectious particle production data with FRET results from the dimerization assay, it is also possible that mutations of P164 affect NS2 dimer formation, as this proline is important for positioning the linker between the N- and C-terminal subdomains. Both mutations, Pro 164 to

alanine or to glycine showed the same phenotype (Fig. 4-1). Pro 164 has a cis conformation that is thought to bend the peptide backbone to establish the correct geometry of the Glu 163 side chain for catalysis; Studies of the NS2-3 protein of the distantly related pestivirus, classical swine fever virus, have similarly shown that the NS2 protease activity is dispensable for infectious virus production (206). However, a histidine-to-arginine mutation within the active site abolished infectivity without affecting NS2-3 expression (206).

A similar correlation can be observed for residue Tyr 141. Tyr 141 mutated to an alanine was replication defective and did not produce high levels of NS2 dimer in our FRET assay while a substitution to a phenylalanine showed wild type levels for both, RNA replication as well as FRET signal (Fig. 3 publication 1, Fig. 4-9). Residues Tyr 141 and Pro 164 are important for NS2 dimerization. Failure to dimerize or inefficient dimerization results in a cleavage deficiency leading to an inhibition of RNA replication and fatality of the virus. Leu 144 is thought to create the correct active site architecture similar to Tyr 141, but we found that an alanine mutation allowed NS2-3 processing while a charged lysine substitution abolished the function of the active site, changing the geometry and possibly preventing His 143 to function (Fig.3 publication 1).

It is also possible that minimum levels of NS2 dimer are required for infectious particle production, which accentuates that NS2 might act as a molecular switch, shifting viral processes from RNA replication to particle production.

Structural data suggested that the NS2 crossover region positions the subdomains to create two composite active sites and mutations in this region were thought to disrupt dimer stability and NS2-3 processing. RNA replication of a monocistronic genome, however, was impaired only by substitution of W177 to cysteine or by a triple mutation of Met 170 Ala / Ile 175 Ala / Trp 177 Ala, suggesting that single point mutations may not have a drastic effect on dimer integrity. $NS2^{pro}$ stability assays (unpublished data) and the significant buried surface area between the monomers indicate that the $NS2^{pro}$ dimer is highly stable (167). While NS2-3 processing was not really impaired, several mutations affected infectious virus production. Interestingly, many crossover region residues are exposed on the surface as shown in Fig. 9 publication 1 and residues in this region may be necessary for crucial viral and host protein-protein interactions in assembly and virus production. In fact NS2 has been described to interact with many viral proteins and characterization of our anti-NS2 antibody revealed the epitope at position 197 to 208 of the NS2 protein (55). Genetic and physical interactions with structural proteins core, and E2 as well as with nonstructural proteins p7, NS3, NS4A, and NS5A have previously been

reported (119, 126, 155, 211, 229, 246, 305). In addition, we also identified an adaptive mutation in E1 (Ala 269 Thr), suggesting an interaction between NS2 and E1 (Fig.1 publication 1).

The C-terminal subdomain of NS2 contributes the catalytic cysteine to the composite active site and deletion analysis revealed that even a single amino acid truncation at the C-terminus severely impaired infectious virus production. Given that RNA replication was not affected, mutations of the C-terminal residue leucine 217 only tolerated a substitution to an isoleucine to produce infectious virus in the bicistronic background, although at very low titers. All other residues abolished infectivity completely (Fig. 7 publication 1). No infectious particles were produced in a monocistronic background, and only an alanine substitution allowed RNA replication while other mutations did not replicate (Fig. 2 publication 2) possibly due to a cleavage deficiency.

Residue Leu 217 has an essential role in infectious virus production that is also accentuated by the high level of conservation compared to the high variability of the NS2 protein across all genotypes. The structure of the post-cleavage form of $NS2^{pro}$ shows that Leu 217 occupies the active site through contacts with H143 and C184 (112, 167). This conformation has been suggested to render the protease inactive after a single auto-proteolytic processing event (167). NS2 expression and stability were not dramatically altered by most C-terminal substitutions, but it is possible that deletion of Leu 217 changes the structure of NS2 by liberating the C-terminus from the active site that in counterpart could prevent essential interactions, such as dimerization or heterotypic associations with viral or host proteins. Distinct similarities have been noted in the catalytic cleft architecture of the NS2 protease and the alpha virus capsid protein (167). The alpha virus capsid, also an autoprotease, is involved in infectious virus production via its C-terminus and analogous to NS2, the highly conserved C-terminal tryptophan of the alphavirus capsid occupies the active site post-cleavage (43).

Mutation of this C-terminal tryptophan to alanine or arginine in a system that uncoupled proteolysis from infectious alphavirus production almost completely abolished nucleocapsid assembly; substitution of the terminal tryptophan with phenylalanine, however, was tolerated (253). Similarly, mutations in the alphavirus capsid that displaced the terminal tryptophan from the active site pocket were found to be highly deleterious to its function (42). These observations suggest that the location of the C-terminus, as well as the presence of a leucine or similar residue at position 217, may be critical to the structure and post-cleavage functions of these viral proteases.

In addition, C-terminal extensions into NS3 were highly deleterious; even one additional amino acid reduced viral titers by three to five folds. Similar results have previously been reported, where ubiquitin fused to the NS2 C-terminus abolished infectious virus production (112). Together, the data suggests the requirement of a free leucine at the C-terminus that remains locked in the active site, limiting the protease activity to a single event and assuring a specific post cleavage NS2 C-terminal and active site structure essential for NS2 functions in infectious particle production.

The C-terminal extensions demonstrated for the first time in a functional HCV virus, that the minimal length of NS3 residues required for proteolytic cleavage is not 181 amino acids, but far less since our extensions with 31, 40, and 90 amino acids showed NS2-3 cleavage. The 181 residues only seem to be required for efficient cleavage. Schregel et al. have similarly demonstrated residual enzymatic activity of NS2 followed by only 2 amino acids of NS3 (245).

Although cleaved NS2 could be detected, no infectious particles were produced. There might be the need for a critical, minimal level of cleaved NS2 to switch from RNA replication to infectious virus production. Insufficient quantities of mature NS2 are produced by suboptimal cleavage or short fragments of NS3 impair infectivity, possibly by acting as dominant-negative inhibitors of interactions between NS2 and full-length NS3 (126). For pestiviruses, the uncleaved NS2-3 precursor is essential for infectious virus production while fused residues from NS3 are deleterious to the role of HCV NS2 infectivity (2, 206). In both viruses NS2 and NS3 form functional associations during virion morphogenesis, suggesting conserved strategies between HCV and other members of the family *flaviviridae* (210).

Further, revertants obtained by passaging the C-terminal NS2 mutations Asp 207 Ala, and Leu 217 Ala point towards an interaction with NS3. Residue Glu 221 in NS3 has been identified as an important residue, as both initial constructs Asp 207 Ala and Leu 217 Ala showed a substitution at this amino acid, either to a leucine (D207A) or a histidine (Leu 217 Ala). Construct Leu 217 Ala presented an additional change in NS3 at position Thr 478 where the threonine was substituted to a proline (Fig. 8 publication 2). Various host factors such as cellular kinase CKII also appear to associate and phosphorylate NS2 (78). NS2 may interact with additional host factors to influence apoptosis (66) and cellular gene expression (62). More recently, an interaction with CsA has been described that inhibits replication of full-length HCV mediated through cyclophilin A (47).

We determined that the proteolytic activity and the role in virus assembly/virus production are essential but two distinct functions of NS2. A number of substitutions in the dimer crossover region and C-terminal subdomain affected infectious titers, but not protease activity, and L217 was found to be dispensable for processing but critical for infectious virus production. Similarly, the finding that NS2 functions in assembly do not tolerate C-terminal extensions contrasts with the requirement for the NS3 protease domain for optimal NS2-3 cleavage.

TM domains of NS2 play critical roles in infectivity (112) but are not absolutely required for protease activity (84, 218, 242, 268), while the active cleft is essential for the protease function but predominantly dispensable for infectivity ((112, 114); this study). Both the TM domains and the protease domain are essential to mediate infectious virus production.

13.2 NS2 dimerization

Results from purified $NS2^{pro}$ (unpublished data) and structural data predicted NS2 to be present as a dimer. After measuring distances between various residues in the $NS2^{pro}$ model, we chose a couple of appropriate crosslinker for an initial screen. DSS with a 11.4 Å spacer arm and and EGS [Ethylene glycolbis(succinimidylsuccinate)] with a 16.1 Å demonstrated the most efficient crosslinking properties for purified $NS2^{pro}$, overexpressed NS2 alone and full-length genomes.

$NS2^{pro}$ could be crosslinked by adding various molar ratios of DSS. Similar, various $NS2^{pro}$ protein concentrations added to a constant DSS concentration produced a concentration range (Fig. 4-2). Successful crosslinking was only possible at low to room temperatures while crosslinking at 60 °C probably only denaturated the protein.
Overexpressed NS2 from an NS2-NS3 or a full-length expressing construct could be crosslinked in U2OS and in Huh-7.5 cells. Already low concentrations of DSS (0.5 mM) were able to produce an NS2 dimer (Fig. 4-3). DSS is by no means NS2 specific and reacts with any primary amine to form stable amino bonds specifically with side chains of lysine (K). Full-length genotype 1a NS2 contains seven lysines all through out the protein with five in the protease domain. Similar, genotype 2A NS2 includes six lysines with four in the protease domain. Experiments with full-length genome revealed a higher affinity to E2 than any other protein we tested for. NS2 possesses similarities to the KUNV NS1 protein, which acquires a partially hydrophobic

character (295, 296). Interestingly, a single mutation causes a virus growth defect in culture and was severely attenuating in mice (93).

Taken together, we were able to confirm that NS2 is present as a dimer *in vitro* and *in vivo* and that dimer formation is critical for NS2/3 cleavage. There seems to be a necessary threshold of NS2 protein levels for cleavage and production of active replicase complexes and *de novo* initiation of RNA synthesis. A delay of RNA replication allows for accumulation of NS3-4A complexes that potentially antagonize induction of type I interferon by the host cell.
The NS2 dimer may even play a role in assembly steps, as the dimeric structure appears to be extremely stable. It is not known whether NS2 monomers or oligomers play a role in these steps as NS2 could interact with NS3 in an oligomeric state similar to core, which is also thought to organize proteins in particle assembly at the site of lipid droplets (LD) (207). NS2 could act mutually with core in bringing the various proteins together at the site of LDs assuring the presence of essential factors for viral assembly.

13.3 Role(s) of the NS2-NS3 cleavage site

NS2 is essential for the HCV life cycle due to its role in infectious particle production and the protease function that, together with the N-terminal region of NS3, cleaves itself from the polyprotein (114, 228). More recently, NS2 has been found to be critical for the production of infectious particles (55, 112, 226). We have shown that several mutations in the NS2 protease domain affect RNA replication through dimer destabilization or a cleavage deficiency. Other mutations only impaired infectious virus production. To investigate the importance of residues at the NS2/3 cleavage site, as well as their function in RNA replication and infectious virus production we mutated the NS2 P1 position as well as P1', P2', P3', P4' at the N-terminus of NS3.

Position P1 of the cleavage site, which is represented by the NS2 C-terminal residue L217 allows an alanine substitution for cleavage and RNA replication (fig. 1 publication 2) but only an isoleucine at this position is able to maintain the essential role of the leucine to some extend in infectious particle production. The isoleucine mutation does not support cleavage or RNA replication in monocistronic constructs. Consistent with our results, work in polyprotein overexpression systems found 69% cleavage efficiency for a L217A change, whereas a proline

substitution completely prevented cleavage (236). Position P1 is highly conserved across genotypes and our results emphasize how indispensable this leucine at the end of NS2 is. It cannot be substituted by any other amino acid to maintain both functions in cleavage and infectious virus production.

The alanine at the N-terminus of NS3, position P1' of the cleavage site only tolerates a lysine. A lysine is the only residue allowing NS2/3 cleavage, replication and infectious virus production, while other mutants supported only one or the other function (Figs. 3 and 4 publication 2). Proline and aspartic acid at this position had previously been shown to be cleavage deficient at 11% for A1D and 0% for A1P (236). Changes in P1 and P1' affecting the conformation severely inhibit cleavage, and therefore RNA replication and virus production (102). The region, with residues P1 and P1' represents an attractive target for the development of future drugs and therapies.

Alanine and lysine substitutions at position P2' can replicate and produce virus which is in accordance to Reed *et al*., who found a 70% efficiency for P2A although did not analyze P2K (236). Interestingly a leucine at this position abolishes NS2/3 cleavage and by consequence inhibits RNA replication and infectivity. Leucine seems to be the preferred residue for infectious virus production alone as the bicistronic construct showed increased replication and infectivity (Figs. 4A and B).

NS2/3 processing is inhibited by isoleucine to alanine, glutamic acid, and proline changes at position P3'. Similar polyprotein processing results had been shown with overexpression of NS2/3 mutants I3A and I3E that allowed up to 70% cleavage efficiency (236). The P3' position may not be essential for processing but could affect RNA structures important for RNA replication. Isoleucine P3' also plays a crucial role in infectious virus production, as all the mutants were lacking infectivity in the bicistronic background (Fig. 4 publication 2).

Position P4' tolerated an alanine but not a proline for cleavage and, although replication of T4A was similar to wild type, neither was infectious (Figs.3 and 4 publication 2). This could indicate that residues further away from the actual cleavage between NS2 and NS3 are less important for the cleavage per se, but maintain an important role for the production of infectious particles through other protein-protein interactions.

The highly conserved region at the C-terminus of NS2 and the N-terminus at NS3 plays a major role in the viral life cycle as a cleavage deficiency abolishes RNA replication and the ability of the

virus to propagate. The C-terminal NS2 residues manage two essential functions, the protease activity and infectious particle production. Infectivity can only be assured by the presence of a proper cleaved NS2 protein (55). Similar, N-terminal NS3 residues manage cleavage efficiency and play an important role in infectious virus production through various protein-protein interactions, one being an NS2-NS3 post cleavage contact.

13.4 NS2-NS3 interplay

NS3 with its serine protease at the N-terminus and a C-terminal RNA helicase function is an essential protein for HCV and therefore represents the number one target for the design of HCV inhibitors. In addition to the interplay between the terminal residues during cleavage, NS2 and NS3 are thought to associate after processing to accomplish further roles in the life cycle. There is growing evidence that NS2 and NS3 work together, as post-cleavage interactions of the proteins have been detected in co-localization and co-immunoprecipitation studies (58, 99, 126). We developed several NS2-NS3 interaction models based on known structural data of these two non-structural proteins. Analysis of all models led to a single, most probable NS2/3 structure that served as the basis of the mutagenesis of key residues, essential for these interactions.
(Fig. 5A publication 2).

Potential interacting residues NS2 S211 and NS3 D168 are important for replication that is disrupted by substituting either to an alanine. Previous research showed that the NS3 protease activity requires a catalytic triad (S139, H57 and D81) and an oxyanion hole (backbone amides of Gly 137 and Ser 139) (167). Mutation of Asp 81 abolished replication completely in an NS2/3 cleavage independent manner, while substitution of Ser 139 heavily impaired RNA replication but allowed reduced infectious virus production in a bicistronic background. Necessary interactions for assembly and release are therefore still possible, including an NS2-NS3 contact. Interestingly, mutation of a residue involved in HCV inhibitor resistance (R155), which potentially interacts with NS2 residues W214 and R161, showed impaired infectious virus production in the bicistronic background (125). Treatment with macrocyclic and linear protease inhibitors data never revealed an alanine substitution at position 155 while lysine, glutamine, serine and threonine are fairly common (11, 36, 125, 139). It is possible that mutations prevent necessary interactions with the cofactor, thus destabilizing the NS3 N-terminal or hinder zinc coordination (187, 299). NS3 protease activity requires its cofactor NS4A as well as the right coordination of Zn^{2+} by the protease active site residues Cys 1123, Cys 1125, Cys 1171, and His 1175 (19, 70,

149). NS2 mutations could also have a dominant negative effect on NS3 thus impairing RNA replication.

13.5 Viral interactions

Passaging and analysis of NS2 and NS3 mutations presented genetic evidence for an interaction with other viral proteins. Initial mutations in NS2 exposed second site mutations in E1 and NS3. Interestingly, sequence analysis of NS2 mutations Leu 217 Val and Leu 217 Ile presented the same E1 mutation Ala 269 Thr, which had previously been described to enhance release of infectious particle production for a J6/H77NS2/JFH, a J6/JFH construct with a full length H77 NS2 (55). An important role can be attributed to residue NS3 Glu 221. A change at this position had been detected with two different NS2 mutant constructs. Passaging of NS2 Asp 207 Ala resulted in a leucine substitution while NS2 L217A gave rise to a histidine change at position 221 in NS3. An additional change to a proline in NS3 at position Thr 478 could be found for construct Leu 217 Ala (Fig. 8 publication 2). This may indicate that a histidine substitution at position 221 might not be enough to overcome the defects caused by the initial mutation and the proline at 478 is needed, possibly for an inter- or intra-molecular interaction. Phan et al. have shown that an NS3 Q221L mutation lowers the affinity of native, full-length NS3-4A for functional RNA binding and is able to enhance NS2 mutations (226).

In fact, genetic evidence of NS2 interacting with core, E1, E2, p7, NS3, NS4A and NS5A has been described earlier (116, 226). In addition to this genetic evidence, we were also able to show an interaction between NS2 and NS3 in a pull-down assay producing infectious particles using a tagged NS2. The mass spectrometry also revealed for the first time to our knowledge a physical interaction between NS2 and E2. Further, NS3 could be linked to E2 while analyzing a passaged NS3 mutation construct that gave rise to two E2 residue changes at position A192G, and A263G (Fig. 8B publication 2). E2 could potentially act on NS3 in a direct, or indirect way, through another host or viral protein, like NS2.

13.6 Host interactions

Numerous NS2 interacting host proteins have been identified using a pull-down assay. NS2 is essential for assembly steps and seems to bring together glycoproteins and nascent particles to form fully infectious HCV virions. In accordance to this, we determined host cell proteins involved in vesicle transport, apoptosis, ER secretory pathways and clathrin mediated transport and assembly to interact with NS2. A larger secondary group involved cytoskeleton proteins such as actin/myosin and tubulin in NS2 interactions and chaperones from the HSP family. Interestingly, Hsp90 is thought to regulate gene expression in mammalian cells and has been identified as the target for a gyrase B inhibitor, coumermycin A1 (C-A1), a potent antiviral. Further, interplay between C-A1 and cyclophilin A could be observed in the context of an HIV infection, while the NS2 protease function of liberating NS2 and NS3 is cyclophilin dependent (47, 285). To create a full map of NS2 interacting proteins, and their respective pathways, more functional assays and characterization is needed. The role of NS2 in infectious virus production is defined by interacting with E1, E2, NS3 and cellular factors to bring all other necessary proteins together to form infectious particles. NS2 could also be an important factor to establish a chronic infection due to its regulation of apoptosis and inhibition of cellular gene expression allowing survival of an HCV infected cell.

13.7 Conclusions

To summarize, we found that residues around the active site of the NS2 protease domain play an important role in NS2/3 cleavage, thus RNA replication and dimerization. The $NS2^{pro}$ crossover region and the C-terminus are mainly involved in infectious virus production through various protein-protein interactions. HCV requires a free NS2 C-terminus with an essential leucine to mediate infectivity. Adding of amino acids to the C-terminus, or deletion of residues result in failure to produce infectious particles.

NS2 dimerization could be validated by chemical crosslinking as well as FRET assays and lead to the understanding of dimerization defects in NS2 active site region mutations.

The NS2/3 cleavage site with its residues does not only serve as a signal sequence for cleavage, but also exerts an important function in infectious virus production.

The proposed NS2-NS3 post-cleavage interaction structure revealed several important residues in NS2 and NS3, crucial for infectious virus production. Absence of NS2/NS3 interactions could

result in these viral defects, although indirect interactions through other proteins cannot be excluded at this point.

We investigated the role of the non-structural protein 2 in the viral life cycle and were able to identify two distinct functions, a protease function and a function in virus assembly. Various regions within NS2, essential for either cleavage or infectious particle production could be determined. In addition, we showed that NS2 interacts with E1, E2, NS3, and numerous host proteins to assure virus assembly and infectious particle production. This study clearly shows the significance of NS2 in the viral life cycle and establishes NS2 as an attractive anti-viral drug target in addition to current protease and polymerase inhibitors currently in clinical trials targeting NS3 and NS5B. The development of new compounds against NS2 or one of its interaction partners identified in this study, will help to improve medical treatments and the patients response, thus leading to an increased number of cured patients across all genotypes.

14 References

1. 2004. Global burden of disease (GBD) for hepatitis C. J Clin Pharmacol **44:**20-29.
2. **Agapov, E. V., C. L. Murray, I. Frolov, L. Qu, T. M. Myers, and C. M. Rice.** 2004. Uncleaved NS2-3 is required for production of infectious bovine viral diarrhea virus. J Virol **78:**2414-2425.
3. **Agnello, V., G. Abel, M. Elfahal, G. B. Knight, and Q. X. Zhang.** 1999. Hepatitis C virus and other flaviviridae viruses enter cells via low density lipoprotein receptor. Proc Natl Acad Sci U S A **96:**12766-12771.
4. **Ago, H., T. Adachi, A. Yoshida, M. Yamamoto, N. Habuka, K. Yatsunami, and M. Miyano.** 1999. Crystal structure of the RNA-dependent RNA polymerase of hepatitis C virus. Structure **7:**1417-1426.
5. **Aizaki, H., K. J. Lee, V. M. Sung, H. Ishiko, and M. M. Lai.** 2004. Characterization of the hepatitis C virus RNA replication complex associated with lipid rafts. Virology **324:**450-461.
6. **Ali, N., and A. Siddiqui.** 1995. Interaction of polypyrimidine tract-binding protein with the 5' noncoding region of the hepatitis C virus RNA genome and its functional requirement in internal initiation of translation. J Virol **69:**6367-6375.
7. **Allander, T., A. Beyene, S. H. Jacobson, L. Grillner, and M. A. Persson.** 1997. Patients infected with the same hepatitis C virus strain display different kinetics of the isolate-specific antibody response. J Infect Dis **175:**26-31.
8. **Alter, H. J., and L. B. Seeff.** 2000. Recovery, persistence, and sequelae in hepatitis C virus infection: a perspective on long-term outcome. Semin Liver Dis **20:**17-35.
9. **Alter, M. J.** 2007. Epidemiology of hepatitis C virus infection. World J Gastroenterol **13:**2436-2441.
10. **Amberg, S. M., A. Nestorowicz, D. W. McCourt, and C. M. Rice.** 1994. NS2B-3 proteinase-mediated processing in the yellow fever virus structural region: in vitro and in vivo studies. J Virol **68:**3794-3802.
11. **Anderson, J., C. Schiffer, S. K. Lee, and R. Swanstrom.** 2009. Viral protease inhibitors. Handb Exp Pharmacol**:**85-110.
12. **Andre, P., F. Komurian-Pradel, S. Deforges, M. Perret, J. L. Berland, M. Sodoyer, S. Pol, C. Brechot, G. Paranhos-Baccala, and V. Lotteau.** 2002. Characterization of low- and very-low-density hepatitis C virus RNA-containing particles. J Virol **76:**6919-6928.
13. **Anwar, A., N. Ali, R. Tanveer, and A. Siddiqui.** 2000. Demonstration of functional requirement of polypyrimidine tract-binding protein by SELEX RNA during hepatitis C virus internal ribosome entry site-mediated translation initiation. J Biol Chem **275:**34231-34235.
14. **Appel, N., T. Pietschmann, and R. Bartenschlager.** 2005. Mutational analysis of hepatitis C virus nonstructural protein 5A: potential role of differential phosphorylation in RNA replication and identification of a genetically flexible domain. J Virol **79:**3187-3194.
15. **Appel, N., M. Zayas, S. Miller, J. Krijnse-Locker, T. Schaller, P. Friebe, S. Kallis, U. Engel, and R. Bartenschlager.** 2008. Essential role of domain III of nonstructural protein 5A for hepatitis C virus infectious particle assembly. PLoS Pathog **4:**e1000035.
16. **Barba, G., F. Harper, T. Harada, M. Kohara, S. Goulinet, Y. Matsuura, G. Eder, Z. Schaff, M. J. Chapman, T. Miyamura, and C. Brechot.** 1997. Hepatitis C virus core protein shows a cytoplasmic localization and associates to cellular lipid storage droplets. Proc Natl Acad Sci U S A **94:**1200-1205.
17. **Barbato, G., D. O. Cicero, M. C. Nardi, C. Steinkuhler, R. Cortese, R. De Francesco, and R. Bazzo.** 1999. The solution structure of the N-terminal proteinase domain of the hepatitis C virus (HCV) NS3 protein provides new insights into its activation and catalytic mechanism. J Mol Biol **289:**371-384.
18. **Baril, M., and L. Brakier-Gingras.** 2005. Translation of the F protein of hepatitis C virus is initiated at a non-AUG codon in a +1 reading frame relative to the polyprotein. Nucleic Acids Res **33:**1474-1486.

19. **Bartenschlager, R., L. Ahlborn-Laake, J. Mous, and H. Jacobsen.** 1994. Kinetic and structural analyses of hepatitis C virus polyprotein processing. J Virol **68:**5045-5055.
20. **Bartenschlager, R., L. Ahlborn-Laake, J. Mous, and H. Jacobsen.** 1993. Nonstructural protein 3 of the hepatitis C virus encodes a serine-type proteinase required for cleavage at the NS3/4 and NS4/5 junctions. J Virol **67:**3835-3844.
21. **Bartenschlager, R., M. Frese, and T. Pietschmann.** 2004. Novel insights into hepatitis C virus replication and persistence. Adv Virus Res **63:**71-180.
22. **Bartosch, B., J. Dubuisson, and F. L. Cosset.** 2003. Infectious hepatitis C virus pseudo-particles containing functional E1-E2 envelope protein complexes. J Exp Med **197:**633-642.
23. **Bartosch, B., G. Verney, M. Dreux, P. Donot, Y. Morice, F. Penin, J. M. Pawlotsky, D. Lavillette, and F. L. Cosset.** 2005. An interplay between hypervariable region 1 of the hepatitis C virus E2 glycoprotein, the scavenger receptor BI, and high-density lipoprotein promotes both enhancement of infection and protection against neutralizing antibodies. J Virol **79:**8217-8229.
24. **Behrens, S. E., C. W. Grassmann, H. J. Thiel, G. Meyers, and N. Tautz.** 1998. Characterization of an autonomous subgenomic pestivirus RNA replicon. J Virol **72:**2364-2372.
25. **Behrens, S. E., L. Tomei, and R. De Francesco.** 1996. Identification and properties of the RNA-dependent RNA polymerase of hepatitis C virus. EMBO J **15:**12-22.
26. **Blight, K. J., A. A. Kolykhalov, and C. M. Rice.** 2000. Efficient initiation of HCV RNA replication in cell culture. Science **290:**1972-1974.
27. **Blight, K. J., J. A. McKeating, J. Marcotrigiano, and C. M. Rice.** 2003. Efficient replication of hepatitis C virus genotype 1a RNAs in cell culture. J Virol **77:**3181-3190.
28. **Blight, K. J., J. A. McKeating, and C. M. Rice.** 2002. Highly permissive cell lines for subgenomic and genomic hepatitis C virus RNA replication. J Virol **76:**13001-13014.
29. **Boni, S., J. P. Lavergne, S. Boulant, and A. Cahour.** 2005. Hepatitis C virus core protein acts as a trans-modulating factor on internal translation initiation of the viral RNA. J Biol Chem **280:**17737-17748.
30. **Bradley, D., K. McCaustland, K. Krawczynski, J. Spelbring, C. Humphrey, and E. H. Cook.** 1991. Hepatitis C virus: buoyant density of the factor VIII-derived isolate in sucrose. J Med Virol **34:**206-208.
31. **Bradley, D. W., J. E. Maynard, H. Popper, E. H. Cook, J. W. Ebert, K. A. McCaustland, C. A. Schable, and H. A. Fields.** 1983. Posttransfusion non-A, non-B hepatitis: physicochemical properties of two distinct agents. J Infect Dis **148:**254-265.
32. **Bradley, D. W., K. A. McCaustland, E. H. Cook, C. A. Schable, J. W. Ebert, and J. E. Maynard.** 1985. Posttransfusion non-A, non-B hepatitis in chimpanzees. Physicochemical evidence that the tubule-forming agent is a small, enveloped virus. Gastroenterology **88:**773-779.
33. **Branch, A. D., D. D. Stump, J. A. Gutierrez, F. Eng, and J. L. Walewski.** 2005. The hepatitis C virus alternate reading frame (ARF) and its family of novel products: the alternate reading frame protein/F-protein, the double-frameshift protein, and others. Semin Liver Dis **25:**105-117.
34. **Brass, V., E. Bieck, R. Montserret, B. Wolk, J. A. Hellings, H. E. Blum, F. Penin, and D. Moradpour.** 2002. An amino-terminal amphipathic alpha-helix mediates membrane association of the hepatitis C virus nonstructural protein 5A. J Biol Chem **277:**8130-8139.
35. **Bressanelli, S., L. Tomei, A. Roussel, I. Incitti, R. L. Vitale, M. Mathieu, R. De Francesco, and F. A. Rey.** 1999. Crystal structure of the RNA-dependent RNA polymerase of hepatitis C virus. Proc Natl Acad Sci U S A **96:**13034-13039.
36. **Brown, N. A.** 2009. Progress towards improving antiviral therapy for hepatitis C with hepatitis C virus polymerase inhibitors. Part I: Nucleoside analogues. Expert Opin Investig Drugs **18:**709-725.
37. **Butcher, S. J., J. M. Grimes, E. V. Makeyev, D. H. Bamford, and D. I. Stuart.** 2001. A mechanism for initiating RNA-dependent RNA polymerization. Nature **410:**235-240.
38. **Cai, Z., C. Zhang, K. S. Chang, J. Jiang, B. C. Ahn, T. Wakita, T. J. Liang, and G. Luo.** 2005. Robust production of infectious hepatitis C virus (HCV) from stably HCV cDNA-transfected human hepatoma cells. J Virol **79:**13963-13973.

39. **Calisher, C. H., R. E. Shope, W. Brandt, J. Casals, N. Karabatsos, F. A. Murphy, R. B. Tesh, and M. E. Wiebe.** 1980. Proposed antigenic classification of registered arboviruses I. Togaviridae, Alphavirus. Intervirology **14:**229-232.
40. **Carrere-Kremer, S., C. Montpellier, L. Lorenzo, B. Brulin, L. Cocquerel, S. Belouzard, F. Penin, and J. Dubuisson.** 2004. Regulation of hepatitis C virus polyprotein processing by signal peptidase involves structural determinants at the p7 sequence junctions. J Biol Chem **279:**41384-41392.
41. **Chambers, T. J., R. C. Weir, A. Grakoui, D. W. McCourt, J. F. Bazan, R. J. Fletterick, and C. M. Rice.** 1990. Evidence that the N-terminal domain of nonstructural protein NS3 from yellow fever virus is a serine protease responsible for site-specific cleavages in the viral polyprotein. Proc Natl Acad Sci U S A **87:**8898-8902.
42. **Choi, H. K., S. Lee, Y. P. Zhang, B. R. McKinney, G. Wengler, M. G. Rossmann, and R. J. Kuhn.** 1996. Structural analysis of Sindbis virus capsid mutants involving assembly and catalysis. J Mol Biol **262:**151-167.
43. **Choi, H. K., L. Tong, W. Minor, P. Dumas, U. Boege, M. G. Rossmann, and G. Wengler.** 1991. Structure of Sindbis virus core protein reveals a chymotrypsin-like serine proteinase and the organization of the virion. Nature **354:**37-43.
44. **Choo, Q.-L., G. Kuo, and A. Weiner.** 1989. Isolation of a cDNA clone derived from a blood-borne non-A, non-B viral hepatitis genome. Science **244:**359-362.
45. **Choukhi, A., S. Ung, C. Wychowski, and J. Dubuisson.** 1998. Involvement of endoplasmic reticulum chaperones in the folding of hepatitis C virus glycoproteins. J Virol **72:**3851-3858.
46. **Ciczora, Y., N. Callens, C. Montpellier, B. Bartosch, F. L. Cosset, A. Op de Beeck, and J. Dubuisson.** 2005. Contribution of the charged residues of hepatitis C virus glycoprotein E2 transmembrane domain to the functions of the E1E2 heterodimer. J Gen Virol **86:**2793-2798.
47. **Ciesek, S., E. Steinmann, H. Wedemeyer, M. P. Manns, J. Neyts, N. Tautz, V. Madan, R. Bartenschlager, T. von Hahn, and T. Pietschmann.** 2009. Cyclosporine A inhibits hepatitis C virus nonstructural protein 2 through cyclophilin A. Hepatology **50:**1638-1645.
48. **Clarke, D., S. Griffin, L. Beales, C. S. Gelais, S. Burgess, M. Harris, and D. Rowlands.** 2006. Evidence for the formation of a heptameric ion channel complex by the hepatitis C virus p7 protein in vitro. J Biol Chem **281:**37057-37068.
49. **Cocquerel, L., C. Wychowski, F. Minner, F. Penin, and J. Dubuisson.** 2000. Charged residues in the transmembrane domains of hepatitis C virus glycoproteins play a major role in the processing, subcellular localization, and assembly of these envelope proteins. J Virol **74:**3623-3633.
50. **Cormier, E. G., R. J. Durso, F. Tsamis, L. Boussemart, C. Manix, W. C. Olson, J. P. Gardner, and T. Dragic.** 2004. L-SIGN (CD209L) and DC-SIGN (CD209) mediate transinfection of liver cells by hepatitis C virus. Proc Natl Acad Sci U S A **101:**14067-14072.
51. **Cormier, E. G., F. Tsamis, F. Kajumo, R. J. Durso, J. P. Gardner, and T. Dragic.** 2004. CD81 is an entry coreceptor for hepatitis C virus. Proc Natl Acad Sci U S A **101:**7270-7274.
52. **Cristofari, G., R. Ivanyi-Nagy, C. Gabus, S. Boulant, J. P. Lavergne, F. Penin, and J. L. Darlix.** 2004. The hepatitis C virus Core protein is a potent nucleic acid chaperone that directs dimerization of the viral (+) strand RNA in vitro. Nucleic Acids Res **32:**2623-2631.
53. **De Francesco, R., and G. Migliaccio.** 2005. Challenges and successes in developing new therapies for hepatitis C. Nature **436:**953-960.
54. **Deleersnyder, V., A. Pillez, C. Wychowski, K. Blight, J. Xu, Y. S. Hahn, C. M. Rice, and J. Dubuisson.** 1997. Formation of native hepatitis C virus glycoprotein complexes. J Virol **71:**697-704.
55. **Dentzer, T. G., I. C. Lorenz, M. J. Evans, and C. M. Rice.** 2009. Determinants of hepatitis C virus nonstructural protein 2 protease domain required for production of infectious virus. J Virol.
56. **Di Bisceglie, A. M.** 1997. Hepatitis C and hepatocellular carcinoma. Hepatology **26:**34S-38S.
57. **Di Bisceglie, A. M., R. L. Carithers, Jr., and G. J. Gores.** 1998. Hepatocellular carcinoma. Hepatology **28:**1161-1165.

58. **Dimitrova, M., I. Imbert, M. P. Kieny, and C. Schuster.** 2003. Protein-protein interactions between hepatitis C virus nonstructural proteins. J Virol **77:**5401-5414.
59. **Drummer, H. E., K. A. Wilson, and P. Poumbourios.** 2005. Determinants of CD81 dimerization and interaction with hepatitis C virus glycoprotein E2. Biochem Biophys Res Commun **328:**251-257.
60. **Dubuisson, J., S. Duvet, J. C. Meunier, A. Op De Beeck, R. Cacan, C. Wychowski, and L. Cocquerel.** 2000. Glycosylation of the hepatitis C virus envelope protein E1 is dependent on the presence of a downstream sequence on the viral polyprotein. J Biol Chem **275:**30605-30609.
61. **Dubuisson, J., H. H. Hsu, R. C. Cheung, H. B. Greenberg, D. G. Russell, and C. M. Rice.** 1994. Formation and intracellular localization of hepatitis C virus envelope glycoprotein complexes expressed by recombinant vaccinia and Sindbis viruses. J Virol **68:**6147-6160.
62. **Dumoulin, F. L., A. von dem Bussche, J. Li, L. Khamzina, J. R. Wands, T. Sauerbruch, and U. Spengler.** 2003. Hepatitis C virus NS2 protein inhibits gene expression from different cellular and viral promoters in hepatic and nonhepatic cell lines. Virology **305:**260-266.
63. **Egger, D., B. Wolk, R. Gosert, L. Bianchi, H. E. Blum, D. Moradpour, and K. Bienz.** 2002. Expression of hepatitis C virus proteins induces distinct membrane alterations including a candidate viral replication complex. J Virol **76:**5974-5984.
64. **El-Hage, N., and G. Luo.** 2003. Replication of hepatitis C virus RNA occurs in a membrane-bound replication complex containing nonstructural viral proteins and RNA. J Gen Virol **84:**2761-2769.
65. **Elazar, M., P. Liu, C. M. Rice, and J. S. Glenn.** 2004. An N-terminal amphipathic helix in hepatitis C virus (HCV) NS4B mediates membrane association, correct localization of replication complex proteins, and HCV RNA replication. J Virol **78:**11393-11400.
66. **Erdtmann, L., N. Franck, H. Lerat, J. Le Seyec, D. Gilot, I. Cannie, P. Gripon, U. Hibner, and C. Guguen-Guillouzo.** 2003. The hepatitis C virus NS2 protein is an inhibitor of CIDE-B-induced apoptosis. J Biol Chem **278:**18256-18264.
67. **Evans, M. J., C. M. Rice, and S. P. Goff.** 2004. Phosphorylation of hepatitis C virus nonstructural protein 5A modulates its protein interactions and viral RNA replication. Proc Natl Acad Sci U S A **101:**13038-13043.
68. **Evans, M. J., T. von Hahn, D. M. Tscherne, A. J. Syder, M. Panis, B. Wolk, T. Hatziioannou, J. A. McKeating, P. D. Bieniasz, and C. M. Rice.** 2007. Claudin-1 is a hepatitis C virus co-receptor required for a late step in entry. Nature **446:**801-805.
69. **Everhart, J. E., Y. Wei, H. Eng, M. R. Charlton, D. H. Persing, R. H. Wiesner, J. J. Germer, J. R. Lake, R. K. Zetterman, and J. H. Hoofnagle.** 1999. Recurrent and new hepatitis C virus infection after liver transplantation. Hepatology **29:**1220-1226.
70. **Failla, C., L. Tomei, and R. De Francesco.** 1994. Both NS3 and NS4A are required for proteolytic processing of hepatitis C virus nonstructural proteins. J Virol **68:**3753-3760.
71. **Fan, Z., Q. R. Yang, J. S. Twu, and A. H. Sherker.** 1999. Specific in vitro association between the hepatitis C viral genome and core protein. J Med Virol **59:**131-134.
72. **Farci, P., A. Shimoda, D. Wong, T. Cabezon, D. De Gioannis, A. Strazzera, Y. Shimizu, M. Shapiro, H. J. Alter, and R. H. Purcell.** 1996. Prevention of hepatitis C virus infection in chimpanzees by hyperimmune serum against the hypervariable region 1 of the envelope 2 protein. Proc Natl Acad Sci U S A **93:**15394-15399.
73. **Feinstone, S. M., K. B. Mihalik, T. Kamimura, H. J. Alter, W. T. London, and R. H. Purcell.** 1983. Inactivation of hepatitis B virus and non-A, non-B hepatitis by chloroform. Infect Immun **41:**816-821.
74. **Flint, M., and J. A. McKeating.** 1999. The C-terminal region of the hepatitis C virus E1 glycoprotein confers localization within the endoplasmic reticulum. J Gen Virol **80 (Pt 8):**1943-1947.
75. **Florese, R. H., M. Nagano-Fujii, Y. Iwanaga, R. Hidajat, and H. Hotta.** 2002. Inhibition of protein synthesis by the nonstructural proteins NS4A and NS4B of hepatitis C virus. Virus Res **90:**119-131.

76. **Foy, E., K. Li, R. Sumpter, Jr., Y. M. Loo, C. L. Johnson, C. Wang, P. M. Fish, M. Yoneyama, T. Fujita, S. M. Lemon, and M. Gale, Jr.** 2005. Control of antiviral defenses through hepatitis C virus disruption of retinoic acid-inducible gene-I signaling. Proc Natl Acad Sci U S A **102:**2986-2991.
77. **Foy, E., K. Li, C. Wang, R. Sumpter, Jr., M. Ikeda, S. M. Lemon, and M. Gale, Jr.** 2003. Regulation of interferon regulatory factor-3 by the hepatitis C virus serine protease. Science **300:**1145-1148.
78. **Franck, N., J. Le Seyec, C. Guguen-Guillouzo, and L. Erdtmann.** 2005. Hepatitis C virus NS2 protein is phosphorylated by the protein kinase CK2 and targeted for degradation to the proteasome. J Virol **79:**2700-2708.
79. **Friebe, P., J. Boudet, J. P. Simorre, and R. Bartenschlager.** 2005. Kissing-loop interaction in the 3' end of the hepatitis C virus genome essential for RNA replication. J Virol **79:**380-392.
80. **Friebe, P., V. Lohmann, N. Krieger, and R. Bartenschlager.** 2001. Sequences in the 5' nontranslated region of hepatitis C virus required for RNA replication. J Virol **75:**12047-12057.
81. **Gastaminza, P., S. B. Kapadia, and F. V. Chisari.** 2006. Differential biophysical properties of infectious intracellular and secreted hepatitis C virus particles. J Virol **80:**11074-11081.
82. **Giannini, C., and C. Brechot.** 2003. Hepatitis C virus biology. Cell Death Differ **10 Suppl 1:**S27-38.
83. **Gosert, R., D. Egger, V. Lohmann, R. Bartenschlager, H. E. Blum, K. Bienz, and D. Moradpour.** 2003. Identification of the hepatitis C virus RNA replication complex in Huh-7 cells harboring subgenomic replicons. J Virol **77:**5487-5492.
84. **Grakoui, A., D. W. McCourt, C. Wychowski, S. M. Feinstone, and C. M. Rice.** 1993. Characterization of the hepatitis C virus-encoded serine proteinase: determination of proteinase-dependent polyprotein cleavage sites. J Virol **67:**2832-2843.
85. **Grakoui, A., D. W. McCourt, C. Wychowski, S. M. Feinstone, and C. M. Rice.** 1993. A second hepatitis C virus-encoded proteinase. Proc Natl Acad Sci U S A **90:**10583-10587.
86. **Grakoui, A., C. Wychowski, C. Lin, S. M. Feinstone, and C. M. Rice.** 1993. Expression and identification of hepatitis C virus polyprotein cleavage products. J Virol **67:**1385-1395.
87. **Grassmann, C. W., H. Yu, O. Isken, and S. E. Behrens.** 2005. Hepatitis C virus and the related bovine viral diarrhea virus considerably differ in the functional organization of the 5' non-translated region: implications for the viral life cycle. Virology **333:**349-366.
88. **Griffin, S., D. Clarke, C. McCormick, D. Rowlands, and M. Harris.** 2005. Signal peptide cleavage and internal targeting signals direct the hepatitis C virus p7 protein to distinct intracellular membranes. J Virol **79:**15525-15536.
89. **Griffin, S. D., L. P. Beales, D. S. Clarke, O. Worsfold, S. D. Evans, J. Jaeger, M. P. Harris, and D. J. Rowlands.** 2003. The p7 protein of hepatitis C virus forms an ion channel that is blocked by the antiviral drug, Amantadine. FEBS Lett **535:**34-38.
90. **Griffin, S. D., R. Harvey, D. S. Clarke, W. S. Barclay, M. Harris, and D. J. Rowlands.** 2004. A conserved basic loop in hepatitis C virus p7 protein is required for amantadine-sensitive ion channel activity in mammalian cells but is dispensable for localization to mitochondria. J Gen Virol **85:**451-461.
91. **Gritsun, T. S., V. A. Lashkevich, and E. A. Gould.** 2003. Tick-borne encephalitis. Antiviral Res **57:**129-146.
92. **Grun, J. B., and M. A. Brinton.** 1987. Dissociation of NS5 from cell fractions containing West Nile virus-specific polymerase activity. J Virol **61:**3641-3644.
93. **Hall, R. A., A. A. Khromykh, J. M. Mackenzie, J. H. Scherret, T. I. Khromykh, and J. S. Mackenzie.** 1999. Loss of dimerisation of the nonstructural protein NS1 of Kunjin virus delays viral replication and reduces virulence in mice, but still allows secretion of NS1. Virology **264:**66-75.
94. **He, L. F., D. Alling, T. Popkin, M. Shapiro, H. J. Alter, and R. H. Purcell.** 1987. Determining the size of non-A, non-B hepatitis virus by filtration. J Infect Dis **156:**636-640.

95. **He, Y., and M. G. Katze.** 2002. To interfere and to anti-interfere: the interplay between hepatitis C virus and interferon. Viral Immunol **15:**95-119.
96. **He, Y., H. Nakao, S. L. Tan, S. J. Polyak, P. Neddermann, S. Vijaysri, B. L. Jacobs, and M. G. Katze.** 2002. Subversion of cell signaling pathways by hepatitis C virus nonstructural 5A protein via interaction with Grb2 and P85 phosphatidylinositol 3-kinase. J Virol **76:**9207-9217.
97. **Heimann, M., G. Roman-Sosa, B. Martoglio, H. J. Thiel, and T. Rumenapf.** 2006. Core protein of pestiviruses is processed at the C terminus by signal peptide peptidase. J Virol **80:**1915-1921.
98. **Higginbottom, A., E. R. Quinn, C. C. Kuo, M. Flint, L. H. Wilson, E. Bianchi, A. Nicosia, P. N. Monk, J. A. McKeating, and S. Levy.** 2000. Identification of amino acid residues in CD81 critical for interaction with hepatitis C virus envelope glycoprotein E2. J Virol **74:**3642-3649.
99. **Hijikata, M., H. Mizushima, T. Akagi, S. Mori, N. Kakiuchi, N. Kato, T. Tanaka, K. Kimura, and K. Shimotohno.** 1993. Two distinct proteinase activities required for the processing of a putative nonstructural precursor protein of hepatitis C virus. J Virol **67:**4665-4675.
100. **Hijikata, M., H. Mizushima, Y. Tanji, Y. Komoda, Y. Hirowatari, T. Akagi, N. Kato, K. Kimura, and K. Shimotohno.** 1993. Proteolytic processing and membrane association of putative nonstructural proteins of hepatitis C virus. Proc Natl Acad Sci U S A **90:**10773-10777.
101. **Hijikata, M., Y. K. Shimizu, H. Kato, A. Iwamoto, J. W. Shih, H. J. Alter, R. H. Purcell, and H. Yoshikura.** 1993. Equilibrium centrifugation studies of hepatitis C virus: evidence for circulating immune complexes. J Virol **67:**1953-1958.
102. **Hirowatari, Y., M. Hijikata, Y. Tanji, H. Nyunoya, H. Mizushima, K. Kimura, T. Tanaka, N. Kato, and K. Shimotohno.** 1993. Two proteinase activities in HCV polypeptide expressed in insect cells using baculovirus vector. Arch Virol **133:**349-356.
103. **Hoofnagle, J. H.** 2002. Course and outcome of hepatitis C. Hepatology **36:**S21-29.
104. **Hsu, M., J. Zhang, M. Flint, C. Logvinoff, C. Cheng-Mayer, C. M. Rice, and J. A. McKeating.** 2003. Hepatitis C virus glycoproteins mediate pH-dependent cell entry of pseudotyped retroviral particles. Proc Natl Acad Sci U S A **100:**7271-7276.
105. **Huang, L., J. Hwang, S. D. Sharma, M. R. Hargittai, Y. Chen, J. J. Arnold, K. D. Raney, and C. E. Cameron.** 2005. Hepatitis C virus nonstructural protein 5A (NS5A) is an RNA-binding protein. J Biol Chem **280:**36417-36428.
106. **Hugle, T., F. Fehrmann, E. Bieck, M. Kohara, H. G. Krausslich, C. M. Rice, H. E. Blum, and D. Moradpour.** 2001. The hepatitis C virus nonstructural protein 4B is an integral endoplasmic reticulum membrane protein. Virology **284:**70-81.
107. **Hussy, P., H. Langen, J. Mous, and H. Jacobsen.** 1996. Hepatitis C virus core protein: carboxy-terminal boundaries of two processed species suggest cleavage by a signal peptide peptidase. Virology **224:**93-104.
108. **Hwang, S. B., S. Y. Lo, J. H. Ou, and M. M. Lai.** 1995. Detection of Cellular Proteins and Viral Core Protein Interacting with the 5' Untranslated Region of Hepatitis C Virus RNA. J Biomed Sci **2:**227-236.
109. **Ito, T., and M. M. Lai.** 1999. An internal polypyrimidine-tract-binding protein-binding site in the hepatitis C virus RNA attenuates translation, which is relieved by the 3'-untranslated sequence. Virology **254:**288-296.
110. **Ivashkina, N., B. Wolk, V. Lohmann, R. Bartenschlager, H. E. Blum, F. Penin, and D. Moradpour.** 2002. The hepatitis C virus RNA-dependent RNA polymerase membrane insertion sequence is a transmembrane segment. J Virol **76:**13088-13093.
111. **Ji, H., C. S. Fraser, Y. Yu, J. Leary, and J. A. Doudna.** 2004. Coordinated assembly of human translation initiation complexes by the hepatitis C virus internal ribosome entry site RNA. Proc Natl Acad Sci U S A **101:**16990-16995.
112. **Jirasko, V., R. Montserret, N. Appel, A. Janvier, L. Eustachi, C. Brohm, E. Steinmann, T. Pietschmann, F. Penin, and R. Bartenschlager.** 2008. Structural and functional characterization of non-structural protein 2 for its role in hepatitis C virus assembly. J Biol Chem.

113. **Johnson, C. L., and M. Gale, Jr.** 2005. CARD games between virus and host get a new player. Trends Immunol.
114. **Jones, C. T., C. L. Murray, D. K. Eastman, J. Tassello, and C. M. Rice.** 2007. Hepatitis C Virus p7 and NS2 Proteins Are Essential for Production of Infectious Virus. J Virol **81:**8374-8383.
115. **Jones, C. T., C. G. Patkar, and R. J. Kuhn.** 2005. Construction and applications of yellow fever virus replicons. Virology **331:**247-259.
116. **Jones, D. M., and J. McLauchlan.** 2010. Hepatitis C virus: assembly and release of virus particles. J Biol Chem **285:**22733-22739.
117. **Jones, D. M., A. H. Patel, P. Targett-Adams, and J. McLauchlan.** 2009. The hepatitis C virus NS4B protein can trans-complement viral RNA replication and modulates production of infectious virus. J Virol **83:**2163-2177.
118. **Jouvenet, N., S. M. Simon, and P. D. Bieniasz.** 2009. Imaging the interaction of HIV-1 genomes and Gag during assembly of individual viral particles. Proc Natl Acad Sci U S A **106:**19114-19119.
119. **Kanaoka, Y., H. Ago, E. Inagaki, T. Nanayama, M. Miyano, R. Kikuno, Y. Fujii, N. Eguchi, H. Toh, Y. Urade, and O. Hayaishi.** 1997. Cloning and crystal structure of hematopoietic prostaglandin D synthase. Cell **90:**1085-1095.
120. **Kaneko, T., Y. Tanji, S. Satoh, M. Hijikata, S. Asabe, K. Kimura, and K. Shimotohno.** 1994. Production of two phosphoproteins from the NS5A region of the hepatitis C viral genome. Biochem Biophys Res Commun **205:**320-326.
121. **Kanto, T., N. Hayashi, T. Takehara, H. Hagiwara, E. Mita, M. Oshita, K. Katayama, A. Kasahara, H. Fusamoto, and T. Kamada.** 1995. Serial density analysis of hepatitis C virus particle populations in chronic hepatitis C patients treated with interferon-alpha. J Med Virol **46:**230-237.
122. **Kapadia, S. B., and F. V. Chisari.** 2005. Hepatitis C virus RNA replication is regulated by host geranylgeranylation and fatty acids. Proc Natl Acad Sci U S A **102:**2561-2566.
123. **Kato, J., N. Kato, H. Yoshida, S. K. Ono-Nita, Y. Shiratori, and M. Omata.** 2002. Hepatitis C virus NS4A and NS4B proteins suppress translation in vivo. J Med Virol **66:**187-199.
124. **Kato, Y., S. Hiraoka, Y. Tada, and T. Nomura.** 2001. Performance of a shaking vessel with current pole. Biochem. Eng. J. **7:**143-151.
125. **Kieffer, T. L., A. D. Kwong, and G. R. Picchio.** 2010. Viral resistance to specifically targeted antiviral therapies for hepatitis C (STAT-Cs). J Antimicrob Chemother **65:**202-212.
126. **Kiiver, K., A. Merits, M. Ustav, and E. Zusinaite.** 2006. Complex formation between hepatitis C virus NS2 and NS3 proteins. Virus Res **117:**264-272.
127. **Kim, J. L., K. A. Morgenstern, C. Lin, T. Fox, M. D. Dwyer, J. A. Landro, S. P. Chambers, W. Markland, C. A. Lepre, E. T. O'Malley, S. L. Harbeson, C. M. Rice, M. A. Murcko, P. R. Caron, and J. A. Thomson.** 1996. Crystal structure of the hepatitis C virus NS3 protease domain complexed with a synthetic NS4A cofactor peptide. Cell **87:**343-355.
128. **Kim, S. J., J. H. Kim, Y. G. Kim, H. S. Lim, and J. W. Oh.** 2004. Protein kinase C-related kinase 2 regulates hepatitis C virus RNA polymerase function by phosphorylation. J Biol Chem **279:**50031-50041.
129. **Kim, Y. K., C. S. Kim, S. H. Lee, and S. K. Jang.** 2002. Domains I and II in the 5' nontranslated region of the HCV genome are required for RNA replication. Biochem Biophys Res Commun **290:**105-112.
130. **Koch, J. O., and R. Bartenschlager.** 1999. Modulation of hepatitis C virus NS5A hyperphosphorylation by nonstructural proteins NS3, NS4A, and NS4B. J Virol **73:**7138-7146.
131. **Kolykhalov, A. A., E. V. Agapov, K. J. Blight, K. Mihalik, S. M. Feinstone, and C. M. Rice.** 1997. Transmission of hepatitis C by intrahepatic inoculation with transcribed RNA. Science **277:**570-574.
132. **Kolykhalov, A. A., S. M. Feinstone, and C. M. Rice.** 1996. Identification of a highly conserved sequence element at the 3' terminus of hepatitis C virus genome RNA. J Virol **70:**3363-3371.

133. **Kolykhalov, A. A., K. Mihalik, S. M. Feinstone, and C. M. Rice.** 2000. Hepatitis C virus-encoded enzymatic activities and conserved RNA elements in the 3' nontranslated region are essential for virus replication in vivo. J Virol **74:**2046-2051.
134. **Konan, K. V., T. H. Giddings, Jr., M. Ikeda, K. Li, S. M. Lemon, and K. Kirkegaard.** 2003. Nonstructural protein precursor NS4A/B from hepatitis C virus alters function and ultrastructure of host secretory apparatus. J Virol **77:**7843-7855.
135. **Konishi, E., S. Pincus, B. A. Fonseca, R. E. Shope, E. Paoletti, and P. W. Mason.** 1991. Comparison of protective immunity elicited by recombinant vaccinia viruses that synthesize E or NS1 of Japanese encephalitis virus. Virology **185:**401-410.
136. **Krey, T., H. J. Thiel, and T. Rumenapf.** 2005. Acid-resistant bovine pestivirus requires activation for pH-triggered fusion during entry. J Virol **79:**4191-4200.
137. **Kuhn, R. J., W. Zhang, M. G. Rossmann, S. V. Pletnev, J. Corver, E. Lenches, C. T. Jones, S. Mukhopadhyay, P. R. Chipman, E. G. Strauss, T. S. Baker, and J. H. Strauss.** 2002. Structure of dengue virus: implications for flavivirus organization, maturation, and fusion. Cell **108:**717-725.
138. **Kummerer, B. M., and C. M. Rice.** 2002. Mutations in the yellow fever virus nonstructural protein NS2A selectively block production of infectious particles. J Virol **76:**4773-4784.
139. **Kwong, A. D., L. McNair, I. Jacobson, and S. George.** 2008. Recent progress in the development of selected hepatitis C virus NS3.4A protease and NS5B polymerase inhibitors. Curr Opin Pharmacol **8:**522-531.
140. **Lackner, T., A. Muller, M. Konig, H. J. Thiel, and N. Tautz.** 2005. Persistence of bovine viral diarrhea virus is determined by a cellular cofactor of a viral autoprotease. J Virol **79:**9746-9755.
141. **Lam, A. M., and D. N. Frick.** 2006. Hepatitis C virus subgenomic replicon requires an active NS3 RNA helicase. J Virol **80:**404-411.
142. **Lanford, R. E., D. Chavez, F. V. Chisari, and C. Sureau.** 1995. Lack of detection of negative-strand hepatitis C virus RNA in peripheral blood mononuclear cells and other extrahepatic tissues by the highly strand-specific rTth reverse transcriptase PCR. J Virol **69:**8079-8083.
143. **Lavillette, D., A. W. Tarr, C. Voisset, P. Donot, B. Bartosch, C. Bain, A. H. Patel, J. Dubuisson, J. K. Ball, and F. L. Cosset.** 2005. Characterization of host-range and cell entry properties of the major genotypes and subtypes of hepatitis C virus. Hepatology **41:**265-274.
144. **Lesburg, C. A., M. B. Cable, E. Ferrari, Z. Hong, A. F. Mannarino, and P. C. Weber.** 1999. Crystal structure of the RNA-dependent RNA polymerase from hepatitis C virus reveals a fully encircled active site. Nat Struct Biol **6:**937-943.
145. **Leung, J. Y., G. P. Pijlman, N. Kondratieva, J. Hyde, J. M. Mackenzie, and A. A. Khromykh.** 2008. Role of nonstructural protein NS2A in flavivirus assembly. J Virol **82:**4731-4741.
146. **Levin, M. K., Y. H. Wang, and S. S. Patel.** 2004. The functional interaction of the hepatitis C virus helicase molecules is responsible for unwinding processivity. J Biol Chem **279:**26005-26012.
147. **Li, W., Y. Li, N. Kedersha, P. Anderson, M. Emara, K. M. Swiderek, G. T. Moreno, and M. A. Brinton.** 2002. Cell proteins TIA-1 and TIAR interact with the 3' stem-loop of the West Nile virus complementary minus-strand RNA and facilitate virus replication. J Virol **76:**11989-12000.
148. **Liang, T. J., and T. Heller.** 2004. Pathogenesis of hepatitis C-associated hepatocellular carcinoma. Gastroenterology **127:**S62-71.
149. **Lin, C., J. A. Thomson, and C. M. Rice.** 1995. A central region in the hepatitis C virus NS4A protein allows formation of an active NS3-NS4A serine proteinase complex in vivo and in vitro. J Virol **69:**4373-4380.
150. **Lindenbach, B. D., M. J. Evans, A. J. Syder, B. Wolk, T. L. Tellinghuisen, C. C. Liu, T. Maruyama, R. O. Hynes, D. R. Burton, J. A. McKeating, and C. M. Rice.** 2005. Complete replication of hepatitis C virus in cell culture. Science **309:**623-626.

151. **Lindenbach, B. D., and C. M. Rice.** 2006. *Flaviviridae*: The viruses and their replication, p. 991-1041. *In* D. M. Knipe and P. M. Howley (ed.), Fields Virology, Fifth ed, vol. 1. Lippincott-Raven Publishers, Philadelphia.
152. **Lindenbach, B. D., and C. M. Rice.** 2001. Flaviviridae: The Viruses and Their Replication, p. 991-1041. *In* D. M. Knipe, P. M. Howley, D. E. Griffin, R. A. Lamb, M. A. Martin, B. Roizman, and S. E. Straus (ed.), Fields Virology. Lippincott Williams & Wilkins, Philadelphia, PA.
153. **Lindenbach, B. D., and C. M. Rice.** 1997. trans-Complementation of yellow fever virus NS1 reveals a role in early RNA replication. J Virol **71:**9608-9617.
154. **Lindenbach, B. D., and C. M. Rice.** 2005. Unravelling hepatitis C virus replication from genome to function. Nature **436:**933-938.
155. **Liu, Q., R. A. Bhat, A. M. Prince, and P. Zhang.** 1999. The hepatitis C virus NS2 protein generated by NS2-3 autocleavage is required for NS5A phosphorylation. Biochem Biophys Res Commun **254:**572-577.
156. **Liu, Q., C. Tackney, R. A. Bhat, A. M. Prince, and P. Zhang.** 1997. Regulated processing of hepatitis C virus core protein is linked to subcellular localization. J Virol **71:**657-662.
157. **Liu, S., I. H. Ansari, S. C. Das, and A. K. Pattnaik.** 2006. Insertion and deletion analyses identify regions of non-structural protein 5A of Hepatitis C virus that are dispensable for viral genome replication. J Gen Virol **87:**323-327.
158. **Liu, W. J., H. B. Chen, and A. A. Khromykh.** 2003. Molecular and functional analyses of Kunjin virus infectious cDNA clones demonstrate the essential roles for NS2A in virus assembly and for a nonconservative residue in NS3 in RNA replication. J Virol **77:**7804-7813.
159. **Lo, S. Y., M. J. Selby, and J. H. Ou.** 1996. Interaction between hepatitis C virus core protein and E1 envelope protein. J Virol **70:**5177-5182.
160. **Lobigs, M.** 1993. Flavivirus premembrane protein cleavage and spike heterodimer secretion require the function of the viral proteinase NS3. Proc Natl Acad Sci U S A **90:**6218-6222.
161. **Locatelli, G. A., S. Spadari, and G. Maga.** 2002. Hepatitis C virus NS3 ATPase/helicase: an ATP switch regulates the cooperativity among the different substrate binding sites. Biochemistry **41:**10332-10342.
162. **Logvinoff, C., M. E. Major, D. Oldach, S. Heyward, A. Talal, P. Balfe, S. M. Feinstone, H. Alter, C. M. Rice, and J. A. McKeating.** 2004. Neutralizing antibody response during acute and chronic hepatitis C virus infection. Proc Natl Acad Sci U S A **101:**10149-10154.
163. **Lohmann, V., F. Korner, U. Herian, and R. Bartenschlager.** 1997. Biochemical properties of hepatitis C virus NS5B RNA-dependent RNA polymerase and identification of amino acid sequence motifs essential for enzymatic activity. J Virol **71:**8416-8428.
164. **Lohmann, V., F. Korner, J. Koch, U. Herian, L. Theilmann, and R. Bartenschlager.** 1999. Replication of subgenomic hepatitis C virus RNAs in a hepatoma cell line. Science **285:**110-113.
165. **Lohmann, V., F. Korner, J. Koch, U. Herian, L. Theilmann, and R. Bartenschlager.** 1999. Replication of subgenomic hepatitis C virus RNAs in a hepatoma cell line. Science **285:**110-113.
166. **Lohmann, V., A. Roos, F. Korner, J. O. Koch, and R. Bartenschlager.** 1998. Biochemical and kinetic analyses of NS5B RNA-dependent RNA polymerase of the hepatitis C virus. Virology **249:**108-118.
167. **Lorenz, I. C., J. Marcotrigiano, T. G. Dentzer, and C. M. Rice.** 2006. Structure of the catalytic domain of the hepatitis C virus NS2-3 protease. Nature **442:**831-835.
168. **Love, R. A., H. E. Parge, J. A. Wickersham, Z. Hostomsky, N. Habuka, E. W. Moomaw, T. Adachi, and Z. Hostomska.** 1996. The crystal structure of hepatitis C virus NS3 proteinase reveals a trypsin-like fold and a structural zinc binding site. Cell **87:**331-342.
169. **Lozach, P. Y., A. Amara, B. Bartosch, J. L. Virelizier, F. Arenzana-Seisdedos, F. L. Cosset, and R. Altmeyer.** 2004. C-type lectins L-SIGN and DC-SIGN capture and transmit infectious hepatitis C virus pseudotype particles. J Biol Chem **279:**32035-32045.
170. **Ludwig, I. S., A. N. Lekkerkerker, E. Depla, F. Bosman, R. J. Musters, S. Depraetere, Y. van Kooyk, and T. B. Geijtenbeek.** 2004. Hepatitis C virus targets DC-SIGN and L-SIGN to escape lysosomal degradation. J Virol **78:**8322-8332.

171. **Lundin, M., M. Monne, A. Widell, G. Von Heijne, and M. A. Persson.** 2003. Topology of the membrane-associated hepatitis C virus protein NS4B. J Virol **77:**5428-5438.
172. **Luo, G., R. K. Hamatake, D. M. Mathis, J. Racela, K. L. Rigat, J. Lemm, and R. J. Colonno.** 2000. De novo initiation of RNA synthesis by the RNA-dependent RNA polymerase (NS5B) of hepatitis C virus. J Virol **74:**851-863.
173. **Luo, G., S. Xin, and Z. Cai.** 2003. Role of the 5'-proximal stem-loop structure of the 5' untranslated region in replication and translation of hepatitis C virus RNA. J Virol **77:**3312-3318.
174. **Ma, H. C., C. H. Ke, T. Y. Hsieh, and S. Y. Lo.** 2002. The first hydrophobic domain of the hepatitis C virus E1 protein is important for interaction with the capsid protein. J Gen Virol **83:**3085-3092.
175. **Ma, Y., J. Yates, Y. Liang, S. M. Lemon, and M. Yi.** 2008. NS3 helicase domains involved in infectious intracellular hepatitis C virus particle assembly. J Virol **82:**7624-7639.
176. **Mackenzie, J. M., A. A. Khromykh, M. K. Jones, and E. G. Westaway.** 1998. Subcellular localization and some biochemical properties of the flavivirus Kunjin nonstructural proteins NS2A and NS4A. Virology **245:**203-215.
177. **Mackenzie, J. M., and E. G. Westaway.** 2001. Assembly and maturation of the flavivirus Kunjin virus appear to occur in the rough endoplasmic reticulum and along the secretory pathway, respectively. J Virol **75:**10787-10799.
178. **Mackenzie, J. S., D. J. Gubler, and L. R. Petersen.** 2004. Emerging flaviviruses: the spread and resurgence of Japanese encephalitis, West Nile and dengue viruses. Nat Med **10:**S98-109.
179. **Mackintosh, S. G., J. Z. Lu, J. B. Jordan, M. K. Harrison, B. Sikora, S. D. Sharma, C. E. Cameron, K. D. Raney, and J. Sakon.** 2006. Structural and biological identification of residues on the surface of NS3 helicase required for optimal replication of the hepatitis C virus. J Biol Chem **281:**3528-3535.
180. **Macovei, A., N. Zitzmann, C. Lazar, R. A. Dwek, and N. Branza-Nichita.** 2006. Brefeldin A inhibits pestivirus release from infected cells, without affecting its assembly and infectivity. Biochem Biophys Res Commun **346:**1083-1090.
181. **Maillard, P., K. Krawczynski, J. Nitkiewicz, C. Bronnert, M. Sidorkiewicz, P. Gounon, J. Dubuisson, G. Faure, R. Crainic, and A. Budkowska.** 2001. Nonenveloped nucleocapsids of hepatitis C virus in the serum of infected patients. J Virol **75:**8240-8250.
182. **Manabe, S., I. Fuke, O. Tanishita, C. Kaji, Y. Gomi, S. Yoshida, C. Mori, A. Takamizawa, I. Yosida, and H. Okayama.** 1994. Production of nonstructural proteins of hepatitis C virus requires a putative viral protease encoded by NS3. Virology **198:**636-644.
183. **Manns, M. P., J. G. McHutchison, S. C. Gordon, V. K. Rustgi, M. Shiffman, R. Reindollar, Z. D. Goodman, K. Koury, M. Ling, and J. K. Albrecht.** 2001. Peginterferon alfa-2b plus ribavirin compared with interferon alfa-2b plus ribavirin for initial treatment of chronic hepatitis C: a randomised trial. Lancet **358:**958-965.
184. **Masaki, T., R. Suzuki, K. Murakami, H. Aizaki, K. Ishii, A. Murayama, T. Date, Y. Matsuura, T. Miyamura, T. Wakita, and T. Suzuki.** 2008. Interaction of hepatitis C virus nonstructural protein 5A with core protein is critical for the production of infectious virus particles. J Virol **82:**7964-7976.
185. **Matusan, A. E., M. J. Pryor, A. D. Davidson, and P. J. Wright.** 2001. Mutagenesis of the Dengue virus type 2 NS3 protein within and outside helicase motifs: effects on enzyme activity and virus replication. J Virol **75:**9633-9643.
186. **McCormick, C. J., S. Maucourant, S. Griffin, D. J. Rowlands, and M. Harris.** 2006. Tagging of NS5A expressed from a functional hepatitis C virus replicon. J Gen Virol **87:**635-640.
187. **McCoy, M. A., M. M. Senior, J. J. Gesell, L. Ramanathan, and D. F. Wyss.** 2001. Solution structure and dynamics of the single-chain hepatitis C virus NS3 protease NS4A cofactor complex. J Mol Biol **305:**1099-1110.
188. **McKeating, J. A., L. Q. Zhang, C. Logvinoff, M. Flint, J. Zhang, J. Yu, D. Butera, D. D. Ho, L. B. Dustin, C. M. Rice, and P. Balfe.** 2004. Diverse hepatitis C virus glycoproteins mediate viral infection in a CD81-dependent manner. J Virol **78:**8496-8505.

189. **McLauchlan, J.** 2000. Properties of the hepatitis C virus core protein: a structural protein that modulates cellular processes. Journal of viral hepatitis **7:**2-14.
190. **McLauchlan, J., M. K. Lemberg, G. Hope, and B. Martoglio.** 2002. Intramembrane proteolysis promotes trafficking of hepatitis C virus core protein to lipid droplets. EMBO J **21:**3980-3988.
191. **Mercer, D. F., D. E. Schiller, J. F. Elliott, D. N. Douglas, C. Hao, A. Rinfret, W. R. Addison, K. P. Fischer, T. A. Churchill, J. R. Lakey, D. L. Tyrrell, and N. M. Kneteman.** 2001. Hepatitis C virus replication in mice with chimeric human livers. Nat Med **7:**927-933.
192. **Meuleman, P., L. Libbrecht, R. De Vos, B. de Hemptinne, K. Gevaert, J. Vandekerckhove, T. Roskams, and G. Leroux-Roels.** 2005. Morphological and biochemical characterization of a human liver in a uPA-SCID mouse chimera. Hepatology **41:**847-856.
193. **Meunier, J. C., R. E. Engle, K. Faulk, M. Zhao, B. Bartosch, H. Alter, S. U. Emerson, F. L. Cosset, R. H. Purcell, and J. Bukh.** 2005. Evidence for cross-genotype neutralization of hepatitis C virus pseudo-particles and enhancement of infectivity by apolipoprotein C1. Proc Natl Acad Sci U S A **102:**4560-4565.
194. **Meylan, E., J. Curran, K. Hofmann, D. Moradpour, M. Binder, R. Bartenschlager, and J. Tschopp.** 2005. Cardif is an adaptor protein in the RIG-I antiviral pathway and is targeted by hepatitis C virus. Nature.
195. **Miyanari, Y., K. Atsuzawa, N. Usuda, K. Watashi, T. Hishiki, M. Zayas, R. Bartenschlager, T. Wakita, M. Hijikata, and K. Shimotohno.** 2007. The lipid droplet is an important organelle for hepatitis C virus production. Nat Cell Biol **9:**1089-1097.
196. **Miyanari, Y., M. Hijikata, M. Yamaji, M. Hosaka, H. Takahashi, and K. Shimotohno.** 2003. Hepatitis C virus non-structural proteins in the probable membranous compartment function in viral genome replication. J Biol Chem **278:**50301-50308.
197. **Mizushima, H., M. Hijikata, Y. Tanji, K. Kimura, and K. Shimotohno.** 1994. Analysis of N-terminal processing of hepatitis C virus nonstructural protein 2. J Virol **68:**2731-2734.
198. **Moennig, V., and P. G. Plagemann.** 1992. The pestiviruses. Adv Virus Res **41:**53-98.
199. **Monazahian, M., I. Bohme, S. Bonk, A. Koch, C. Scholz, S. Grethe, and R. Thomssen.** 1999. Low density lipoprotein receptor as a candidate receptor for hepatitis C virus. J Med Virol **57:**223-229.
200. **Moradpour, D., E. Bieck, T. Hugle, W. Wels, J. Z. Wu, Z. Hong, H. E. Blum, and R. Bartenschlager.** 2002. Functional properties of a monoclonal antibody inhibiting the hepatitis C virus RNA-dependent RNA polymerase. J Biol Chem **277:**593-601.
201. **Moradpour, D., C. Englert, T. Wakita, and J. R. Wands.** 1996. Characterization of cell lines allowing tightly regulated expression of hepatitis C virus core protein. Virology **222:**51-63.
202. **Moradpour, D., M. J. Evans, R. Gosert, Z. Yuan, H. E. Blum, S. P. Goff, B. D. Lindenbach, and C. M. Rice.** 2004. Insertion of green fluorescent protein into nonstructural protein 5A allows direct visualization of functional hepatitis C virus replication complexes. J Virol **78:**7400-7409.
203. **Moradpour, D., R. Gosert, D. Egger, F. Penin, H. E. Blum, and K. Bienz.** 2003. Membrane association of hepatitis C virus nonstructural proteins and identification of the membrane alteration that harbors the viral replication complex. Antiviral Res **60:**103-109.
204. **Moradpour, D., F. Penin, and C. M. Rice.** 2007. Replication of hepatitis C virus. Nat Rev Microbiol **5:**453-463.
205. **Mottola, G., G. Cardinali, A. Ceccacci, C. Trozzi, L. Bartholomew, M. R. Torrisi, E. Pedrazzini, S. Bonatti, and G. Migliaccio.** 2002. Hepatitis C virus nonstructural proteins are localized in a modified endoplasmic reticulum of cells expressing viral subgenomic replicons. Virology **293:**31-43.
206. **Moulin, H. R., T. Seuberlich, O. Bauhofer, L. C. Bennett, J. D. Tratschin, M. A. Hofmann, and N. Ruggli.** 2007. Nonstructural proteins NS2-3 and NS4A of classical swine fever virus: essential features for infectious particle formation. Virology **365:**376-389.
207. **Mousseau, G., S. Kota, V. Takahashi, D. Frick, and A. D. Strosberg.** 2010. Dimerization-driven interaction of hepatitis c virus core protein with NS3 helicase. J Gen Virol.

208. **Mukhopadhyay, A., G. E. Lee, and D. W. Wilson.** 2006. The amino terminus of the herpes simplex virus 1 protein Vhs mediates membrane association and tegument incorporation. J Virol **80:**10117-10127.
209. **Mukhopadhyay, S., B. S. Kim, P. R. Chipman, M. G. Rossmann, and R. J. Kuhn.** 2003. Structure of West Nile virus. Science **302:**248.
210. **Murray, C. L., C. T. Jones, and C. M. Rice.** 2008. Architects of assembly: roles of Flaviviridae non-structural proteins in virion morphogenesis. Nat Rev Microbiol **6:**699-708.
211. **Murray, C. L., C. T. Jones, J. Tassello, and C. M. Rice.** 2007. Alanine scanning of the hepatitis C virus core protein reveals numerous residues essential for production of infectious virus. J Virol **81:**10220-10231.
212. **Neddermann, P., M. Quintavalle, C. Di Pietro, A. Clementi, M. Cerretani, S. Altamura, L. Bartholomew, and R. De Francesco.** 2004. Reduction of hepatitis C virus NS5A hyperphosphorylation by selective inhibition of cellular kinases activates viral RNA replication in cell culture. J Virol **78:**13306-13314.
213. **Nestorowicz, A., T. J. Chambers, and C. M. Rice.** 1994. Mutagenesis of the yellow fever virus NS2A/2B cleavage site: effects on proteolytic processing, viral replication, and evidence for alternative processing of the NS2A protein. Virology **199:**114-123.
214. **O'Farrell, D., R. Trowbridge, D. Rowlands, and J. Jager.** 2003. Substrate complexes of hepatitis C virus RNA polymerase (HC-J4): structural evidence for nucleotide import and de-novo initiation. J Mol Biol **326:**1025-1035.
215. **Ogino, T., H. Fukuda, S. Imajoh-Ohmi, M. Kohara, and A. Nomoto.** 2004. Membrane binding properties and terminal residues of the mature hepatitis C virus capsid protein in insect cells. J Virol **78:**11766-11777.
216. **Okamoto, K., K. Moriishi, T. Miyamura, and Y. Matsuura.** 2004. Intramembrane proteolysis and endoplasmic reticulum retention of hepatitis C virus core protein. J Virol **78:**6370-6380.
217. **Otto, G. A., and J. D. Puglisi.** 2004. The pathway of HCV IRES-mediated translation initiation. Cell **119:**369-380.
218. **Pallaoro, M., A. Lahm, G. Biasiol, M. Brunetti, C. Nardella, L. Orsatti, F. Bonelli, S. Orru, F. Narjes, and C. Steinkuhler.** 2001. Characterization of the hepatitis C virus NS2/3 processing reaction by using a purified precursor protein. J Virol **75:**9939-9946.
219. **Pang, P. S., E. Jankowsky, P. J. Planet, and A. M. Pyle.** 2002. The hepatitis C viral NS3 protein is a processive DNA helicase with cofactor enhanced RNA unwinding. EMBO J **21:**1168-1176.
220. **Patargias, G., N. Zitzmann, R. Dwek, and W. B. Fischer.** 2006. Protein-protein interactions: modeling the hepatitis C virus ion channel p7. J Med Chem **49:**648-655.
221. **Patel, J., A. H. Patel, and J. McLauchlan.** 1999. Covalent interactions are not required to permit or stabilize the non-covalent association of hepatitis C virus glycoproteins E1 and E2. J Gen Virol **80 (Pt 7):**1681-1690.
222. **Pavlovic, D., D. C. Neville, O. Argaud, B. Blumberg, R. A. Dwek, W. B. Fischer, and N. Zitzmann.** 2003. The hepatitis C virus p7 protein forms an ion channel that is inhibited by long-alkyl-chain iminosugar derivatives. Proc Natl Acad Sci U S A **100:**6104-6108.
223. **Penin, F., J. Dubuisson, F. A. Rey, D. Moradpour, and J. M. Pawlotsky.** 2004. Structural biology of hepatitis C virus. Hepatology **39:**5-19.
224. **Pestova, T. V., I. N. Shatsky, S. P. Fletcher, R. J. Jackson, and C. U. Hellen.** 1998. A prokaryotic-like mode of cytoplasmic eukaryotic ribosome binding to the initiation codon during internal translation initiation of hepatitis C and classical swine fever virus RNAs. Genes Dev **12:**67-83.
225. **Petracca, R., F. Falugi, G. Galli, N. Norais, D. Rosa, S. Campagnoli, V. Burgio, E. Di Stasio, B. Giardina, M. Houghton, S. Abrignani, and G. Grandi.** 2000. Structure-function analysis of hepatitis C virus envelope-CD81 binding. J Virol **74:**4824-4830.

226. **Phan, T., R. K. Beran, C. Peters, I. C. Lorenz, and B. D. Lindenbach.** 2009. Hepatitis C virus NS2 protein contributes to virus particle assembly via opposing epistatic interactions with the E1-E2 glycoprotein and NS3-NS4A enzyme complexes. J Virol **83:**8379-8395.
227. **Piccininni, S., A. Varaklioti, M. Nardelli, B. Dave, K. D. Raney, and J. E. McCarthy.** 2002. Modulation of the hepatitis C virus RNA-dependent RNA polymerase activity by the non-structural (NS) 3 helicase and the NS4B membrane protein. J Biol Chem **277:**45670-45679.
228. **Pietschmann, T., A. Kaul, G. Koutsoudakis, A. Shavinskaya, S. Kallis, E. Steinmann, K. Abid, F. Negro, M. Dreux, F. L. Cosset, and R. Bartenschlager.** 2006. Construction and characterization of infectious intragenotypic and intergenotypic hepatitis C virus chimeras. Proc Natl Acad Sci U S A **103:**7408-7413.
229. **Pietschmann, T., V. Lohmann, A. Kaul, N. Krieger, G. Rinck, G. Rutter, D. Strand, and R. Bartenschlager.** 2002. Persistent and transient replication of full-length hepatitis C virus genomes in cell culture. J Virol **76:**4008-4021.
230. **Pietschmann, T., V. Lohmann, G. Rutter, K. Kurpanek, and R. Bartenschlager.** 2001. Characterization of cell lines carrying self-replicating hepatitis C virus RNAs. J Virol **75:**1252-1264.
231. **Pileri, P., Y. Uematsu, S. Campagnoli, G. Galli, F. Falugi, R. Petracca, A. J. Weiner, M. Houghton, D. Rosa, G. Grandi, and S. Abrignani.** 1998. Binding of hepatitis C virus to CD81. Science **282:**938-941.
232. **Ploss, A., M. J. Evans, V. A. Gaysinskaya, M. Panis, H. You, Y. P. de Jong, and C. M. Rice.** 2009. Human occludin is a hepatitis C virus entry factor required for infection of mouse cells. Nature **457:**882-886.
233. **Premkumar, A., L. Wilson, G. D. Ewart, and P. W. Gage.** 2004. Cation-selective ion channels formed by p7 of hepatitis C virus are blocked by hexamethylene amiloride. FEBS Lett **557:**99-103.
234. **Quinkert, D., R. Bartenschlager, and V. Lohmann.** 2005. Quantitative analysis of the hepatitis C virus replication complex. J Virol **79:**13594-13605.
235. **Ranjith-Kumar, C. T., R. T. Sarisky, L. Gutshall, M. Thomson, and C. C. Kao.** 2004. De novo initiation pocket mutations have multiple effects on hepatitis C virus RNA-dependent RNA polymerase activities. J Virol **78:**12207-12217.
236. **Reed, K. E., A. Grakoui, and C. M. Rice.** 1995. Hepatitis C virus-encoded NS2-3 protease: cleavage-site mutagenesis and requirements for bimolecular cleavage. J Virol **69:**4127-4136.
237. **Reusken, C. B., T. J. Dalebout, P. Eerligh, P. J. Bredenbeek, and W. J. Spaan.** 2003. Analysis of hepatitis C virus/classical swine fever virus chimeric 5'NTRs: sequences within the hepatitis C virus IRES are required for viral RNA replication. J Gen Virol **84:**1761-1769.
238. **Rijnbrand, R., T. van der Straaten, P. A. van Rijn, W. J. Spaan, and P. J. Bredenbeek.** 1997. Internal entry of ribosomes is directed by the 5' noncoding region of classical swine fever virus and is dependent on the presence of an RNA pseudoknot upstream of the initiation codon. J Virol **71:**451-457.
239. **Robertson, B., G. Myers, C. Howard, T. Brettin, J. Bukh, B. Gaschen, T. Gojobori, G. Maertens, M. Mizokami, O. Nainan, S. Netesov, K. Nishioka, T. Shin i, P. Simmonds, D. Smith, L. Stuyver, and A. Weiner.** 1998. Classification, nomenclature, and database development for hepatitis C virus (HCV) and related viruses: proposals for standardization. International Committee on Virus Taxonomy. Arch Virol **143:**2493-2503.
240. **Sakai, A., M. S. Claire, K. Faulk, S. Govindarajan, S. U. Emerson, R. H. Purcell, and J. Bukh.** 2003. The p7 polypeptide of hepatitis C virus is critical for infectivity and contains functionally important genotype-specific sequences. Proc Natl Acad Sci U S A **100:**11646-11651.
241. **Santolini, E., G. Migliaccio, and N. La Monica.** 1994. Biosynthesis and biochemical properties of the hepatitis C virus core protein. J Virol **68:**3631-3641.
242. **Santolini, E., L. Pacini, C. Fipaldini, G. Migliaccio, and N. Monica.** 1995. The NS2 protein of hepatitis C virus is a transmembrane polypeptide. J Virol **69:**7461-7471.

243. **Scarselli, E., H. Ansuini, R. Cerino, R. M. Roccasecca, S. Acali, G. Filocamo, C. Traboni, A. Nicosia, R. Cortese, and A. Vitelli.** 2002. The human scavenger receptor class B type I is a novel candidate receptor for the hepatitis C virus. EMBO J **21:**5017-5025.
244. **Schmidt-Mende, J., E. Bieck, T. Hugle, F. Penin, C. M. Rice, H. E. Blum, and D. Moradpour.** 2001. Determinants for membrane association of the hepatitis C virus RNA-dependent RNA polymerase. J Biol Chem **276:**44052-44063.
245. **Schregel, V., S. Jacobi, F. Penin, and N. Tautz.** 2009. Hepatitis C virus NS2 is a protease stimulated by cofactor domains in NS3. Proc Natl Acad Sci USA **106:**5342-5347.
246. **Selby, M. J., E. Glazer, F. Masiarz, and M. Houghton.** 1994. Complex processing and protein:protein interactions in the E2:NS2 region of HCV. Virology **204:**114-122.
247. **Serebrov, V., and A. M. Pyle.** 2004. Periodic cycles of RNA unwinding and pausing by hepatitis C virus NS3 helicase. Nature **430:**476-480.
248. **Shim, J. H., G. Larson, J. Z. Wu, and Z. Hong.** 2002. Selection of 3'-template bases and initiating nucleotides by hepatitis C virus NS5B RNA-dependent RNA polymerase. J Virol **76:**7030-7039.
249. **Shimoike, T., S. Mimori, H. Tani, Y. Matsuura, and T. Miyamura.** 1999. Interaction of hepatitis C virus core protein with viral sense RNA and suppression of its translation. J Virol **73:**9718-9725.
250. **Shirota, Y., H. Luo, W. Qin, S. Kaneko, T. Yamashita, K. Kobayashi, and S. Murakami.** 2002. Hepatitis C virus (HCV) NS5A binds RNA-dependent RNA polymerase (RdRP) NS5B and modulates RNA-dependent RNA polymerase activity. J Biol Chem **277:**11149-11155.
251. **Simmonds, P., A. Tuplin, and D. J. Evans.** 2004. Detection of genome-scale ordered RNA structure (GORS) in genomes of positive-stranded RNA viruses: Implications for virus evolution and host persistence. RNA **10:**1337-1351.
252. **Siridechadilok, B., C. S. Fraser, R. J. Hall, J. A. Doudna, and E. Nogales.** 2005. Structural roles for human translation factor eIF3 in initiation of protein synthesis. Science **310:**1513-1515.
253. **Skoging, U., and P. Liljestrom.** 1998. Role of the C-terminal tryptophan residue for the structure-function of the alphavirus capsid protein. J Mol Biol **279:**865-872.
254. **Spahn, C. M., J. S. Kieft, R. A. Grassucci, P. A. Penczek, K. Zhou, J. A. Doudna, and J. Frank.** 2001. Hepatitis C virus IRES RNA-induced changes in the conformation of the 40s ribosomal subunit. Science **291:**1959-1962.
255. **Stadler, K., S. L. Allison, J. Schalich, and F. X. Heinz.** 1997. Proteolytic activation of tick-borne encephalitis virus by furin. J Virol **71:**8475-8481.
256. **Steinmann, E., F. Penin, S. Kallis, A. H. Patel, R. Bartenschlager, and T. Pietschmann.** 2007. Hepatitis C virus p7 protein is crucial for assembly and release of infectious virions. PLoS Pathog **3:**e103.
257. **StGelais, C., T. J. Tuthill, D. S. Clarke, D. J. Rowlands, M. Harris, and S. Griffin.** 2007. Inhibition of hepatitis C virus p7 membrane channels in a liposome-based assay system. Antiviral Res **76:**48-58.
258. **Street, A., A. Macdonald, K. Crowder, and M. Harris.** 2004. The Hepatitis C virus NS5A protein activates a phosphoinositide 3-kinase-dependent survival signaling cascade. J Biol Chem **279:**12232-12241.
259. **Su, A. I., J. P. Pezacki, L. Wodicka, A. D. Brideau, L. Supekova, R. Thimme, S. Wieland, J. Bukh, R. H. Purcell, P. G. Schultz, and F. V. Chisari.** 2002. Genomic analysis of the host response to hepatitis C virus infection. Proc Natl Acad Sci U S A **99:**15669-15674.
260. **Suzich, J. A., J. K. Tamura, F. Palmer-Hill, P. Warrener, A. Grakoui, C. M. Rice, S. M. Feinstone, and M. S. Collett.** 1993. Hepatitis C virus NS3 protein polynucleotide-stimulated nucleoside triphosphatase and comparison with the related pestivirus and flavivirus enzymes. J Virol **67:**6152-6158.
261. **Tamura, J. K., P. Warrener, and M. S. Collett.** 1993. RNA-stimulated NTPase activity associated with the p80 protein of the pestivirus bovine viral diarrhea virus. Virology **193:**1-10.

262. **Tan, B. H., J. Fu, R. J. Sugrue, E. H. Yap, Y. C. Chan, and Y. H. Tan.** 1996. Recombinant dengue type 1 virus NS5 protein expressed in Escherichia coli exhibits RNA-dependent RNA polymerase activity. Virology **216:**317-325.
263. **Tanaka, T., N. Kato, M. J. Cho, and K. Shimotohno.** 1995. A novel sequence found at the 3' terminus of hepatitis C virus genome. Biochem Biophys Res Commun **215:**744-749.
264. **Tanaka, Y., T. Shimoike, K. Ishii, R. Suzuki, T. Suzuki, H. Ushijima, Y. Matsuura, and T. Miyamura.** 2000. Selective binding of hepatitis C virus core protein to synthetic oligonucleotides corresponding to the 5' untranslated region of the viral genome. Virology **270:**229-236.
265. **Tellinghuisen, T. L., K. L. Foss, and J. Treadaway.** 2008. Regulation of hepatitis C virion production via phosphorylation of the NS5A protein. PLoS Pathog **4:**e1000032.
266. **Tellinghuisen, T. L., J. Marcotrigiano, A. E. Gorbalenya, and C. M. Rice.** 2004. The NS5A protein of hepatitis C virus is a zinc metalloprotein. J Biol Chem **279:**48576-48587.
267. **Tellinghuisen, T. L., and C. M. Rice.** 2002. Interaction between hepatitis C virus proteins and host cell factors. Curr Opin Microbiol **5:**419-427.
268. **Thibeault, D., R. Maurice, L. Pilote, D. Lamarre, and A. Pause.** 2001. In vitro characterization of a purified NS2/3 protease variant of hepatitis C virus. J Biol Chem **276:**46678-46684.
269. **Thomssen, R., S. Bonk, C. Propfe, K. H. Heermann, H. G. Kochel, and A. Uy.** 1992. Association of hepatitis C virus in human sera with beta-lipoprotein. Med Microbiol Immunol (Berl) **181:**293-300.
270. **Thomssen, R., S. Bonk, and A. Thiele.** 1993. Density heterogeneities of hepatitis C virus in human sera due to the binding of beta-lipoproteins and immunoglobulins. Med Microbiol Immunol **182:**329-334.
271. **Tischendorf, J. J., C. Beger, M. Korf, M. P. Manns, and M. Kruger.** 2004. Polypyrimidine tract-binding protein (PTB) inhibits Hepatitis C virus internal ribosome entry site (HCV IRES)-mediated translation, but does not affect HCV replication. Arch Virol **149:**1955-1970.
272. **Tomei, L., C. Failla, E. Santolini, R. De Francesco, and N. La Monica.** 1993. NS3 is a serine protease required for processing of hepatitis C virus polyprotein. J Virol **67:**4017-4026.
273. **Tomori, O.** 2004. Yellow fever: the recurring plague. Crit Rev Clin Lab Sci **41:**391-427.
274. **Tscherne, D. M., C. T. Jones, M. J. Evans, B. D. Lindenbach, J. A. McKeating, and C. M. Rice.** 2006. Time- and temperature-dependent activation of hepatitis C virus for low-pH-triggered entry. J Virol **80:**1734-1741.
275. **Tsuchihara, K., T. Tanaka, M. Hijikata, S. Kuge, H. Toyoda, A. Nomoto, N. Yamamoto, and K. Shimotohno.** 1997. Specific interaction of polypyrimidine tract-binding protein with the extreme 3'-terminal structure of the hepatitis C virus genome, the 3'X. J Virol **71:**6720-6726.
276. **Tsukiyama-Kohara, K., N. Iizuka, M. Kohara, and A. Nomoto.** 1992. Internal ribosome entry site within hepatitis C virus RNA. J Virol **66:**1476-1483.
277. **Tuplin, A., J. Wood, D. J. Evans, A. H. Patel, and P. Simmonds.** 2002. Thermodynamic and phylogenetic prediction of RNA secondary structures in the coding region of hepatitis C virus. RNA **8:**824-841.
278. **Urbani, A., R. Bazzo, M. C. Nardi, D. O. Cicero, R. De Francesco, C. Steinkuhler, and G. Barbato.** 1998. The metal binding site of the hepatitis C virus NS3 protease. A spectroscopic investigation. J Biol Chem **273:**18760-18769.
279. **van Dijk, A. A., E. V. Makeyev, and D. H. Bamford.** 2004. Initiation of viral RNA-dependent RNA polymerization. J Gen Virol **85:**1077-1093.
280. **Van Itallie, C. M., and J. M. Anderson.** 2006. Claudins and epithelial paracellular transport. Annu Rev Physiol **68:**403-429.
281. **Vassilaki, N., and P. Mavromara.** 2003. Two alternative translation mechanisms are responsible for the expression of the HCV ARFP/F/core+1 coding open reading frame. J Biol Chem **278:**40503-40513.
282. **Verna, E. C., and R. S. Brown, Jr.** 2006. Hepatitis C virus and liver transplantation. Clin Liver Dis **10:**919-940.

283. **Voisset, C., and J. Dubuisson.** 2004. Functional hepatitis C virus envelope glycoproteins. Biol Cell **96:**413-420.
284. **von Hahn, T., B. D. Lindenbach, A. Boullier, O. Quehenberger, M. Paulson, C. M. Rice, and J. A. McKeating.** 2006. Oxidized low-density lipoprotein inhibits hepatitis C virus cell entry in human hepatoma cells. Hepatology **43:**932-942.
285. **Vozzolo, L., B. Loh, P. J. Gane, M. Tribak, L. Zhou, I. Anderson, E. Nyakatura, R. G. Jenner, D. Selwood, and A. Fassati.** 2010. A gyrase B inhibitor impairs HIV-1 replication by targeting HSP90 and the capsid protein. J Biol Chem.
286. **Wakita, T., T. Pietschmann, T. Kato, T. Date, M. Miyamoto, Z. Zhao, K. Murthy, A. Habermann, H. G. Krausslich, M. Mizokami, R. Bartenschlager, and T. J. Liang.** 2005. Production of infectious hepatitis C virus in tissue culture from a cloned viral genome. Nat Med **11:**791-796.
287. **Walker, C. M.** 1997. Comparative features of hepatitis C virus infection in humans and chimpanzees. Springer Semin Immunopathol **19:**85-98.
288. **Warrener, P., and M. S. Collett.** 1995. Pestivirus NS3 (p80) protein possesses RNA helicase activity. J Virol **69:**1720-1726.
289. **Watashi, K., M. Hijikata, M. Hosaka, M. Yamaji, and K. Shimotohno.** 2003. Cyclosporin A suppresses replication of hepatitis C virus genome in cultured hepatocytes. Hepatology **38:**1282-1288.
290. **Watashi, K., N. Ishii, M. Hijikata, D. Inoue, T. Murata, Y. Miyanari, and K. Shimotohno.** 2005. Cyclophilin B is a functional regulator of hepatitis C virus RNA polymerase. Mol Cell **19:**111-122.
291. **Watson, J. P., D. J. Bevitt, G. P. Spickett, G. L. Toms, and M. F. Bassendine.** 1996. Hepatitis C virus density heterogeneity and viral titre in acute and chronic infection: a comparison of immunodeficient and immunocompetent patients. J Hepatol **25:**599-607.
292. **Welbourn, S., R. Green, I. Gamache, S. Dandache, V. Lohmann, R. Bartenschlager, K. Meerovitch, and A. Pause.** 2005. Hepatitis C virus NS2/3 processing is required for NS3 stability and viral RNA replication. J Biol Chem **280:**29604-29611.
293. **Wellnitz, S., B. Klumpp, H. Barth, S. Ito, E. Depla, J. Dubuisson, H. E. Blum, and T. F. Baumert.** 2002. Binding of hepatitis C virus-like particles derived from infectious clone H77C to defined human cell lines. J Virol **76:**1181-1193.
294. **Wengler, G.** 1991. The carboxy-terminal part of the NS 3 protein of the West Nile flavivirus can be isolated as a soluble protein after proteolytic cleavage and represents an RNA-stimulated NTPase. Virology **184:**707-715.
295. **Winkler, G., S. E. Maxwell, C. Ruemmler, and V. Stollar.** 1989. Newly synthesized dengue-2 virus nonstructural protein NS1 is a soluble protein but becomes partially hydrophobic and membrane-associated after dimerization. Virology **171:**302-305.
296. **Winkler, G., V. B. Randolph, G. R. Cleaves, T. E. Ryan, and V. Stollar.** 1988. Evidence that the mature form of the flavivirus nonstructural protein NS1 is a dimer. Virology **162:**187-196.
297. **Wiskerchen, M., S. K. Belzer, and M. S. Collett.** 1991. Pestivirus gene expression: the first protein product of the bovine viral diarrhea virus large open reading frame, p20, possesses proteolytic activity. J Virol **65:**4508-4514.
298. **Wiskerchen, M., and M. S. Collett.** 1991. Pestivirus gene expression: protein p80 of bovine viral diarrhea virus is a proteinase involved in polyprotein processing. Virology **184:**341-350.
299. **Wolk, B., D. Sansonno, H. G. Krausslich, F. Dammacco, C. M. Rice, H. E. Blum, and D. Moradpour.** 2000. Subcellular localization, stability, and trans-cleavage competence of the hepatitis C virus NS3-NS4A complex expressed in tetracycline-regulated cell lines. J Virol **74:**2293-2304.
300. **Wunschmann, S., J. D. Medh, D. Klinzmann, W. N. Schmidt, and J. T. Stapleton.** 2000. Characterization of hepatitis C virus (HCV) and HCV E2 interactions with CD81 and the low-density lipoprotein receptor. J Virol **74:**10055-10062.

301. **Yamada, N., K. Tanihara, A. Takada, T. Yorihuzi, M. Tsutsumi, H. Shimomura, T. Tsuji, and T. Date.** 1996. Genetic organization and diversity of the 3' noncoding region of the hepatitis C virus genome. Virology **223:**255-261.
302. **Yamashita, T., S. Kaneko, Y. Shirota, W. Qin, T. Nomura, K. Kobayashi, and S. Murakami.** 1998. RNA-dependent RNA polymerase activity of the soluble recombinant hepatitis C virus NS5B protein truncated at the C-terminal region. J Biol Chem **273:**15479-15486.
303. **Yan, Y., Y. Li, S. Munshi, V. Sardana, J. L. Cole, M. Sardana, C. Steinkuehler, L. Tomei, R. De Francesco, L. C. Kuo, and Z. Chen.** 1998. Complex of NS3 protease and NS4A peptide of BK strain hepatitis C virus: a 2.2 A resolution structure in a hexagonal crystal form. Protein Sci **7:**837-847.
304. **Yanagi, M., R. H. Purcell, S. U. Emerson, and J. Bukh.** 1997. Transcripts from a single full-length cDNA clone of hepatitis C virus are infectious when directly transfected into the liver of a chimpanzee. Proc Natl Acad Sci U S A **94:**8738-8743.
305. **Yi, M., Y. Ma, J. Yates, and S. M. Lemon.** 2007. Compensatory mutations in E1, p7, NS2, and NS3 enhance yields of cell culture-infectious intergenotypic chimeric hepatitis C virus. J Virol **81:**629-638.
306. **Yi, M., Y. Nakamoto, S. Kaneko, T. Yamashita, and S. Murakami.** 1997. Delineation of regions important for heteromeric association of hepatitis C virus E1 and E2. Virology **231:**119-129.
307. **You, S., D. D. Stump, A. D. Branch, and C. M. Rice.** 2004. A cis-acting replication element in the sequence encoding the NS5B RNA-dependent RNA polymerase is required for hepatitis C virus RNA replication. J Virol **78:**1352-1366.
308. **Yu, I. M., W. Zhang, H. A. Holdaway, L. Li, V. A. Kostyuchenko, P. R. Chipman, R. J. Kuhn, M. G. Rossmann, and J. Chen.** 2008. Structure of the immature dengue virus at low pH primes proteolytic maturation. Science **319:**1834-1837.
309. **Yu, M. Y., B. Bartosch, P. Zhang, Z. P. Guo, P. M. Renzi, L. M. Shen, C. Granier, S. M. Feinstone, F. L. Cosset, and R. H. Purcell.** 2004. Neutralizing antibodies to hepatitis C virus (HCV) in immune globulins derived from anti-HCV-positive plasma. Proc Natl Acad Sci U S A **101:**7705-7710.
310. **Yuan, Z. H., U. Kumar, H. C. Thomas, Y. M. Wen, and J. Monjardino.** 1997. Expression, purification, and partial characterization of HCV RNA polymerase. Biochem Biophys Res Commun **232:**231-235.
311. **Zhang, C., Z. Cai, Y. C. Kim, R. Kumar, F. Yuan, P. Y. Shi, C. Kao, and G. Luo.** 2005. Stimulation of hepatitis C virus (HCV) nonstructural protein 3 (NS3) helicase activity by the NS3 protease domain and by HCV RNA-dependent RNA polymerase. J Virol **79:**8687-8697.
312. **Zhang, J., G. Randall, A. Higginbottom, P. Monk, C. M. Rice, and J. A. McKeating.** 2004. CD81 is required for hepatitis C virus glycoprotein-mediated viral infection. J Virol **78:**1448-1455.
313. **Zhang, J., O. Yamada, H. Yoshida, T. Iwai, and H. Araki.** 2002. Autogenous translational inhibition of core protein: implication for switch from translation to RNA replication in hepatitis C virus. Virology **293:**141-150.
314. **Zhang, W., P. R. Chipman, J. Corver, P. R. Johnson, Y. Zhang, S. Mukhopadhyay, T. S. Baker, J. H. Strauss, M. G. Rossmann, and R. J. Kuhn.** 2003. Visualization of membrane protein domains by cryo-electron microscopy of dengue virus. Nat Struct Biol **10:**907-912.
315. **Zhang, Y., J. Corver, P. R. Chipman, W. Zhang, S. V. Pletnev, D. Sedlak, T. S. Baker, J. H. Strauss, R. J. Kuhn, and M. G. Rossmann.** 2003. Structures of immature flavivirus particles. EMBO J **22:**2604-2613.
316. **Zhang, Y., B. Kaufmann, P. R. Chipman, R. J. Kuhn, and M. G. Rossmann.** 2007. Structure of immature West Nile virus. J Virol **81:**6141-6145.
317. **Zhang, Y., V. A. Kostyuchenko, and M. G. Rossmann.** 2007. Structural analysis of viral nucleocapsids by subtraction of partial projections. J Struct Biol **157:**356-364.

318. **Zheng, Y., B. Gao, L. Ye, L. Kong, W. Jing, X. Yang, and Z. Wu.** 2005. Hepatitis C virus non-structural protein NS4B can modulate an unfolded protein response. J Microbiol **43:**529-536.
319. **Zhong, J., P. Gastaminza, G. Cheng, S. Kapadia, T. Kato, D. R. Burton, S. F. Wieland, S. L. Uprichard, T. Wakita, and F. V. Chisari.** 2005. Robust hepatitis C virus infection in vitro. Proc Natl Acad Sci U S A **102:**9294-9299.
320. **Zhong, W., L. L. Gutshall, and A. M. Del Vecchio.** 1998. Identification and characterization of an RNA-dependent RNA polymerase activity within the nonstructural protein 5B region of bovine viral diarrhea virus. J Virol **72:**9365-9369.
321. **Zhong, W., A. S. Uss, E. Ferrari, J. Y. Lau, and Z. Hong.** 2000. De novo initiation of RNA synthesis by hepatitis C virus nonstructural protein 5B polymerase. J Virol **74:**2017-2022.
322. **Zibert, A., H. Meisel, W. Kraas, A. Schulz, G. Jung, and M. Roggendorf.** 1997. Early antibody response against hypervariable region 1 is associated with acute self-limiting infections of hepatitis C virus. Hepatology **25:**1245-1249.